OESG Scientific Report

Annex 3: Multi-media Case Studies

Case study: Impacts of reductions in mercury emissions on the Flin Flon ecosystem

Marlene Evans, Environment and Climate Change Canada

Background and description for the Flin Flon case study: The copper-zinc smelter at Flin Flon, Manitoba, began its operation in 1930, using two short (53 and 69 m tall) stacks to release its emissions. It was until improvements were made in the operation of its Zn processing facility in 1982, the single largest Hg emitter in North America (Pai et al. 2000, Wiklund et al. 2017) with emissions of 20,000 kg in 1990, representing 57% of total Canadian emissions (Outridge et al. 2011, Environment and Climate Change Canada 2016). It also was a major emitter of Pb, Zn and other heavy metals with an average particulate emission rate of 7,150 t/yr over 1931-1974 and 6,834 t/yr over 1985-1995 (McMartin et al. 1999) and the fourth 4th largest single SO_2 emitter in Canada emitting 192,320 tonnes/yr (Franklin et al. 1985). In 1974, as part of strategies to reduce the impacts of acidifying emissions on the environment, the two original short stacks were replaced with a 251 m stack to reduce local deposition of particulate emissions while dispersing over them over a broader area (Harrison and Klaverkamp 1990). A series of snow and water investigations were conducted over 1974-1982 and within ~40 km of the smelter to investigate spatial variability in metal and SO_2 deposition on the landscape (Van Loon and Beamish 1977, Franzin et al. 1979, McFarlane et al. 1979, Franzin and McFarlane 1981) with the construction of the new stack although mercury was not included in these studies. The studies did not investigate time trends. Studies also investigated soils, garden produce and peat (Hogan and Wotton 1984, Zoltai 1988, Pip 1991).

A limited number of biological studies also were conducted (Jackson 1978, Franzin and McFarlane 1980, McFarlane and Franzin 1980, Jackson 1984) with Harrison and Klaverkamp (1990) showing that cadmium, copper, mercury, selenium and zinc occurred in highly elevated concentrations in lake sediments within 7 km of the smelter with concentrations decreasing with increasing distance from the smelter. There was also some evidence from sediment core studies that metal deposition had increased at sites located 68-84 km north of the smelter and decreased at lakes located within 7 km of the smelter and in close proximity to Flin Flon. Mercury concentrations were lowest in Northern Pike (*Esox lucius*) at lakes located within 7 km of the smelter, averaging less than 0.09 µg/g; 0.20 µg/g at lakes 21-43 km from the smelter; and 0.47 µg/g at lakes 68-84 km northwest of the smelter where lakes tended to be acidic (surface pH 5.9-6.5) based on a single measurement made of surface waters in June 1982. Low mercury concentrations in northern pike (and white sucker) in lakes close to the smelter despite high mercury deposition rates and high mercury concentrations in lake sediments were related to high selenium concentrations which may have reduced Hg uptake and/or to Cu, Cd, and Zn toxicity which reduced mercury methylation rates (Jackson 1984, Harrison and Klaverkamp 1990) Similar reductions in mercury in yellow perch (*Perca flavescens*) and crayfish mercury concentrations were observed in lakes close to the Sudbury smelter and attributed to high selenium loading which interfered with mercury uptake an/or metal concentrations which impacted metal toxicity and mercury methylation (Nriagu et al. 1982, Nriagu and Wong 1983, Wren and Stokes 1988). However, unlike Flin Flon, mercury emission rates from Sudbury smelters are low (Evans et al. In review)with a later study showing that mercury concentrations are low in Sudbury lake sediments (Hechler 2006).

In an effort to reduce toxic emissions from smelters, The Government of Canada (2006) set 2008 and 2015 target releases. For Flin Flon, the 2008 SO_2 target release was 187,000 tonnes/yr with further reductions to 33,500 tonnes/yr by 2015, reductions to 88% and 16% respectively of the 212,000 tons/yr releases in the late 1970s and early 1980s (Franklin et al. 1985). Target reductions for particulates was 930 tonnes/yr by 2008 and 616 tonnes/yr by 2015 down to 14% and 9% respectively of 1975-1997 average dust emissions of 6,834 t/yr (McMartin et al. 1999). Individual targets were not set for metals except for Hg to 373 kg/y by 2008 down to 4% of 1975-1997 average emissions of 9.3 t/yr (McMartin et al. 1999) and 2% of peak estimates of 20 tonnes/y estimates in the late 1970s early 1980s (Wiklund et al. 2017). Challenges were encountered in meeting target SO_2 emissions and the Cu smelter Description closed in 2010 although the zinc refinery continued to operate through the early 2020s.

Methodology: Several studies have been conducted in the Flin Flon area to better understand the long-term impacts on emissions from the Flin Flon and broader area landscape. These studies included published studies of mercury concentrations in soils surrounding Flin Flon (McMartin et al. 1999, McMartin et al. 2002); mercury emissions from soils in the Flin Flon area (Eckley et al. 2013, Eckley et al. 2015)' sediment core studies to investigate mercury deposition to lakes close to Flin Flon and at some distance (Outridge et al. 2011, Wiklund et al. 2017, Roberts et al. 2021). Methodology is explained in these papers. In addition, surveys were conducted of Flin Flon lakes over 2008-2017 expanding on the studies conducted by Harrison and Klaverkamp (1990) with a broad suite of metal concentrations measured in surface sediments; metals and major ions concentrations in lake waters, and temperature, specific conductivity, pH, and dissolved oxygen profiles measured. The findings of these studies, along with reported metal and SO_2 have recently been submitted to a scientific journal for publication (Evans et al. In review). Studies also were conducted of mercury concentrations in northern pike (and other species) and influencing factors with presentations given at scientific meetings (Evans et al. 2017) and a manuscript in preparation. Data on emission rates from Flin Flon were obtained from the National Pollutant Release Inventory (2025).

Major findings

Reductions in Hg and other emissions: Flin Flon met with some success in reducing its emissions to meet The Government of Canada (2006) 2008 and 2015 target releases (Fig 1). The 2008 target for SO_2 was only slightly lower than historic emissions and was met as the 2015 target by the closure of the copper smelter in 2010. Particulate emission targets were met in both years, again facilitated by the closure of the copper smelter. Hg emissions began to decline after 1980 from ca. 20,000 kg to ca. 4,200 kg in 1995 with further declines through to 2010 (Wiklund et al. 2017); the 2008 target was not met with Hg emissions decreasing below this target with the 2010 closure of the copper smelter. No reductions were set for other metals, including Cd which has been implicated as having toxic impacts, including on mercury methylation (Jackson 1978, Jackson 1984, Harrison and Klaverkamp 1990). Cd emissions trends followed that of particulates, plunging in 2010. Similar reductions in Hg emissions were observed at the Trail smelter in British Columbia, coal-fired plants in Alberta and Saskatchewan and the Fort McMurray oil sands (Rutila 2018, Evans et al. In review)

Spatial and temporal patterns in mercury in soils, peat bogs, and lake sediments

Interest in Flin Flon as a study location based on its mercury and other metal emissions resumed in the late 1990s with early programs funded by the Hudson Bay Mining and Smelting Corporation. Mercury and other metal concentrations were measured in soil and humus in the broader Flin Flon area (Henderson and McMartin 1995, Henderson et al. 1998, McMartin et al. 1999) with a later study comparing Flin Flon with the smelters at Sudbury and Rouyn-Noranda, and the inactive Pinchi Lake gold mine (McMartin et al. 2002). Overall, the researchers determined that the metal concentrations were extremely high close to the smelter and decreased with increasing distance from the smelter, with additional spatial variation due to variability in the organic content of B horizon and substrate geology. The distances to reach regional background concentration ranged from 70 km for Cd, 85 km for Hg to 104 km for As. Mercury concentrations tend to be highest in humus with a median concentration of 900 µg/g versus 10 µg/g in the B horizon and 5 µg/g in the C horizon. Mean Hg concentration in humus was 6,320 µg/g with a maximum 100,000 µg/g. Clearly, large amounts of metals have been deposited in the landscape over the decades of smelter operation and are available to be eroded into creeks and rivers with rainfall, snowmelt, and wind events with lakes located within 10 km of the smelter the most vulnerable.

Outridge et al. (2011) investigated Hg and Zn deposition in a series of sediment cores collected from peat bogs, which are impacted primarily by atmospheric deposition and lakes which are impacted by atmospheric deposition and inputs from the watershed. Hg concentration and flux increased significantly in the cores after the smelter opened. One peat core showed

Substantial reductions in Hg and Zn concentrations after 1980, apparently coincidence with reductions in these metal emissions while no substantial declines were observed in the lake cores with Hg and Zn fluxes increasing substantially since 1988. Outridge et al. suggested that this increase was due to catchment soil saturation by the historically deposited metals over the decades of smelter operation, a hypothesis first proposed by Nriagu et al. (1998), which were now being mobilized to enter the lakes from the contaminated watershed. This mobilization is dependent on a number of factors including how well various metals are retained in the watershed, catchment features, and the volatility of the metal (Blais and Kalff 1993, Goodarzi et al. 2002). Climate change, through warming trends, affects a longer ice-free season, permafrost melt, and increased lake productivity all of which can increase total flux and associated metals to lakes (Outridge et al. 2007, Carrie et al. 2010).

The Canadian Mercury Science Assessment Report (Environment and Climate Change Canada 2016) identified several knowledge gaps about Hg in the Canadian environment and led to several research programs initially under the Clear Air Regulatory Agenda (CRA). One major gap was in western Canada, where only a few studies have been conducted in lakes around several significant Hg emitters. The Cu-Zn smelter at Flin Flon was of special interest.

One of the first studies was conducted by Wiklund et al. (2017) who collected sediment cores in 9 lakes located 5-75 km from Flin Flon measuring anthropogenic Hg flux and total inventory within each lake which varied by two orders of magnitude over the study area. Most of the Hg released in emissions contributed to the global transport of mercury with only about 11% of the released Hg deposited on the landscape within 50 km of the smelter. This mercury budget changed after the year 2000 when Hg emissions from the smelter were reduced more than 10-fold and the observed Hg deposition to lakes exceeded smelter releases. Tis suggested that the landscape is re-emitting/remobilizing legacy Hg as has become a major ongoing regional source of Hg and continuing to contribute to the global inventory of Hg despite the strong reduction in Hg emissions from the smelter.

Eckley conducted two studies investigating the impact of the closure of the copper on point source mercury emissions from the landscape. In Eckley et al. (2013), they found that total gaseous mercury was significantly elevated while the copper smelter was operational (4.1 ± 3.7 ng m^3), decreased to only 20% during the year following its closure, and remained ~2-fold above background levels while the zinc plant continued too operate. As with Outridge et al. (2011) and Wiklund et al. (2017), this was attributed to significant surface-air fluxes from mercury-contaminated soils in the vicinity of the smelter and or from the tailings area.

More recently, Sun et al. (2022) used mercury stable isotopes to investigate anthropogenic impacts of Hg emissions from the smelter. For much of the smelter's operational history, Hg isotope compositions showed limited variations in the lake sediments <10 km) from the smelter sediments reflecting the strong input from smelter emissions whereas isotopic variation was more variable in lakes 20-75 km from the smelter reflecting multiple Hg sources. For sediments deposited after 2000, fugitive dust from ore tailings dominated Hg deposition in lakes <10 km from the smelter and terrestrial legacy Hg re-emissions dominated Hg deposition in lakes 2-75 km from the smelter. They recommended strong remediation measures of highly contaminated sites such as the ore tailings area.

As noted previously, Harrison and Klaverkamp (1990) measured Hg in addition to Cu, Cd, Se and Se concentrations in the upper 2 cm of lake sediments at distances ranging from 4.5 to 84 km of the smelter (Fig 2). They observed a classic pattern of decreasing concentrations with increasing distance from the smelter due to the increasing dilution of emissions with distance and deposition. Similar patterns have been observed in lake sediments near other smelters (Telmer et al. 2004, Pyle et al. 2005, Shuhaimi-Othman et al. 2006) and in snow deposition (Kelly et al. 2010). In a more recent study, similar patterns were observed in surface sediments collected at the same lakes in 2008 and 2009 (Evans et al. In review). There was little evidence of a significant decline in metal concentrations over the 40 years separating the two studies despite substantial improvements in the operation of the smelter although most improvements

occurred after 1993. Concentrations of several metals above the Canadian Council of Ministers of the Environment (2014) Probable Effects Guideline for the protection of aquatic life in sediments.

Evans et al. (In review) measured the concentrations of several metals in surface and near bottom water on several occasions in these lakes. Surprisingly, there was little difference in metal concentrations in surface and near bottom waters although methyl mercury concentrations may have been elevated relative to surface water concentrations in one lake during periods of anoxia and low pH. There was surprisingly little spatial variability in mercury concentrations in water with highest concentrations in lakes close to the smelter and lakes more than 60 km to the northwest (Fig 3a). Concentrations were not appreciably different from those measured in the Northwest Territories. On the other hand, ,metals such as As, Cd, Cu, Se and Zn showed pronounced spatial gradients of substantially higher concentrations in lakes close to the smelter and decreasing concentrations with increasing distance. These spatial gradients in concentration were not as steep as for metals in sediments. Moreover, many metals exceed CCME chronic guidelines for the protection of aquatic life.

Smelter emissions and the biological environment. Harrison and Klaverkamp (1990) conducted the primary study investigating the impact of smelter emissions on the metal content on Northern pike (*Esox lucius*) and white sucker (*Catostomus commersoni*)from the same 13 lakes located 4.5 to 84 km from smelter where they conducted sediment core studies. They determined, as already noted, that metal concentrations were extremely low in northern pike (and white sucker) in lakes whose sediments were highly contaminated with mercury and other metals. While they did not measure metals in water, we can assume that metals would have shown the same spatial patterns and possibility similar concentration as observed in Evans et al. (In review). Other limnological variables seemed to have little influence on metal concentrations in fish. Over 2009-2017, Evans conducted various studies of mercury concentrations in northern pike (and white suckers) presenting findings at scientific meetings the most recent being Evans et al. (2017) with a manuscript now in preparation building on Evans et al. (In review).and including a closer examination of the mercury fish data reported in Harrison et al. (1989). Despite the high metal concentrations in lake water and sediments in lakes close to the smelter, there was no difference in the mean size, age, and condition factor of fish between the two regions suggesting that fish health was not being adversely affected in lakes close to the smelter. The most interesting and intriguing aspect of the northern pike data is that mercury concentrations have been increasing at lakes 5.6 and 7.6 km from the smelter with less evidence of a trend of increase in more distant lakes. This suggests that the impairment of mercury uptake by pike in lakes in close proximity to the smelter has become weaker in recent years as toxic emissions have declined, a situation also observed at Sudbury (Ažđajić et al. 2020) . The higher mercury concentrations in lakes 74 km to the north is within the normal variability of mercury concentrations in pike and appears to be due to a combination of fish age and undetermined features of the watersheds and lakes.

Simmatis et al. (2022) recently reported on a paleolimnology investigation of how changes in metal deposition to Phantom Lake, located 5.4 km from the smelter, impacted zooplankton, diatom, and benthic invertebrate communities. As noted in other sediment core studies, metal concentrations in the sediments increased through the 1930s, peaked in the 1960s, and declined with later technological improvements but remain highly elevated above background concentrations. Sediment PELs guidelines were exceeded for several metals for prolonged periods of time and presumably water quality chronic guidelines. The diatom record showed no evidence of acidification as the lake was and remained well-buffered. Prior to the operation of the smelter, diatom and invertebrate assemblages were diverse and indicated oligo-mesotrophic conditions. Smelting resulted in the loss of metal-sensitive biological indicators and the emergence of assemblages dominated by metal-tolerant, generalist taxa. Diatom assemblages tracked the substantial reductions in aerial emissions since the 1990s, particularly after the smelter closed, but also indicated that the biological effects of metal pollution persist in Phantom Lake. Mercury concentrations were not determined in this core but were in an earlier core collected by Wiklund et al. (2017). It is

unlikely that mercury had a profound effect on diatoms and invertebrate assemblage composition but more likely operated through biomagnification pathways.

Another study investigated mercury concentrations in small fish and in blood of common loons (*Gavia immer*) in lakes in the Flin Flon area, central Alberta, southern Quebec and Nova Scotia (Scheuhammer et al. 2016). Hg concentrations in the small fish and the blood of loons from the Flin Flon area were low and similar to those from uncontaminated reference lakes. Lake pH was by far the most important single factor influencing perch Hg concentrations in lakes across the four study areas and the best 3 variable model included pH, alkalinity and sediment Se. The greatest potential Hg health risk for perch and for breeding common loons were in lakes where pH was < 6.7 and were located in eastern Canada.

Relevance to effectiveness evaluation: Studies conducted at Flin Flon have shown that while the Cu-Zn smelter was a major mercury emitter, these mercury emissions appear to have had little negative impact on the aquatic environment. Unlike studies conducted around pulp and paper mills where large quantities of mercury were released into the aquatic environment where it rapidly entered the food chain reaching dangerously high concentrations in fish (Armstrong and Scott 1979, Gewurtz et al. 2010, Neff et al. 2012), high emission rates of other heavy metals may have occurred in sufficiently high concentrations in the aquatic environment as to impair mercury methylation rates; high concentrations of selenium may have interfered with mercury uptake. Moreover, despite high SO_2 emission rates, lakes near the smelter were largely circumneutral because of watershed features and because the base metal/fly ash was sufficient to counteract any potential acidification caused by the SO_2 emissions (Harrison and Klaverkamp 1990, Scott 2000, Evans et al. In review) and thus mercury methylation was not enhanced by acidic conditions as has been observed in other environments (Miskimmin et al. 1992, Scheuhammer and Graham 1999). Sediment core studies have provided strong evidence of the effectiveness of Hg (and other metal) controls in reducing deposition to lakes and the landscape. The recent strong reduction in Hg emissions with the copper smelter closure in 2010 is particularly noteworthy. On the other hand, mercury deposited on the landscape over decades of smelter operation and residing in the tailings pond are subject to reentry to the environment through wind activity, particularly over the tailings area, and revitalization.

Information and capacity needs: There are several research needs for the Flin Flon area including a better understanding of the factors affecting the low mercury concentrations in northern pike in lakes near the smelter. The potential role of heavy metal toxicity in affecting mercury methylation rates requires a fuller understanding. Furthermore, if high concentrations of Se are interfering with Hg uptake, this needs to be better understood as it potentially could be used as a remedy elsewhere in limiting Hg uptake including through the consumption of organisms containing high mercury concentrations.

More information is needed on the impacts of smelter emissions on the health of fish and other organisms using more modern techniques to detect impaired reproductive impairment, physiological function, etc. (Saha et al. 2023, Zahran et al. 2025).

Apart from Simmatis et al. (2022) nothing is known abut zooplankton, phytoplankton and benthos community structure, their spatial distribution with the lakes, and their health.

A long-term research and monitoring plan is desirable for Flin Flon to investigate how lake ecosystems respond to declining emissions and the re-entry of metals into lakes from the watershed. Fish mercury monitoring and studies are particularly desirable in lakes located with 7 km of the smelter. Lakes located 73-84 km to the northwest also are of interest because north pike can have high mercury concentrations in these lakes for reasons not fully understood. Waters are occasionally acidic which may facilitate mercury methylation rates.

Investigations of the loss of mercury and other metals from the exposed tailings area merits some attention.

References

.

Armstrong, F. A. J., and D. P. Scott. 1979. Decrease in mercury content of fishes in Ball Lake, Ontario, since imposition of controls on mercury discharges. Journal of the Fisheries Research Board of Canada **36**:670-672.

Aždajić, M., N. Belzile, J. M. Gunn, J. M. Blais, and A. J. Poulain. 2020. Effects of a decade of selenium emission reductions on mercury accumulation in aquatic biota in the Sudbury region of Ontario. Canadian Journal of Fisheries and Aquatic Sciences **77**:848-856.

Blais, J. M., and J. Kalff. 1993. Atmospheric loading of Zn, Cu, Ni, Cr, and Pb to lake sediments: The role of catchment, lake morphometry, and physico-chemical properties of the elements. Biogeochemistry **23**:1-22.

Canadian Council of Ministers of the Environment. 2014. Canadian environmental quality guidelines. Canadian Council of Ministers of the Environment.

Carrie, J., F. Wang, H. Sanei, R. W. Macdonald, P. M. Outridge, and G. A. Stern. 2010. Increasing contaminant burdens in an arctic fish, burbot (Lota lota), in a warming climate. Environmental Science and Technology **44**:316-322.

Eckley, C. S., P. Blanchard, D. McLennan, R. Mintz, and M. Sekela. 2015. Soil-Air Mercury Flux near a Large Industrial Emission Source before and after Closure (Flin Flon, Manitoba, Canada). Environmental Science and Technology **49**:9750-9757.

Eckley, C. S., M. T. Parsons, R. Mintz, M. Lapalme, M. Mazur, R. Tordon, R. Elleman, J. A. Graydon, P. Blanchard, and V. St Louis. 2013. Impact of closing Canada's Largest Point-Source of Mercury Emissions on Local Atmospheric Mercury Concentrations. Environmental Science and Technology **47**:10339-10348.

Environment and Climate Change Canada. 2016. Canadian Mercury Science Assessment Report. Gatineau QC.

Evans, M. s., J. Kirk, D. Muir, J. Wiklund, J. Keating, A. Gleason, and X. Wang. 2017. Impacts of mercury and other emissions from the smelter at Flin Flon (Manitoba) on lake ecosystems: responses to smelter closure. ICMGP 2017: 13th International Conference on Mercury as a Global Pollutant. July 16-21, 2017, Providence, Rhode Island, USA.

Evans, M. S., J. Kirk, J. A. Wiklund, K. J. Painter, J. P. Smol, K. Ruhland, S. Robert, B. Simmatis, and D. G. C. Muir. In review. Lake water and sediment chemistry responses to reductions in mercury, other heavy metals, and sulfur dioxide emissions from smelter at the Flin Flon, Manitoba, Canada, with historic comparisons to other emitters.

Franklin, C. A., R. T. Burnett, R. Paolini, and M. E. Raizenne. 1985. Health risks from acid rain: a Canadian perspective. Environmental Health Perspectives **63**:155.

Franzin, W., and G. McFarlane. 1980. An analysis of the aquatic macrophyte, Myriophyllum exalbescens, as an indicator of metal contamination of aquatic ecosystems near a base metal smelter. Bulletin of Environmental Contamination and Toxicology **24**:597-605.

Franzin, W. G., and G. A. McFarlane. 1981. Elevated Zn, Cd and Pb concentrations in waters of ice-covered lakes near a base metal smelter during the snow melt, April 1977. Environmental Pollution. Series B, Chemical and Physical **2**:11-19.

Franzin, W. G., G. A. McFarlane, and A. Lutz. 1979. Atmospheric fallout in the vicinity of a base metal smelter at Flin Flon, Manitoba, Canada. Environmental Science and Technology **13**:1513-1522.

Gewurtz, S. B., S. P. Bhavsar, D. A. Jackson, R. Fletcher, E. Awad, R. Moody, and E. J. Reiner. 2010. Temporal and spatial trends of organochlorines and mercury in fishes from the St. Clair River/Lake St. Clair corridor, Canada. Journal of Great Lakes Research **36**:100-112.

Goodarzi, F., H. Sanei, R. G. Garrett, and W. F. Duncan. 2002. Accumulation of trace elements on the surface soil around the trail smelter, British Columbia, Canada. Environmental Geology **43**:29-38.

Government of Canada. 2006. Notice with respect to the Environmental Code of Practice for Base Metals Smelters and Refineries. Notice requiring the preparation and implementation of pollution prevention plans in respect of specified toxic substances released from base metals smelters and refineries and zinc plants. Pages 877-915 *in* C. Gazette, editor. Vol 140, no 7. April 29, 2006. Government of Canada Publications, Public Works and Government Services Canada, Ottawa, Canada.

Harrison, S. E., M. D. Dutton, R. V. Hunt, J. F. Klaverkamp, A. Lutz, W. A. Macdonald, H. S. Majewski, and L. J. Wesson. 1989. Metal Concentrations in Fish and Sediment from Lakes near Flin Flon, Manitoba. Page 74. Canadian Data Report of Fisheries and Aquatic Sciences, Winnipeg, MB.

Harrison, S. E., and J. F. Klaverkamp. 1990. Metal contamination in liver and muscle of northern pike (Esox Lucius) and white sucker (Catostomus commersoni) and in sediments from lakes near the smelter at Flin Flon, Manitoba. Environmental Toxicology and Chemistry **9**:941-956.

Hechler, J. 2006. Distribution and Speciation of Thallium in Sediment Profiles from Ramsey Lake; Sudbury, Ontario, Canada. Laurentian University Sudbury.

Henderson, P. J., and I. McMartin. 1995. Mercury distribution in humus and surficial sediments, Flin Flon, Manitoba, Canada. Water, Air, and Soil Pollution **80**:1043-1046.

Henderson, P. J., I. McMartin, G. E. Hall, J. B. Percival, and D. A. Walker. 1998. The chemical and physical characteristics of heavy meals in humus and till in the vicinity of the base metal smelter at Flin Flon, Manitoba, Canada. Environmental Geology **34**:39-58.

Hogan, G. D., and D. L. Wotton. 1984. Pollutant Distribution and Effects in Forests Adjacent to Smelters. Journal of Environmental Quality **13**:377-382.

Jackson, T. 1984. Effects of inorganic cadmium, zinc, copper, and mercury on methyl mercury production in polluted lake sediments. Environmental Impacts of Smelters:551-578.

Jackson, T. A. 1978. The biogeochemistry of heavy metals in polluted lakes and streams at Flin Flon, Canada, and a proposed method for limiting heavy-metal pollution of natural waters. Environmental Geology **2**:173-189.

Kelly, E. N., D. W. Schindler, P. V. Hodson, J. W. Short, R. Radmanovich, and C. C. Nielsen. 2010. Oil sands development contributes elements toxic at low concentrations to the Athabasca River and its tributaries. Proceedings of the National Academy of Sciences of the United States of America **107**:16178-16183.

McFarlane, G., W. Franzin, and A. Lutz. 1979. Chemical Analyses of Flin Flon Area Lake Waters and Precipitation, 1973 to 1977. Western Region, Fisheries and Marine Service, Canada Department of Fisheries.

McFarlane, G. A., and W. G. Franzin. 1980. An examination of Cd, Cu, and Hg concentrations in livers of northern pike, Esox lucius, and white sucker, Catostomus commersoni, from five lakes near a base metal smelter at Flin Flon, Manitoba. Canadian Journal of Fisheries and Aquatic Sciences **37**:1573-1578.

McMartin, I., P. J. Henderson, and E. Nielsen. 1999. Impact of a base metal smelter on the geochemistry of soils of the Flin Flon region, Manitoba and Saskatchewan. Canadian Journal of Earth Sciences **36**:141-160.

McMartin, I., P. J. Henderson, A. Plouffe, and R. D. Knight. 2002. Comparison of Cu-Hg-Ni-Pb concentrations in soils adjacent to anthropogenic point sources: Examples from four Canadian sites. Geochemistry: Exploration, Environment, Analysis **2**:57-74.

Miskimmin, B. M., J. W. Rudd, and C. A. Kelly. 1992. Influence of dissolved organic carbon, pH, and microbial respiration rates on mercury methylation and demethylation in lake water. Canadian Journal of Fisheries and Aquatic Sciences **49**:17-22.

National Pollutant Release Inventory. 2025. National Pollutant Release Inventory data search. Government of Canada.

Neff, M. R., S. P. Bhavsar, G. B. Arhonditsis, R. Fletcher, and D. A. Jackson. 2012. Long-term changes in fish mercury levels in the historically impacted English-Wabigoon River system (Canada). Journal of Environmental Monitoring **14**:2327-2337.

Nriagu, J. O., and H. K. Wong. 1983. Selenium pollution of lakes near the smelters at Sudbury, Ontario. Nature **301**:55-57.

Nriagu, J. O., H. K. T. Wong, and R. D. Coker. 1982. Deposition and Chemistry of Pollutant Metals in Lakes around the Smelters at Sudbury, Ontario. Environmental Science and Technology **16**:551-560.

Nriagu, J. O., H. K. T. Wong, G. Lawson, and P. Daniel. 1998. Saturation of ecosystems with toxic metals in Sudbury basin, Ontario, Canada. Science of the Total Environment **223**:99-117.

Outridge, P. M., N. Rausch, J. B. Percival, W. Shotyk, and R. McNeely. 2011. Comparison of mercury and zinc profiles in peat and lake sediment archives with historical changes in emissions from the Flin Flon metal smelter, Manitoba, Canada. Science of the Total Environment **409**:548-563.

Outridge, P. M., H. Sanei, G. A. Stern, P. B. Hamilton, and F. Goodarzi. 2007. Evidence for control of mercury accumulation rates in Canadian High Arctic Lake sediments by variations of aquatic primary productivity. Environmental Science and Technology **41**:5259-5265.

Pai, P., D. Niemi, and B. Powers. 2000. A North American inventory of anthropogenic mercury emissions. Fuel Processing Technology **65-66**:101-115.

Pip, E. 1991. Cadmium, copper, and lead in soils and garden produce near a metal smelter at Flin Flon, Manitoba. Bulletin of Environmental Contamination and Toxicology;(United States) **46**.

Pyle, G. G., J. W. Rajotte, and P. Couture. 2005. Effects of industrial metals on wild fish populations along a metal contamination gradient. Ecotoxicology and Environmental Safety **61**:287-312.

Roberts, S. L., J. L. Kirk, D. C. G. Muir, J. A. Wiklund, M. S. Evans, A. Gleason, A. Tam, P. E. Drevnick, A. Dastoor, A. Ryjkov, F. Yang, X. Wang, G. f. C. U. m. D. R. e. a. s. p. Lawson, M. Pilote, J. Keating, B. D. Barst, J. M. E. Ahad, and C. A. Cooke. 2021. Quantification of Spatial and Temporal Trends in Atmospheric Mercury Deposition across Canada over the Past 30 Years. Environmental Science and Technology **55**:15766-15775.

Rutila, E. C. 2018. Geochemical Fingerprinting of Metals from Non-Ferrous Smelting Emissions within Lake Sediments. M. Sc. Oregon State University.

Saha, S., K. Dhara, A. V. Chukwuka, P. Pal, N. C. Saha, and C. Faggio. 2023. Sub-lethal acute effects of environmental concentrations of inorganic mercury on hematological and biochemical parameters in walking catfish, Clarias batrachus. Comparative Biochemistry and Physiology Part - C: Toxicology and Pharmacology **264**.

Scheuhammer, A. M., and J. E. Graham. 1999. The Bioaccumulation of Mercury in Aquatic Organisms from Two Similar Lakes with Differing pH. Ecotoxicology **8**:49-56.

Scheuhammer, A. M., S. I. Lord, M. Wayland, N. M. Burgess, L. Champoux, and J. E. Elliott. 2016. Major correlates of mercury in small fish and common loons (Gavia immer) across four large study areas in Canada. Environmental Pollution **210**:361-370.

Scott, G. 2000. Soil acidity (pH) as influenced by point-source pollution from a base-metal smelter, Flin Flon, Manitoba. Prairie Perspect **3**:97-110.

Shuhaimi-Othman, M., D. Pascoe, U. Borgmann, and W. P. Norwood. 2006. Reduced metals concentrations of water, sediment and Hyalella Azteca from lakes in the vicinity of the sudbury metal smelters, Ontario, Canada. Environmental Monitoring and Assessment **117**:27-44.

Simmatis, B., K. M. Rühland, M. Evans, C. Meyer-Jacob, J. Kirk, D. C. G. Muir, and J. P. Smol. 2022. Metal contamination in alkaline Phantom Lake (Flin Flon, Manitoba, Canada) generates strong responses in multiple paleolimnological proxies. Science of the Total Environment **811**:152299.

Sun, R., H. Hintelmann, J. A. Wiklund, M. S. Evans, D. Muir, and J. L. Kirk. 2022. Mercury Isotope Variations in Lake Sediment Cores in Response to Direct Mercury Emissions from Non-Ferrous Metal Smelters and Legacy Mercury Remobilization. Environmental Science and Technology **56**:8266-8277.

Telmer, K., G. F. Bonham-Carter, D. A. Kliza, and G. E. M. Hall. 2004. The atmospheric transport and deposition of smelter emissions: evidence from the multi-element geochemistry of snow, Quebec, Canada1 1Associate editor: D. J. Vaughan. Geochimica et Cosmochimica Acta **68**:2961-2980.

Van Loon, J., and R. Beamish. 1977. Heavy-metal contamination by atmospheric fallout of several Flin Flon area lakes and the relation to fish populations. J. Fish. Res. Board Can.;(Canada) **34**.

Wiklund, J. A., J. L. Kirk, D. C. G. Muir, M. Evans, F. Yang, J. Keating, and M. T. Parsons. 2017. Anthropogenic mercury deposition in Flin Flon Manitoba and the Experimental Lakes Area Ontario (Canada): A multi-lake sediment core reconstruction. Sci Total Environ **586**:685-695.

Wren, C. D., and P. M. Stokes. 1988. Depressed mercury levels in biota from acid and metal stressed lakes near Sudbury, Ontario. Ambio **17**:28-29.

Zahran, E., A. Z. Mamdouh, S. Elbahnaswy, M. M. A. El-Son, E. Risha, A. ElSayed, M. I. E. Barbary, and M. G. E. Sebaei. 2025. The impact of heavy metal pollution: bioaccumulation, oxidative stress, and histopathological alterations in fish across diverse habitats. Aquaculture International **33**.

Zoltai, S. C. 1988. Distribution of base metals in peat near a smelter at Flin Flon, Manitoba. Water, Air, and Soil Pollution **37**:217-228.

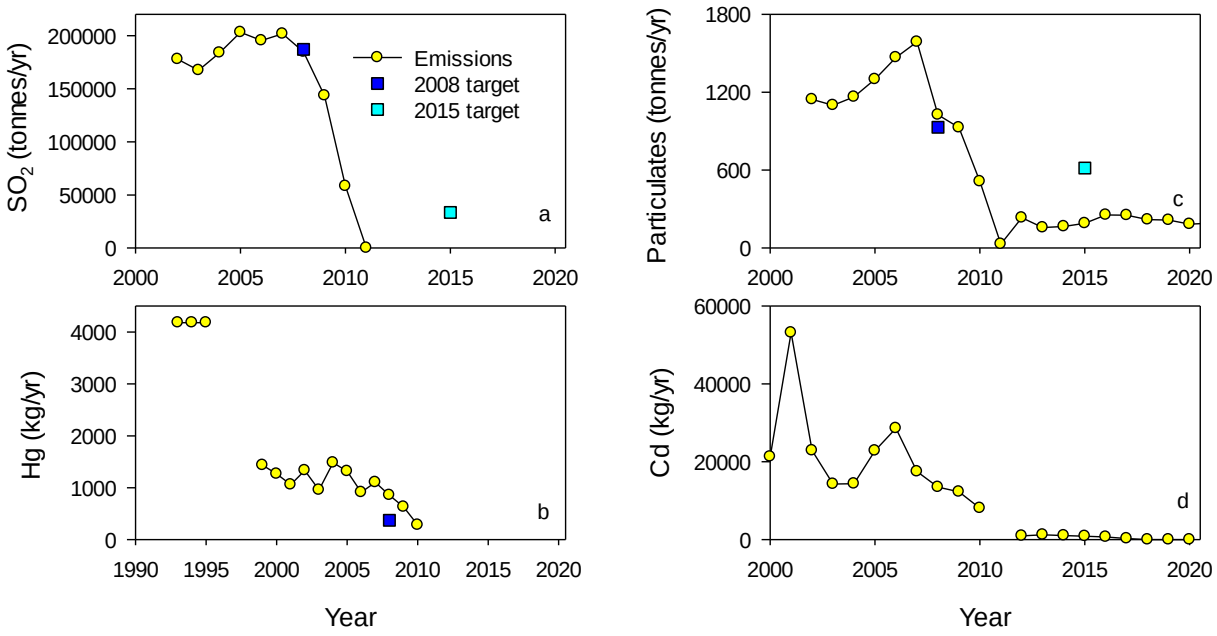

Figure 1. Declines in SO_2 (a), Hg (b), particulates (c) and Cd (d) emissions from the copper zinc smelter at Flin Flon, Manitoba. Also shown are the target reductions in SO_2 , Hg, and particulate emission targets by the Government of Canada (2006). No targets were set for metal other than Hg.

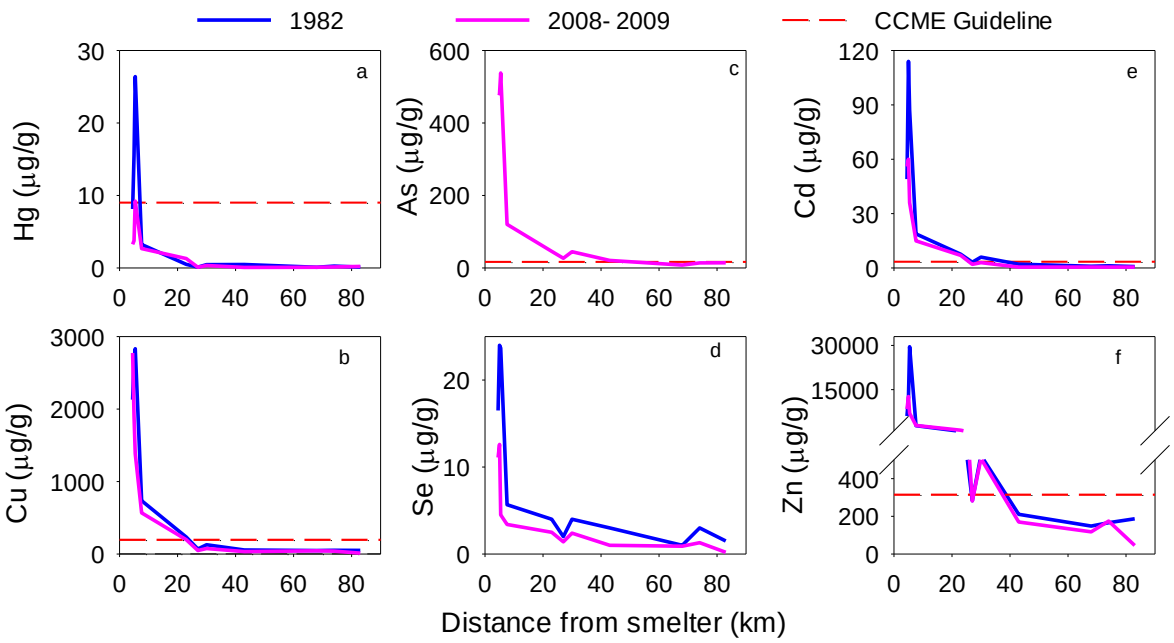

Figure 2. Metal concentrations in surface sediments in lakes at varying distances from the Flin Flon smelter as measured in 1982 by Harrison and Klaverkamp (1990) and in 2008-2009 by Evans et al. (In review). Arsenic (2c) was not measured in 1982. Also shown are the Canadian Council of Ministers of the Environment (2014) Probable Effects Guidelines for the protection of aquatic life in sediments. No guidelines have been established for selenium (Fig. 2 d).

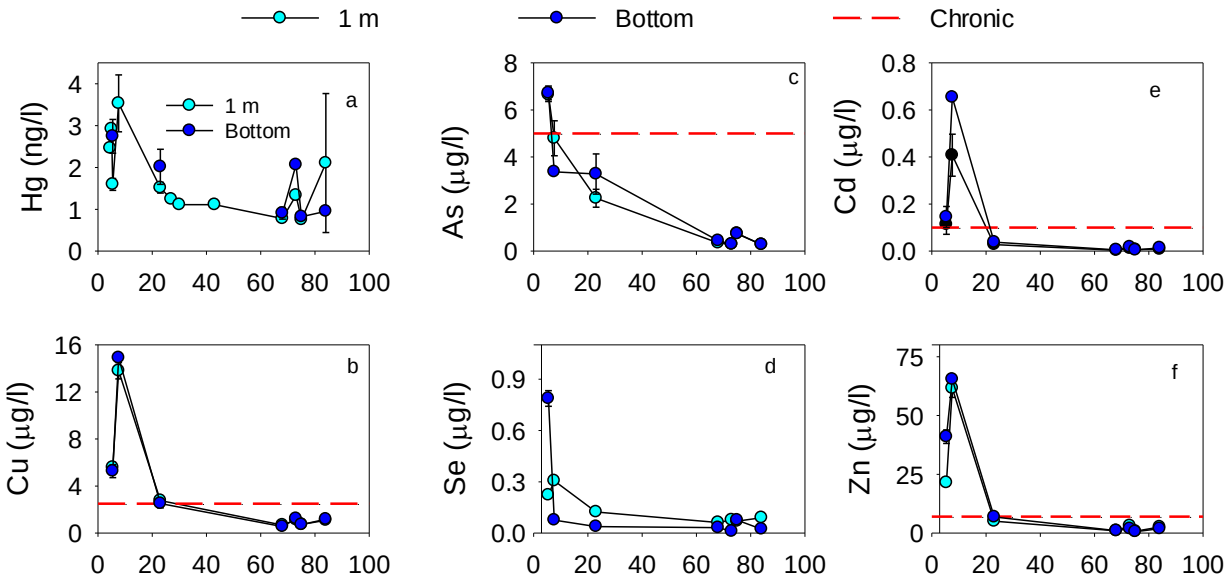

Figure 3. Surface and bottom water metal concentrations from six Flin Flon lakes, presented as averages and standard deviations measured on summer 2009-2016 field trips (Evans et al. In review). Also shown are the Canadian Council of Ministers of the Environment (2014) Chronic Guidelines for the protection of aquatic life in water. No guidelines have been established for selenium and mercury.

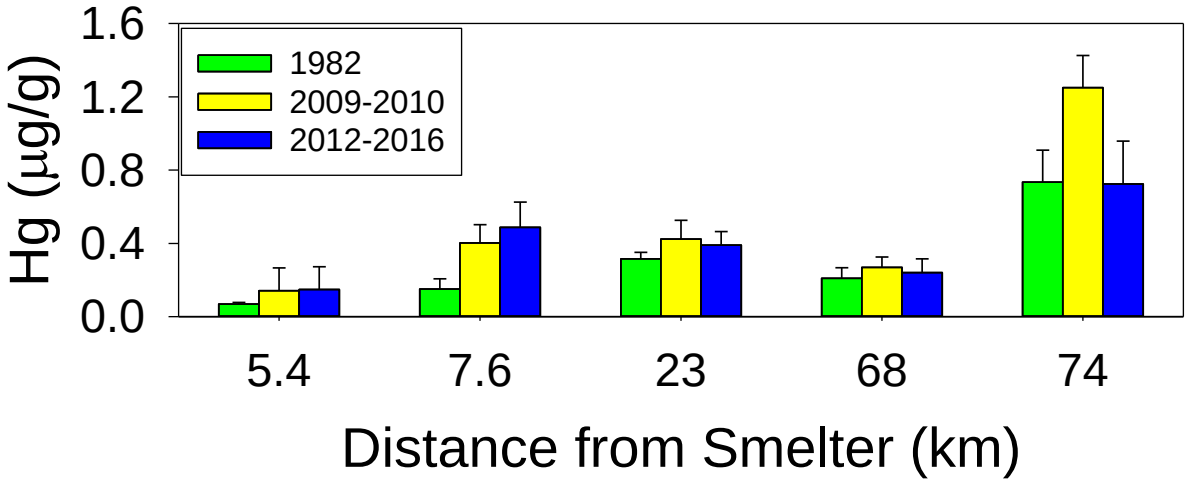

Figure 4. Spatial and temporal trends in mercury concentrations in length-adjusted (525 mm) northern pike fillet in lakes varying distance from the smelter during full smelter operation (1982), shorter before and during the closure of the copper smelter (2009-2010) and subsequent years (2012-2016). From (Evans et al. 2017).

Case study: Oceanic mercury monitoring in the East China Sea

Kohji Marumoto, Environmental Chemistry Section, National Institute for Minamata Disease (NIMD), Japan
Akinori Takeuchi, Strategic Risk Management Research Section, National Institute for Environmental Studies

Are the spatial patterns and temporal trends in Hg observed in soils, sediments, surface and ocean waters consistent with trends in estimated releases to land and water?

Information Used

On the northwestern edge of the Pacific Ocean, there are three marginal seas connected by warm currents branching off from the Kuroshio Current; the East China Sea, the East/Japan Sea, and the Sea of Okhotsk. These seas are important components of the marine system in the northwestern Pacific Ocean, influencing regional weather patterns and supporting diverse marine ecosystems. Especially, the East China Sea is one of the world's richest fishing grounds because its primary production is supported by nutrient supply from various processes, including atmospheric deposition, ocean currents, upwelling, eddies, river and groundwater inflows, and human activities [1,2]. One of the most representative toxic elements, mercury (Hg), exhibits varying toxicity depending on its chemical form. Among the Hg dissolved in seawater, the proportion of methylmercury (MeHg) —a highly toxic form—is several times higher in marginal seas than in the Pacific Ocean. One of the causes of this is the process by which Hg accumulated in shelf sediments as sulfides is methylated by microbial activity in reducing environments and transferred into the water column. We mainly focused on the Kuroshio Current region of the East China Sea, where data are scarce, and examined the vertical and horizontal distributions of dissolved Hg, particulate Hg, and dissolved MeHg in seawater and total Hg and MeHg in the planktons. In addition, Hg evasion fluxes were investigated using a two-layer gas exchange model [3].

Methodology

The sampling of seawaters and planktons for the measurement of total and methyl Hg and other parameters and the observation of air-sea exchange of Hg were performed for the Kuroshio Current region of the East China Sea during an oceanographic cruise (KH-15-3) on the R/V Hakuhou-Maru in October 2015, the survey at the offshore of Kumejima Island in March 2018 using a fishing craft Kiyo-Maru, and another oceanographic cruise on the R/V Kaimei in February 2022. Seawater was collected in a Niskin-X sampler with the protocol of clean technique recommended by the GEOTRACES program [4]. Future ocean surveys, the GEOTRACES-Japan cruise will be planned for the summer of 2028 in the marginal seas of East Asia including the East China Sea, Japan Sea and the Sea of Okhotsk.

Answer/Response

Hg distributions in seawaters and planktons

The total Hg concentrations in the deeper waters were higher than those in surface and subsurface waters. The MeHg concentrations were also higher in deeper waters than in surface waters, and the maximum concentrations were observed in the depth of 500 – 600 m at the several sites. The temperature – salinity diagram shows that North Pacific Intermediate Water (NPIW) flows in this depth. The highest MeHg concentrations in the NPIW were

observed in the other sea areas such as the eastern Pacific Ocean and Equatorial regions. Therefore, it is possible that the horizontal advection of NPIW relates to high MeHg concentrations at the study area. The total Hg and MeHg concentrations in planktons, which were collected using a plankton net with 100 μm of mesh size, were also measured. The both concentrations were higher in the Kuroshio current region than in the continental shelf region. This indicates the opposite phenomenon of bio-dilution because the Kuroshio current is well known to be oligotrophic and biomass is not abundant.

Time series trend of Hg in surface seawaters

In the East China Sea, Hydrographic and Oceanographic Department, Japan Coast Guard (JCG) have observed total Hg in surface seawaters every year [5]. As shown in Figure 1, the decreasing trend of Hg concentrations in surface seawater in the East China Sea as well as North Atlantic Ocean {6}. The collateral decreasing trend of atmospheric gaseous elemental Hg (GEM) at Cape Hedo, Okinawa was observed (Figure 2). In addition, the stronger decreasing trend of GEM was observed in warm season compared with that in the cold season, which air masses including some air pollutants from the Asian continent are transported to the monitoring site by westerlies and northwestern monsoons [7]. Therefore, one possible explanation on these decreasing trends is the influence of the interactions of air-sea exchange.

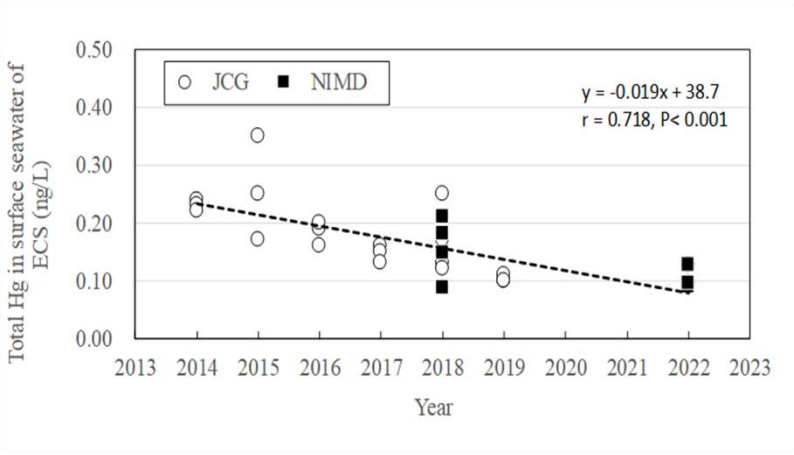

Figure 1 Long-term trends of total Hg in surface seawater of the East China Sea

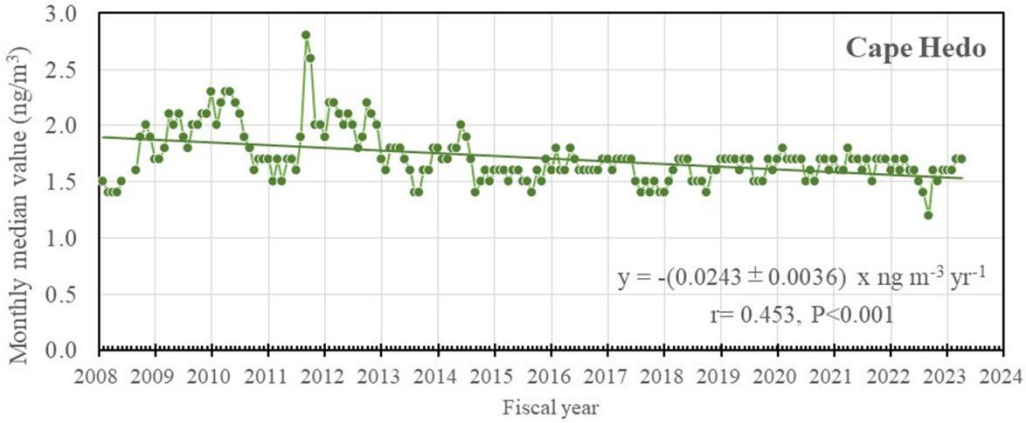

Figure 2 Long-term trends of atmospheric GEM concentration at Cape Hedo, Okinawa [7]

Reference

[1] Chen et al. (1999) JGR-Oceans 104, 20675; [2] Huang et al. (2019) Sci. Rep. 9, 5648; [3] Marumoto et al., (2018) Geochem, J. 52, 1-12. [4] Cutter et al. (2017) GEOTRACES cookbook v3 [5] JCG (2014-2022) REPORT OF MARINE POLLUTION SURVEYS [6] Lee et al. (2016) Environ. Sci. Technol. 2016, 50, 23, 12825–12830 [7] Marumoto et al., (2019) Atmosphere 10, 362.

Case Study:

Mercury in the Mediterranean Region and the Minamata Convention

Authors: Milena Horvat, Jože Kotnik, Igor Živkovič, Jan Gačnik, Oleg Travnikov, Adna Alilović, Janja Snoj Tratnik, Vanja Usenik, David Kocman, Ermira Begu

Department of Environmental Sciences, Jožef Stefan Institute, Slovenia

September, 2025, Ljubljana, Slovenia

Foreword

This document was prepared as part of the Open-Ended Scientific Group (OESG) process under the Minamata Convention on Mercury. During its March 2025 meeting in Minamata, Japan, it was suggested that representative case studies be presented to support discussions on regional mercury issues and their relevance to the Convention's effectiveness evaluation (Article 22).

The Mediterranean was selected as a case study due to its unique combination of natural and anthropogenic mercury sources, long legacy of mining and industrial activities, and strong cultural and economic reliance on seafood. Importantly, the region also benefits from decades of monitoring across environmental compartments and human biomonitoring, making it a valuable test case for understanding how mercury cycles through a semi-enclosed marine system and how international measures may translate into tangible environmental and health outcomes.

This case study does not attempt to review the full breadth of research on mercury in the Mediterranean—hundreds of scientific publications address this subject in detail. Instead, it provides a concise overview of key evidence and trends relevant to the Minamata Convention. It is intended as an accessible synthesis to inform discussions within the OESG and the broader Convention process.

Disclaimer

This document is provided as background information to support the work of the OESG. It is not an official publication of the Minamata Convention and does not represent the views or positions of the Conference of the Parties, the Secretariat, or individual Parties. The summary presented here is illustrative in nature and should not be interpreted as an exhaustive scientific assessment.

Table of Contents

1. Introduction

The Mediterranean is a region where the environment and everyday life are deeply connected. With more than 20 countries bordering its shores and nearly half a billion people living in its catchment, it is a place where seafood is not only a key source of food and income but also a cornerstone of culture. Yet this same connection to the sea brings challenges: mercury (Hg) contamination has long been a concern.

Part of the reason lies in the sea's semi-enclosed nature — water circulates slowly, so pollutants tend to remain and build up over time. Another factor is the region's complex mix of natural and human-related mercury sources. Volcanic activity and hydrothermal vents release mercury naturally, while centuries of mining, industrial development, and energy production have added further pressures.

Figure 1. *Mercury hotspots in the Mediterranean*

Location	Source of pollution
Alboran Sea and Ebro River Delta	atmospheric Hg, Almadén mine, industrial discharges, riverine sediments.
Rhône River Delta, Fos-sur-Mer	Rhône Valley industry, former chlor-alkali plants
Tyrrhenian Sea (Livorno, Piombino)	industrial areas and mining in Monte Amiata
Sicily – Milazzo, Augusta	petrochemical and chlor-alkali industries
Monteponi	Pb and Zn mining
Gulf of Trieste	historical discharges from the Idrija mine
Marano - Grado Lagoon	Idrija Hg mining, industrty
Mestre (Porto Marghera)	chlor-alkali industry
Ravenna	chlor-alkali industry
Kaštela Bay	former chemical industry
Neretva River delta	Secondary contamination from agriculture and river sediment
Pagaseti Bay	Industrial plants, refineries, small mines
Gulf of Antalya	Industry, agriculture
Iskenderun Bay	metallurgy, thermal power plants, fossil fuels
Haifa Bay	petrochemical industry, metallurgy, industrial discharges
Bizerte	Hg mining, petrochemical industry, phosphate industry
Gulf of Gabès	phosphate industry, Hg in fertilizers
Skikda Bay	petrochemical industry and old industrial zones

Figure 1 illustrates major Hg contamination hotspots across the Mediterranean region, together with their primary sources of pollution. The distribution highlights the so-called Mediterranean Hg belt, which includes areas affected by historical Hg mining, industrial discharges, and petrochemical activities. Notable sites include the Almadén mine (Spain), historically the world's largest source of mercury, and Idrija (Slovenia), where past mining activities contributed to Hg accumulation in the Gulf of Trieste and the Marano–Grado Lagoon. Additional industrial sources are located along the Rhône River delta and in northern Italy (Livorno, Piombino, Mestre, Ravenna), linked to chlor-alkali production and petrochemical industries. In southern Europe and North Africa, hotspots include Milazzo and Augusta (Sicily), Monteponi (Sardinia), and several coastal sites in Tunisia and Algeria (e.g., Bizerte, Gulf of Gabès, Skikda Bay), where mining, fertilizer production, and petrochemical activities have released substantial mercury loads. Eastern Mediterranean locations, such as

Kaštela Bay, the Neretva River delta, Iskenderun Bay, and Haifa Bay, further reflect contamination from chemical industries, agriculture, metallurgy, and fossil fuel use. Collectively, the map emphasizes the widespread but heterogeneous distribution of mercury sources, with legacies of mining and industry continuing to shape Hg inputs to Mediterranean coastal and marine environments.

The problem is particularly concerning because mercury, especially in the form of methylmercury, accumulates in fish and seafood. For a population with high seafood consumption, this translates into real human exposure, with vulnerable groups such as children and pregnant women most at risk. Some of the highest mercury concentrations in fish and in human biomonitoring data across Europe have been reported from this region.

At the same time, the Mediterranean offers something valuable: decades of monitoring have generated a relatively strong dataset compared to other regions. We have records of mercury in air, water, sediments, and marine organisms. While gaps remain, the breadth of information provides a solid foundation for and for advancing our understanding of mercury sources, cycling, and fate in a complex semi-enclosed marine system.

This makes the Mediterranean a particularly compelling case study for evaluating the effectiveness of the Minamata Convention on Mercury. The Convention seeks to reduce mercury pollution and its impacts on people and ecosystems. Here, in a region where those impacts are tangible and where data are available, we can begin to test whether policies are making a difference. If reductions are visible, the Mediterranean could serve as evidence of success; if not, the obstacles identified here could help guide efforts in other parts of the world. In this sense, the Mediterranean is more than a local concern — it is a globally relevant lens through which to understand how mercury moves through the environment and how international policy can make a difference.

2. Regional intergovernmental agreements supporting mercury monitoring and control in the Mediterranean

Mercury monitoring and control in the Mediterranean have been strongly shaped by regional agreements and EU policy instruments that translate global commitments, such as the Minamata Convention, into concrete action (Table 1). These frameworks not only provide legally binding obligations but also enable coordination across EU and non-EU countries, ensure coherence of measures, and sustain long-term monitoring. Importantly, a large body of data summarized in the following tables has been generated thanks to substantial support from national programmes and EU Framework-funded projects (e.g. GMOS, GMOS-Train, LIFE initiatives). This combination of governance and research investment has laid the scientific foundation for evaluating the effectiveness of mercury policies in the region.

Table 1. *Some key Regional intergovernmental agreements supporting mercury monitoring and control in the Mediterranean*

Agreement / Instrument	***Relevance***	***Key Contributions***
Barcelona Convention (UNEP/MAP) and Protocols	Main legally binding agreement for Mediterranean marine protection. Mercury addressed via the Land-Based Sources Protocol (LBS) and Strategic Action Programme (SAP MED).	▪ MED POL programme supports long-term contaminant monitoring (including Hg); ▪ Development of pollution reduction measures and National Action Plans (NAPs); ▪ Coordination across EU and non-EU Mediterranean countries
European Union (EU) legislation and policy instruments	EU regulatory and funding frameworks strongly influence Mediterranean mercury policies.	▪ EU Mercury Strategy & Regulation (2017/852), aligned with Minamata; ▪ Water Framework Directive (WFD): monitoring & reporting of Hg in water bodies; ▪ Marine Strategy Framework Directive (MSFD): Good Environmental Status (GES) with Hg in fish as indicator; ▪ Substantial funding for research projects (HBM4EU, GMOS, LIFE MERMED, etc...)
European Monitoring and Evaluation Programme (EMEP) under CLRTAP	Regional air pollution monitoring and modeling, including atmospheric mercury.	▪ Long-term Hg measurements at EMEP stations (e.g. Iskrba, Longobucco, etc...); ▪ Transboundary Hg deposition modeling for source attribution
OSPAR Commission (Northeast Atlantic)	Not Mediterranean-specific but provides methodologies adapted for use in EU/UNEP-MAP contexts.	▪ Tools and indicators for Hg in fish and sediments; ▪ Modeling approaches applied to Mediterranean assessments

3. Overview of available data across media

The Mediterranean is one of the few regions in the world where mercury has been studied across nearly all environmental and biological compartments — air, water, sediment, biota, and even human exposure. This gives researchers a rare opportunity to see how mercury moves through a regional system over time. But while the region is relatively data-rich, the coverage isn't even, and the quality varies depending on the media and the location.

3.1. Air

Air monitoring of mercury in the Mediterranean region has been established through only a few long-term stations, complemented by shorter field campaigns. Continuous measurements of gaseous elemental mercury (GEM) are available from EMEP and GMOS sites such as Iskrba (Slovenia), Longobucco and Monte Curcio (Italy), and Minorca (Spain). In addition to long-term EMEP/GMOS records (e.g., Iskrba, Longobucco, Monte Curcio, Minorca) showing background GEM ≈ 1.4–1.9 ng m^{-3} and gradual Northern Hemisphere declines, shipborne MED-OCEANOR campaigns (13 cruises, 2000–2017) provide basin-scale process evidence that strengthens the Mediterranean picture. Using standardized Tekran analyzer measurements with GMOS QA/QC and co-measured meteorology, these cruises found median GEM typically 1.0–1.8 ng m^{-3} and documented a post-2009 shift to lower means (≈ 1.5–1.6 ng m^{-3}), consistent with GMOS trends. Notably, the 95th-percentile GEM dropped from ~2.5 ng m^{-3} (pre-2009) to ~1.95 ng m^{-3} thereafter, while near-shore excursions (e.g., Rosignano Solvay, Naples, La Spezia, Ravenna, Trieste) remained evident and tied to local sources; offshore values were lower and steadier (Sprovieri et al., 2025).

Speciation/fractionation and sources. Particle bound Hg (PBM) was more variable than GEM and peaked near coastlines and known industrial areas; wildfire seasons likely contribute episodically and may gain importance under climate warming. Gaseous oxidized mercury (GOM) showed diurnal maxima around midday, indicating in-situ photochemical oxidation in the marine boundary layer; observations and modeling support bromine-mediated pathways linked to acidified sea-salt aerosols. Some extreme GOM events were associated with volcanic plumes (e.g., Aeolian Islands, Campanian Archipelago), while others reflected anthropogenic influence along coastal routes (Sprovieri et al., 2025).

Air–sea exchange context. Parallel dissolved gaseous Hg in water (DGM) measurements in surface and deeper waters (with DGM increasing with depth alongside nutrients and lower O_2) and gas-exchange calculations indicate a net gaseous Hg evasion of ~30 Mg yr^{-1} from the Mediterranean—consistent with basin budgets that diagnose a net atmospheric source (evasion > deposition). These campaigns also emphasize method needs: a community-accepted standard protocol for DGM to improve comparability, and GOM denuder intercomparisons (e.g., cation-exchange membranes vs. KCl denuders) so that the historical record can be re-interpreted quantitatively (Sprovieri et al., 2025).

Table 2: Atmospheric mercury monitoring stations in the Mediterranean region and their main characteristics

Station / Location	Country	Type of measurements	Time coverage	Notes
Iskrba (EMEP site)	Slovenia	GEM (gaseous elemental mercury)	Long-term	One of the few consistent regional time series used in Mediterranean assessments; part of EMEP.
Longobucco (GMOS site)	Italy (Calabria)	GEM; wet deposition	Since ~2011	GMOS background site; contributes to regional trends within GMOS QA/QC framework.
Monte Curcio (GMOS site)	Italy	GEM; ancillary meteorology	Since ~2011	Mountain background station for central Mediterranean; complements Longobucco.
Minorca (GMOS site)	Spain (Balearic Islands)	GEM	Since ~2011	Island background site extending western Mediterranean coverage.
MED-OCEANOR ship campaigns (Western & Eastern basins, incl. Adriatic)	Basin-wide	GEM, GOM, PBM (speciation); meteorology	2000–2017 (13 cruises)	Standardized Tekran speciation with GMOS QA/QC; median GEM typically 1.0–1.8 ng m–3; 95th percentile GEM fell from ~2.5 to ~1.95 ng m–3 after 2009; near-shore excursions and volcanic plumes evident; primary speciation basis for the Mediterranean.
Coastal campaign clusters (5 sites, 2003–2004)	Various coasts (W & E Mediterranean)	GEM, GOM, PBM (campaign-based)	Short campaigns	Higher Mediterranean GEM than Northern Europe; diurnal GOM maxima near midday consistent with in-situ photochemical oxidation; valuable process snapshots but not continuous records.

In terms of time trends, the observations show a gradual decline in GEM concentrations, consistent with broader Northern Hemisphere trends. Yet deposition data remain scarce, with only discontinuous wet deposition measurements, making atmospheric modeling essential for constructing regional budgets and assessing source contributions. EU-funded projects such as GMOS, GMOS-Train, Merc-Ox, have been instrumental in expanding the observational basis, harmonizing datasets, and linking measurements with models.

The **multi-model ensemble simulations (MCHgMAP)** for 2010–2020 (see Figure 2) further complement the limited observational record. These simulations indicate a statistically significant decrease in GEM, from about 1.5 to 1.4 ng m^{-3} (≈10% over the decade), with an average annual reduction of 0.015 ng m^{-3} per year. The estimated annual decrease of GOM and PBM is about 0.035 pg m^{-3} y^{-1}, corresponding to a 3% and 6% reduction over the period, respectively. In contrast, wet deposition showed no significant trend, while total atmospheric deposition to the Mediterranean Sea decreased by ≈5% (0.06 g km^{-2} yr^{-1}). These modeled results are broadly consistent with observed declines in GEM and provide basin-wide context that monitoring alone cannot yet deliver (Travnikov et al, 2025, personal communication).

Figure 2: *Simulated trends of atmospheric mercury concentrations and deposition in the Mediterranean basin (2010–2020) based on MCHgMAP multi-model ensemble*[*]

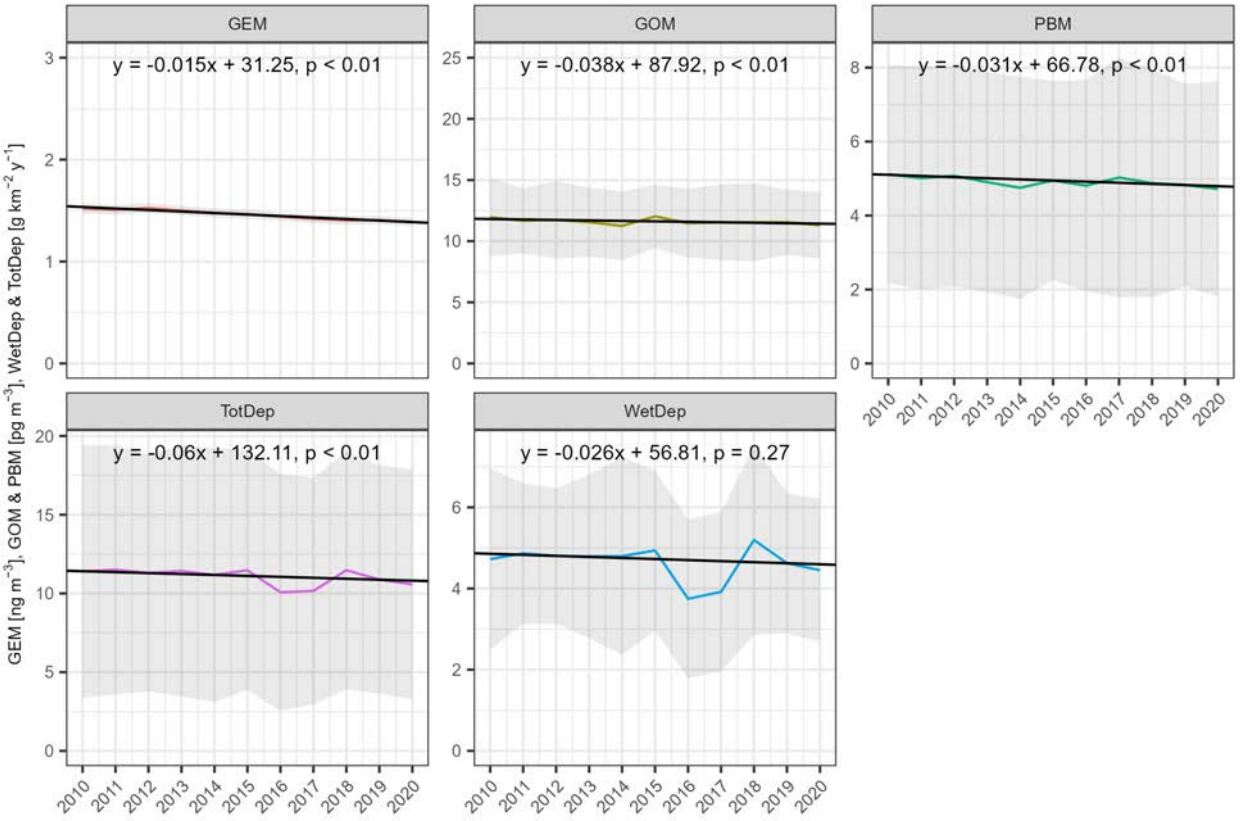

In summary, the Mediterranean has some of the best atmospheric mercury datasets globally thanks to EMEP and GMOS, but the geographical coverage remains uneven. Modeling and EU-funded research efforts are therefore critical for filling gaps and providing robust evidence to assess policy effectiveness under the Minamata Convention and regional frameworks.

3.2. Water and sediments

Water and sediments have been more intensively studied than air, particularly in the western Mediterranean basin. Measurements of total mercury (THg) and methylmercury (MeHg) in seawater and sediments provide insights into historical inputs, ongoing cycling, and long-term burial processes. However, the geographical distribution of studies remains uneven, with the eastern and southern basins comparatively under-sampled.

3.2.1. Mercury in seawater

Concentrations of THg and MeHg in Mediterranean seawater exhibit marked spatial and temporal variability. Figure 3 synthesizes the GMOS ship campaigns (2000–2015) and shows that offshore surface THg clusters in the ~200–470 pg L^{-1} envelope across most of the basin, with localized

[*] *The simulations indicate a statistically significant decline in GEM, reactive mercury species (GOM, PBM), and total deposition, while wet deposition shows no significant trend.*

hotspots in the western Mediterranean and the northern Adriatic/Gulf of Trieste, where riverine/legacy influences elevate concentrations. Surface MeHg is patchier (typically ~8–40 pg L^{-1}) and increases below the mixed layer; depth profiles reveal a thermocline/intermediate maximum (order ~50–150 pg L^{-1}) and occasional near-bottom rises consistent with diffusive sediment fluxes. These patterns align with the updated ranges (Table 3) and reinforce the mechanistic view: enhanced in-basin transformations (methylation at intermediate depths; photoreduction at/near the surface) and elevated DGM at depth, to which natural geogenic inputs (hydrothermal/volcanic seepage and tectonically driven degassing along seismically active margins) can contribute.

What is distinctive is the speciation presented in Table 3. The fraction of THg present as methylmercury (MeHg) and as dissolved gaseous mercury (DGM) is consistently higher than other oceans, especially below the surface. At the surface, MeHg is typically ~8–32 pg L^{-1} (≈ 3–10% of THg) and DGM ~12–106 pg L^{-1} (≈ 5–20% of THg). In the thermocline/intermediate layer—the Mediterranean's main MeHg production zone—MeHg rises to ~20–180 pg L^{-1} (means ~90 pg L^{-1}; ≈ 15–40% of THg) and DGM commonly reaches ~32–94 pg L^{-1} (≈ 15–30% of THg). These elevated MeHg and DGM fractions point to faster or more efficient in-basin transformations—enhanced methylation at intermediate depths and photoreduction at/near the surface—driven by warm, saline, stratified waters, intense remineralization/low-O_2 layers, and reactive halogen chemistry in the marine boundary layer. Additionally, natural (geogenic) Hg inputs—hydrothermal/volcanic seepage and tectonically driven degassing along faulted, seismically active margins—can inject reduced Hg into deeper waters, sustaining DGM maxima and feeding in-situ MeHg formation.

Figure 3: *Spatial distribution of total mercury (THg) and methylmercury (MeHg) in Mediterranean seawater during GMOS ship campaigns (2000–2015), highlighting hotspots in the Gulf of Trieste, Adriatic, and western basin (Kotnik et al., 2014).*

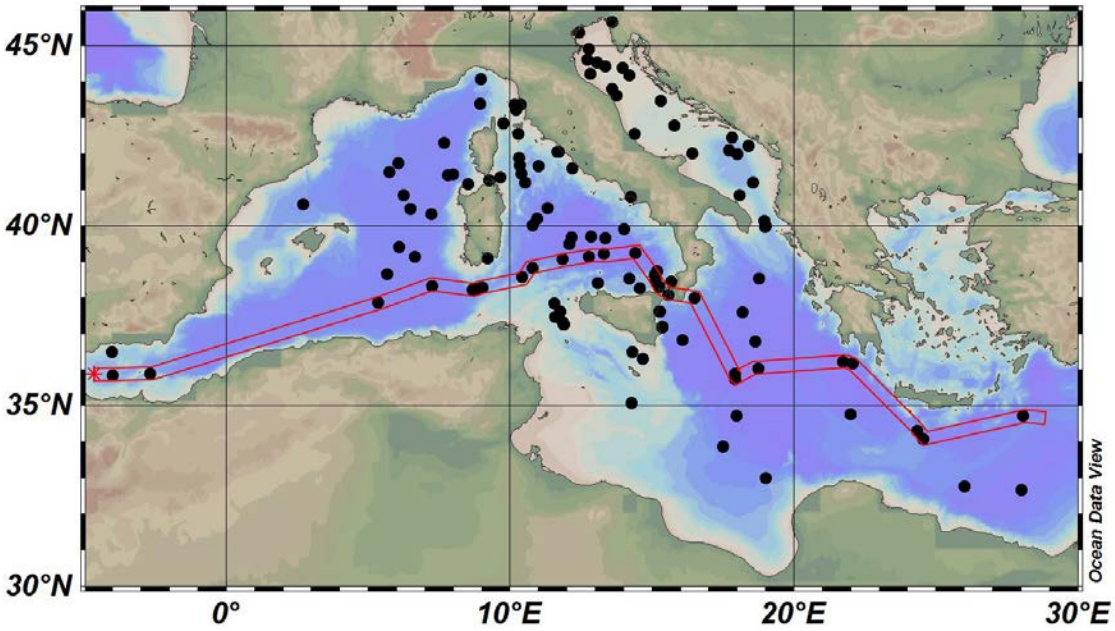

Note: Sampling locations of surficial and vertical profiles. All GMOS cruises together 2000 – 2015. The red line shown in Figure 3 marks a representative transect where vertical depth profiles of total mercury (THg) and methylmercury (MeHg) were collected. These depth profiles are presented in the following figures, providing detailed insight into how concentrations vary with depth compared to the basin-scale surface distributions illustrated here (Kotnik et al., 2014).

Total Hg in surface waters (ng/L)

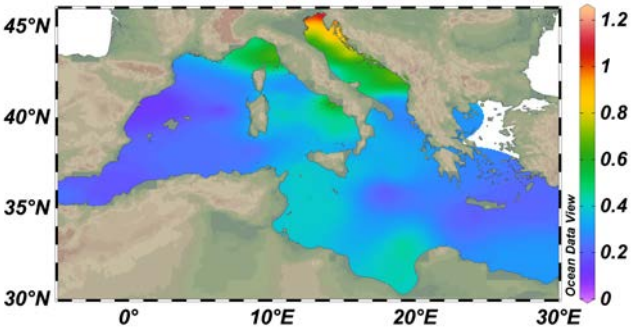

MeHg in surface waters (pg/L)

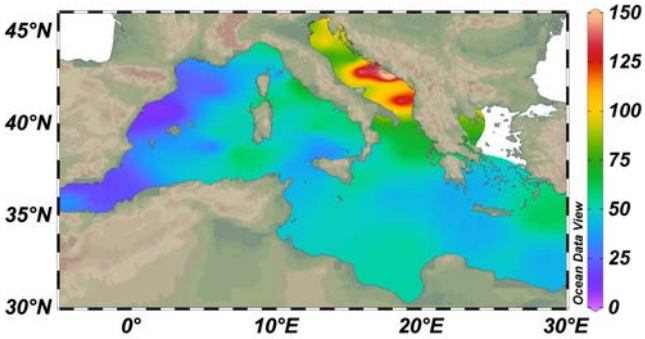

Total Hg in depth profiles (ng/L)

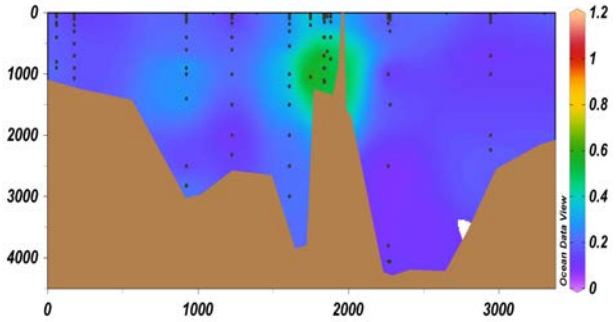

MeHg in depth profiles (pg/L)

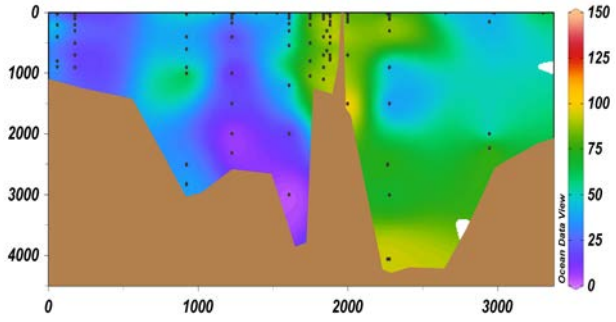

Table 3: *Total and MeHg concentrations in seawater of the Medietrranena in comparison to Atlantic Pacific waters*

Region / Layer	**THg** (pg/L) **range**	**THg** (pg/L) **mean**	**MeHg** (pg/L) **range**	**MeHg** (pg/L) **mean**	**%THg as MeHg** (range)	**%THg as MeHg** (mean)	**DGM** (pg/L) **range**	**DGM** (pg/L) **mean**	**%THg as DGM** (range)	**%THg as DGM** (mean)
Mediterranean — Open sea (surface)	162–467	0.29	8–32	15	2.7–11	**5.1**	12–106	40	**4.1–36**	13.7
Mediterranean — Thermocline / intermediate	162–467	0.29	19–177	91	6.4–60	**31**	32–94	60	**11–32**	20.5
Mediterranean — Deep (>1,500 m)	162–467	0.29	22–112	62	7.5–38	**21**	32–94	70	**11–32**	24.0
Atlantic/Pacific — Open ocean (surface)	161–401	0.24	5–15	8	2.1–6.2	**3.3**	6.0–20	10	**2.5–8.3**	4.1
Atlantic/Pacific — Thermocline	161 –401	0.24	20–60	40	8.3–253	**16.6**	14–30	20	**5.8–12**	8.3

Because MeHg is the bioaccumulative form, a higher MeHg/THg ratio in seawater translates into more MeHg available to food webs, helping explain why several Mediterranean top-predator fish remain above EU Hg thresholds even when bulk THg in water is not exceptional. In short: the Mediterranean differs less in how much mercury it has than in how quickly and efficiently it turns that mercury into MeHg and DGM forms - a reactivity signal that ultimately shows up as higher MeHg in fish and elevated human exposure in high-seafood, coastal populations.

Time trends:

At the scale of the open Mediterranean, no robust multi-decadal trend in dissolved THg has been detected from compiled profiles; however, boundary waters show a significant decline: between 1989 and 2012, THg decreased by ~30% in the deep outflow from the Mediterranean and by ~50% in the Atlantic inflow (Strait of Gibraltar sections). For MeHg, repeated sections (e.g., Ligurian Sea) reveal interannual variability and tight coupling to oxygen consumption in the thermocline rather than a monotonic trend (Cossa et al., 2022). Taken together, the present evidence supports process-driven fluctuations overlaid on stable basin-average THg, with the clearest trend signal appearing at the Atlantic–Mediterranean boundary. At the same time, observations and a basin 3-D model agree that MeHg variability is process-driven: a subsurface (thermocline) maximum builds under summer stratification and is redistributed/diluted by winter deep convection. The model further indicates that weaker winter convection under warming tends to raise MeHg in the biologically active zone, increasing lower-trophic exposure (BCF/TMF), even without large changes in bulk THg (Rosati et al., 2022).

3.2.2. Mercury in sediments

Surface sediments in the Mediterranean Sea display marked spatial heterogeneity in both total mercury (THg) and methylmercury (MeHg) concentrations. Among the different sub-basins, the Adriatic Sea emerges as the most contaminated area, with THg levels reaching up to ~1000 ng g^{-1} and MeHg concentrations up to 5 ng g^{-1}. These exceptionally high values are largely a consequence of the Idrija mercury mine in Slovenia, historically one of the world's largest, as well as downstream industrial and urban activities that have contributed to mercury enrichment in sediments. The semi-enclosed nature of the Adriatic, together with limited water exchange, further enhances the persistence and accumulation of mercury in this basin.

In comparison, sediments from the eastern Mediterranean basin are characterized by substantially lower contamination, with THg generally ≤100 ng g^{-1} and MeHg <2.5 ng g^{-1}. This pattern reflects both the reduced historical inputs of mercury and the oligotrophic conditions of the basin, which limit the availability of organic matter that can promote mercury methylation. The western Mediterranean basin shows intermediate conditions, with spatially variable but notable concentrations (THg up to ~75 ng g^{-1}; MeHg ~3 ng g^{-1}). These values indicate localized anthropogenic influences, including industrial discharges and riverine inputs, superimposed on natural background levels.

Taken together, these spatial contrasts highlight the strong influence of historical mining legacies, regional hydrography, and biogeochemical processes on mercury distribution across Mediterranean sediments. The persistence of elevated concentrations in the Adriatic underscores the long-term impact of past industrial activities, while the relatively moderate to low levels in the eastern and western basins illustrate the heterogeneity of mercury contamination and the need for region-specific assessments and management strategies (Cossa et al., 2022).

Sediment cores provide a historical perspective: mercury accumulation increased markedly during the early 20th century, peaking during the post-war industrial boom, and has since stabilized or declined slightly in many locations. Current burial fluxes are estimated at ~5.8 Mg yr^{-1} in deep-sea sediments and ~6.8 Mg yr^{-1} on continental shelves, confirming the importance of sediments as a long-term sink for mercury in the basin (Cossa et al., 2022).

Figure 4: *Sediment core profiles showing historical mercury accumulation trends across Mediterranean basins: Total Hg concentration (THg) profiles in sediment cores from the abyssal plain (bottom >2000 m) of the Western Mediterranean (A) and Eastern Mediterranean (B). (DYC) Ligurian Sea;103 (WP13, W1B, 16 and 17) Algero-Provençal basin; (E1A and E1B) Ionian Sea; (WP5) Levantine Sea (adopted from Cossa et al., 2022)*

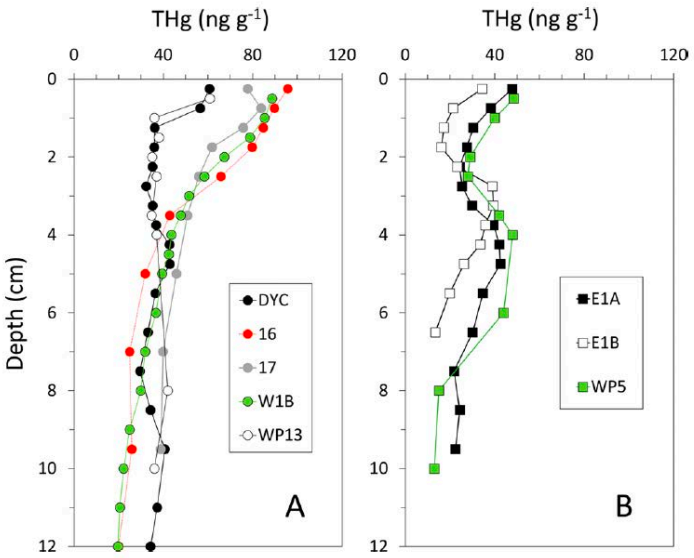

In the Minamata Convention monitoring guidance, mercury stable isotopes are a higher-tier/advanced tool used when we need source attribution and process diagnostics rather than just concentrations. Ogrinc et al,2029, demonstrated that in In Mediterranean sediments, **isotope fingerprints** consistently show positive odd-mass MIF (Δ^{199}Hg, Δ^{201}Hg) with near-zero Δ^{200}Hg—evidence that mercury underwent sunlight-driven reactions in seawater before burial—while δ^{202}Hg (MDF) varies with source mix and post-burial processing. Simple δ^{202}–Δ^{199} mixing indicates that gaseous elemental mercury (GEM) dry deposition dominates the atmospheric contribution to recent surface sediments (with site-dependent wet deposition and industrial/urban inputs). Down-core, isotopes reveal site-specific histories (post-industrial enrichment at some locations, volcanic/tectonic signals at others) and help separate true source changes from diagenetic shifts, so the record supports process-driven variability rather than a single basin-wide trend. For

example, a simple δ^{202}–Δ^{199} mixing model resolves site-specific source patterns: industrial Hg dominates in Algerian and Western Basin surface sediments and at two Adriatic sites, whereas urban contributions are highest at the Strait of Otranto and across other Adriatic surfaces; precipitation contributes ~10–37% depending on location. Basin-wide, the atmospheric share to recent sediments is mostly GEM dry deposition (~58 ± 11%), not wet deposition—consistent with a Med system where air–sea exchange and strong photochemistry shape the record; Levantine sediment behaves as a low-Hg, background end-member. Together, these isotope constraints add who/where/how context to concentration data and make time-trend interpretation more robust by separating true source shifts from post-depositional effects.

In summary, seawater and sediment studies highlight the heterogeneous nature of mercury cycling in the Mediterranean. Local hotspots (Figure 1), such as the Adriatic Sea and Gulf of Trieste, reveal the long-lasting legacy of historical mining and industrial activity, while western basin sites illustrate more recent variability linked to industrial discharges and riverine inputs. The eastern and southern Mediterranean remain under-sampled, creating uncertainties in basin-wide budgets.

Future efforts should focus on integrating seawater and sediment observations with models to better constrain fluxes and assess the effectiveness of policy interventions under the Minamata Convention.

3.3. Biota

Biota represents one of the largest Hg datasets, particularly for larger, commercially important fish species like tuna, swordfish, mullets, and hake. In many cases, these species have Hg concentrations that exceed EU regulatory thresholds for safe consumption (European Commission, 2023). There is also a fair amount of data on invertebrates, seabirds, and marine mammals. However, we still lack good coverage of the lower levels of the food web, i.e., plankton, which is essential for understanding how MeHg enters and moves up the trophic chain.

The observations presented here are part of a wider effort to consolidate long-term mercury measurements, as demonstrated in Global mercury concentrations in biota, their use as a basis for a global biomonitoring framework (Evers et al., 2024) and Mercury concentrations in biota in the Mediterranean Sea, a compilation of 40 years of surveys (Cinnirella et al., 2019), which highlight the value of harmonized datasets for trend detection and policy evaluation.

Concentrations of Hg across biological compartments in the Mediterranean region reveal both spatial and temporal dynamics relevant to the assessment of Minamata Convention targets. Long-term monitoring of *Mullus* spp., a widely distributed demersal fish, provides one of the most consistent datasets available for the Mediterranean region. Average THg concentrations compiled from 1974 (Figure 5) indicate pronounced geographic heterogeneity, with hotspots often aligning with known sources of anthropogenic contamination in (semi)enclosed bays, like the Adriatic.

Figure 5. *Average THg concentrations (in µg/g wet weight) in fish Mullus spp. across the Mediterranean Sea. Data range from 1974 – 2025.*

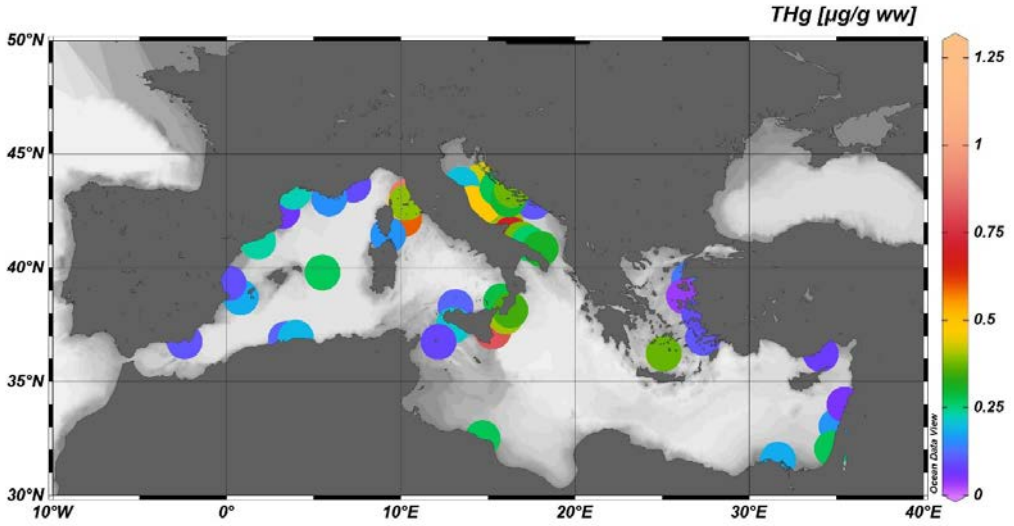

When pooled into broader time intervals (decades), the *Mullus* spp. records provide insight into long-term dynamics. The box-and-whisker plots (Figure 6) reveal modest reductions in median THg concentrations in recent decade, suggesting that regulatory and emission control measures may have contributed to gradual declines in Hg content. However, certain high values (outliers) indicate that localized contamination sources and site-specific factors continue to govern Hg content in fish.

Figure 6. *Box-and-whiskers plots (5, 10, 25, 50, 75, 90, and 95th percentile) of the average THg concentrations (in µg/g wet weight) in fish Mullus spp. from the Mediterranean Sea, pooled in four time periods.*

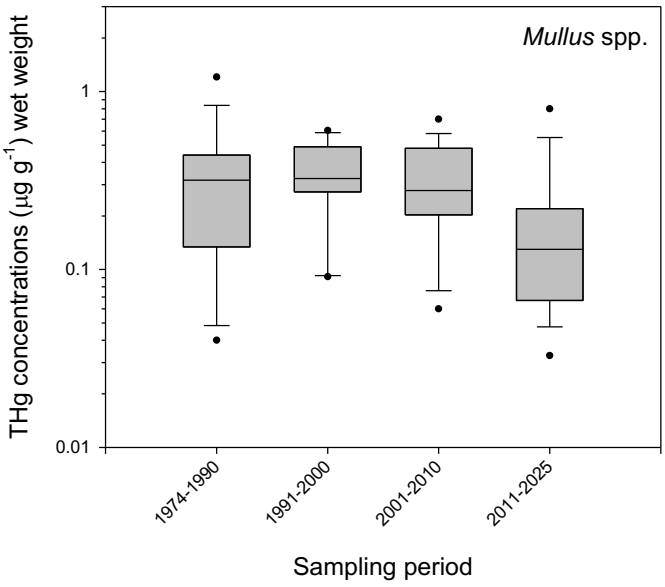

Comparative analyses of 58 fish species highlight how Hg data are distributed across trophic levels. The availability of data beyond commercially important fish species offers a greater insight into Hg distribution within Mediterranean food webs. The strong correlation between MeHg

concentrations and trophic position (Figure 7) highlights the extent of MeHg biomagnification within regional food webs. Fish species at the top of the food webs commonly have elevated MeHg concentrations and are therefore commonly monitored in the context of human exposure to Hg (e.g., tuna).

Figure 7. *Correlation of the average MeHg concentrations (in µg/g wet weight) in 58 fish species from the Mediterranean Sea with the trophic level of the fish species.*

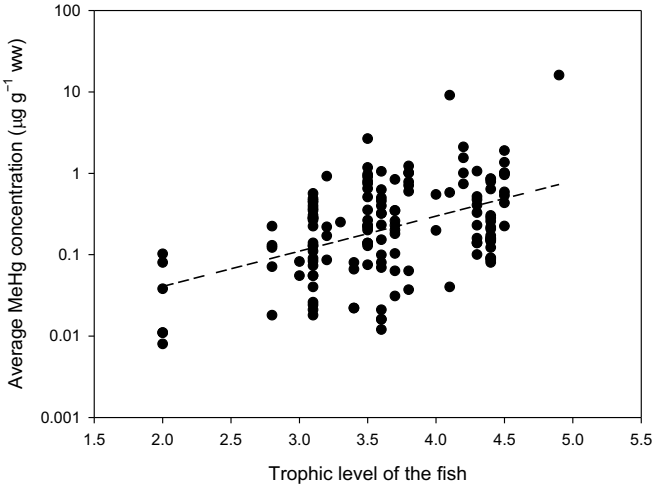

At lower trophic levels, data from Adriatic zooplankton (Figure 8) show the variability of Hg concentrations across space and time, reflecting both natural gradients and proximity to natural and anthropogenic inputs (e.g., the Gulf of Trieste in the Northern Adriatic). Changes in THg concentrations with time in the Adriatic zooplankton are considerable. The decrease in natural and anthropogenic Hg inputs (closure of Idrija mine and chlor-alkali plants) is responsible for an approximately 10-fold decrease in zooplankton THg (Živković et al., 2017). While slight downward temporal trends are seen in certain fish species (Figure 6), the base of the food web remains a dynamic reservoir of Hg inputs to higher trophic levels.

Figure 8. *Box-and-whiskers plots of the geographical distribution of THg in zooplankton from the Adriatic Sea. Figure from (Živković et al., 2017).*

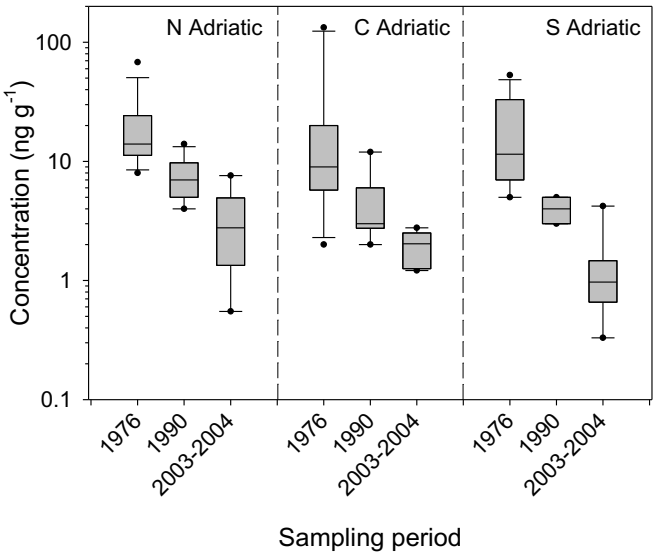

A broader perspective emerges when Mediterranean data are compared to other world seas (Figure 9). While MeHg concentrations in zooplankton are broadly similar to those in other basins, the proportion of THg occurring as MeHg is notably higher in the Adriatic (Živković et al., 2017). This suggests that regional conditions favor more efficient Hg methylation, thereby sustaining elevated risks of Hg transfer to higher trophic levels.

Figure 9. *Comparison of recent THg and MeHg concentrations and percentage of THg as MeHg in zooplankton from different world seas. Figure from (Živković et al., 2017).*

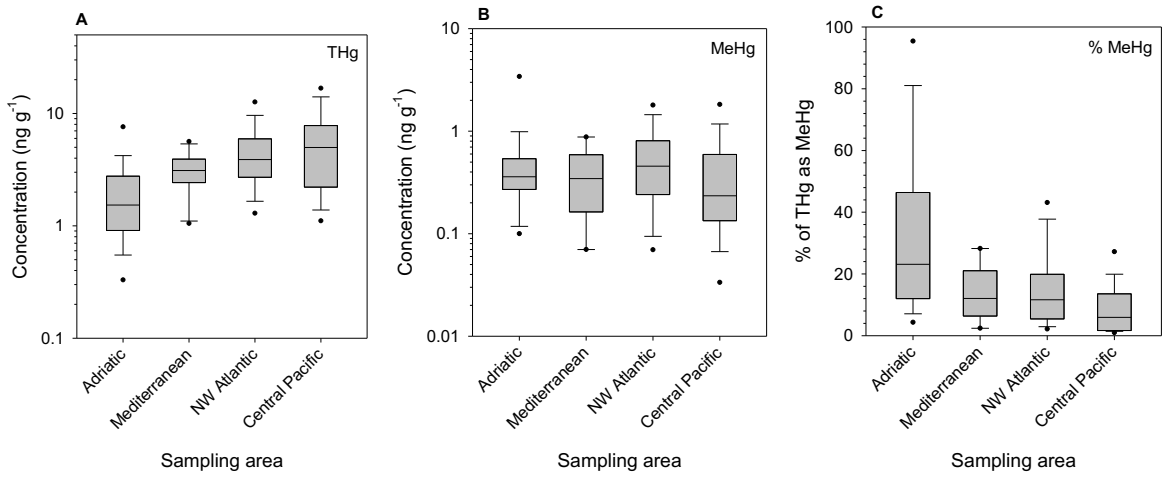

The integration of fish and zooplankton datasets therefore reveals a consistent trend: even as declines in certain fish species hint at regulatory progress, the base of the food web remains an active and efficient source of MeHg to the ecosystem.

3.4. Human biomonitoring

Human exposure to mercury is commonly assessed using hair, urine, blood and cord blood; the choice of biomarker depends on source, chemical form and life stage. The organic form, methylmercury (MeHg), is a potent neurotoxicant with the developing fetus as the most sensitive life stage; for the general population, fish and seafood consumption is the dominant exposure pathway, with other sources contributing far less by comparison. Spatial differences in human exposure within Europe largely track seafood intake and the biogeochemistry of regional seas. In the Mediterranean (MED), efficient MeHg production and transfer through food webs, and the frequent exceedance of EU thresholds in several top-predator species, sustain comparatively higher exposure potential while calling for risk communication that preserves the nutritional benefits of fish rather than discouraging consumption outright (Katsouri et al., 2024).

As part of the OESG process the new compilation of Human biomonitoring (HBM) data from national and European campaigns over ~2000–2024 (hair, blood, and cord blood) reveal clear geographic patterns in mercury exposure across Europe that align with seafood consumption and coastal residence. Figure 10 synthesizes these studies by mapping total mercury (THg) in hair (■),

blood (●), and cord blood (▲), with concentration classes harmonized for visual comparison. For interpretation across biomarkers we apply commonly used conversion anchors—~250 for hair:blood and ~1.7 for cord:maternal blood—which facilitate pattern recognition without altering original reported values. The map shows a denser occurrence of higher categories along Mediterranean and Atlantic littorals (e.g., Iberia, Italy, parts of Greece), consistent with diet-driven methylmercury (MeHg) exposure.

Across adults, Mediterranean cohorts more often sit in higher concentration classes than inland populations. Examples include Spain, where national and regional studies report blood medians ≥3.3 ng mL^{-1} and hair medians near 2.0 µg g^{-1} in high-consumption areas (e.g., Valencia, Barcelona), versus generally lower values in central/northern Europe. Similarly, coastal Italy (e.g., Sicily, Trieste) shows elevated central tendencies, while inland Slovenia's DEMOCOPHES mothers are typically lower (hair GM ~0.23 µg g^{-1}).

Among children and adolescents, Mediterranean datasets again skew higher than inland comparators: Spanish schoolchildren in the Valencian region show hair GMs around 0.79–0.88 µg g^{-1}, whereas DEMOCOPHES series report lower medians in Slovenia (0.17 µg g^{-1}) and Switzerland (0.08 µg g^{-1}). Greek RHEA cohorts report child blood medians of 0.69–0.73 ng mL^{-1}.

Pregnancy and newborn indicators confirm this gradient. Cord-blood medians reach 6.2 ng mL^{-1} in Greek island cohorts and4.0 ng mL^{-1} in Trieste, with lower central values in Slovenia (1.7 ng mL^{-1}) and intermediate levels in Tarragona, Spain (2.8 ng mL^{-1}). Such differences follow frequency and type of local seafood consumption.

Figure 10. *Total mercury (THg) in European human biomonitoring (HBM) studies, 2000–2024: hair, blood, and cord blood.*

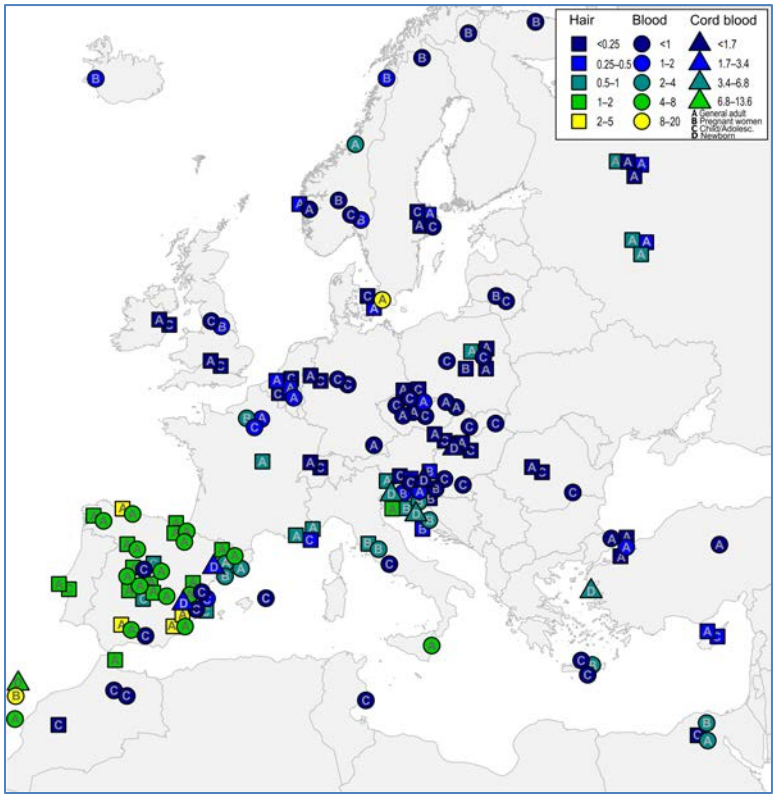

Note: Symbols denote biomarker type (■ hair, ● blood, ▲ cord blood); colours indicate concentration classes as shown in the legend (hair in µg g^{-1}; blood and cord blood in ng mL^{-1}). Letters inside symbols mark study population groups (A–D; see legend). The compilation integrates national and European campaigns over ~two decades and highlights a coastal gradient, with more frequent higher categories in Mediterranean and Atlantic littoral regions compared with inland and northern Europe—consistent with diet-driven exposure patterns. Sources: compiled HBM datasets and published campaigns summarised in the accompanying table and prior European/Mediterranean reviews.

Although fish consumption is the main source of MeHg exposure, it is also an important source of omega-3 fatty acids and other nutrients essential for neurodevelopment (Inoue et al., 2023; Starling et al., 2015). Exposure management should therefore focus on risk–benefit optimization via species-specific advice for vulnerable populations (e.g., pregnant women), rather than discouraging fish consumption altogether. HBM4EU-MOM (MethylMercury-contrOl in expectant Mothers through suitable dietary advice for pregnancy), a multicenter randomized trial, operationalized this principle at the science–policy interface in five coastal countries with high fish consumption (Cyprus, Greece, Iceland, Portugal, Spain). At baseline, seafood intake averaged ~8 meals per month, reaching ≥15 in Portugal and ≥7 in Spain, with frequent consumption of large oily fish (Portugal 89%, Spain 85%; Katsonouri et al., 2023). This trial provides a framework for linking HBM with harmonized, species- and portion-specific dietary advice in prenatal care, offering a template for future Article 22 effectiveness evaluations to complement long-term surveillance.

The multi-decade window captured by these studies, together with earlier works, supports the feasibility of Article 22 effectiveness evaluation under the Minamata Convention: repeated, harmonized human biomonitoring can identify population-level correlations with specific drivers (e.g., dietary guidance, reductions in dental amalgam use) and detect shifts in dominant exposure pathways. Spatial analyses, especially in Mediterranean and coastal regions, highlight sustained diet-linked exposure signals and underscore the importance of continued monitoring in pregnancy and early life.

4. Cross-media integration and observed trends

A consistent basin-scale picture emerges when atmospheric, oceanic, sedimentary, biotic and human biomonitoring (HBM) evidence are viewed together. Since the early 2000s, three independent mass-balance efforts—an early, model-driven **THg** budget for the whole Mediterranean, a layer-resolved update including the first **MeHg** budget, and a recent observation-constrained reassessment—converge on the same qualitative features: **(i)** air–sea exchange dominates the Hg cycle and the basin behaves as a **net atmospheric source** (evasion > deposition); **(ii)** there is a **net export at Gibraltar**, especially for MeHg; and **(iii)** the overall mass budget is near balanced, implying a slow long-term decline in the basin Hg pool as atmospheric and boundary losses slightly exceed inputs.

Basin mass balance through time. The first Mediterranean-wide budget (Rajar 2007) used a coupled hydro-atmospheric modelling framework and early 2000s observations to close the THg cycle. It already placed air–sea exchange as the dominant term (evasion ~50 Mg yr^{-1}, deposition ~23 Mg yr^{-1}) and found outflow > inflow at Gibraltar by ~41 kmol yr^{-1}, i. e. a small, positive net export consistent with slow recovery (Rajar et al, 2007). Building on new measurements and process understanding, Žagar et al. 2014 re-cast the budget into three water-column layers (surface, thermocline, deep), added deep-water formation/upwelling, and produced the first approximate MeHg budget. In that framework, the sign of THg exchange at Gibraltar can be small and sensitive, but MeHg export is robust, reflecting substantial in-basin methylation and transfer to the outflow. The recent Critical Review (Cossa et al., 2022) tightened magnitudes with updated concentrations and transports, confirming net THg export ≈ 1.9 Mg yr^{-1} and MeHg export ≈ 1.35 Mg yr^{-1}, while keeping air–sea evasion in the ~50–100 Mg yr^{-1} envelope with wet+dry deposition each ~20 Mg yr^{-1} (Figure 11).

Atmosphere–ocean coupling. Long-range transport and regional sources supply deposition to the basin, but warm, sunlit surface waters favour reduction to Hg^0 and evasion, sustaining a fast two-way flux that makes the Mediterranean both a sink **and** an efficient re-emitter to the free troposphere—hence the persistent net atmospheric source diagnosed in all three budgets.

Water column, sediments, and legacy signals. Open-water THg and MeHg display coherent spatial structure and depth maxima associated with low-oxygen layers (high methylation capacity), while sediment archives track 20th-century enrichment followed by stabilization/decline. Local legacy hotspots (e.g., heavily impacted embayments) remain active sources via remobilization, which the mass balances capture as benthic exchange and burial terms.

Food webs and human exposure. Efficient MeHg production and biomagnification in Mediterranean food webs leave several top-predator fish above EU thresholds, a pattern mirrored in **HBM** datasets with higher central values in coastal/high-seafood populations than in inland Europe—underscoring the need for **species- and size-specific** risk communication that preserves nutritional benefits.

Figure 11. *Mediterranean mercury mass balance (after Cossa et al., 2022)*

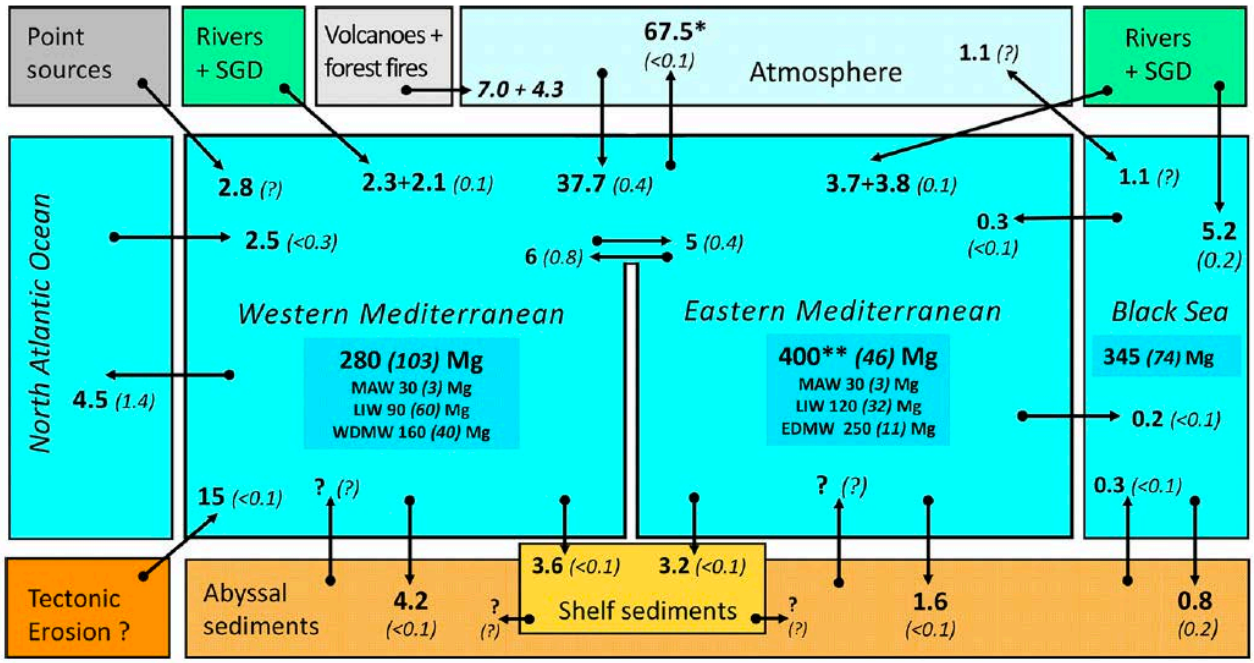

4.1. Relevance to effectiveness evaluation (Minamata Article 22)

The Mediterranean is a responsive test bed for Article 22: short effective residence times and tightly coupled compartments allow policy signals to emerge across media. Independent budgets converge on a **net atmospheric source** and **net Atlantic export**, and the Gibraltar sections document **multi-decadal declines** consistent with global emissions controls. Because speciation is explicit (MeHg, DGM), we can link observed **biogeochemical reactivity** to outcomes that matter—**fish Hg** and **human exposure**. As local point sources wane (e.g., chlor-alkali, dental amalgam), **diet becomes the dominant exposure pathway**; thus, **targeted, species/portion-specific advisories** become the practical lever to protect vulnerable groups while preserving seafood benefits. Together, these features make the Mediterranean a **demonstration region** where cross-media indicators can track Convention effectiveness with credibility.

4.2. What remains to be done

It is essential to institutionalize a cost-effective, multi-compartment observing system that is coupled to a data-assimilative regional model. This system should include sentinel transects and stations linking the atmosphere, surface, thermocline (100–600 m), and deep ocean, with routine speciation of mercury forms such as methylmercury (MeHg) and dissolved gaseous mercury (DGM), along with core hydro-biogeochemical measurements.

Boundary exchange monitoring at key locations such as Gibraltar and the Sicily Channel should be established, with harmonized measurements of total mercury (THg) and MeHg concentrations combined with transport estimates to quantify net export. Sediment archives, including both

sediment traps and well-dated cores from shelf areas and the deep sea, are needed to partition burial from remobilization processes and to attribute sources using stable isotopes.

Monitoring land–sea inputs at major rivers and submarine groundwater outlets will help constrain coastal loads and identify pollution hotspots. In addition, integrated human biomonitoring during pregnancy and early life in high-consumption communities should be implemented, aligned with species- and portion-specific dietary guidance to evaluate the effectiveness of risk communication.

All of these observations should feed into a process-based, assimilating model designed to reconcile budgets, quantify uncertainty, and test management and climate scenarios, thereby closing the loop from detection to decision support.

4.3. Framing for management under natural dominance and climate sensitivity

At the basin scale, natural sources and processes (in-situ MeHg production, volcanic/hydrothermal inputs, sediment–water exchange) are predominant, while the system is highly sensitive to water- and land-management (damming, irrigation, wastewater, coastal development) and to climate forcing (stratification, oxygenation, deep-water formation). These drivers regulate MeHg production, boundary exports, and fish Hg. Management should therefore pair sustained cross-media monitoring with adaptive, seafood-smart risk communication, using indicators that respond to both policy and climate (e.g., depth/inventory of the MeHg maximum, surface DGM, Gibraltar fluxes, sentinel fish exceedance rates, HBM trends).

5. Data gaps and limitations

Current knowledge on mercury in the Mediterranean is constrained by several significant gaps and limitations. Geographic and trophic coverage remains incomplete, with especially limited data available from the eastern and southern Mediterranean. Time series are scarce, particularly for methylmercury (MeHg) and boundary exchange processes, making it difficult to establish long-term trends and variability. Coordinated human biomonitoring (HBM) efforts are limited across high-consumption communities, restricting the ability to assess exposure patterns in populations at greatest risk.

Submarine groundwater discharge and hydrothermal fluxes remain highly uncertain, yet they may represent important sources of mercury input. Speciation and microbial cycling are not routinely measured, even though these processes are central to mercury transformation and bioavailability. In addition, methodological differences across environmental media hinder cross-integration of datasets and complicate the establishment of coherent regional assessments.

Opportunities and recommendations

To address these gaps, spatial and trophic coverage needs to be expanded with a particular focus on under-sampled sub-basins and on top predators that integrate ecosystem exposure. A ecoordinated regional HBM programme should be implemented using common protocols, with an emphasis on high-seafood-consuming populations and on pregnancy and early life stages where risks are greatest. Establishing long-term time series at sentinel sites, including MeHg profiles, surface dissolved gaseous mercury (DGM), Gibraltar boundary sections, and sediment core records, would provide a robust temporal baseline.

Equally important is the systematic assimilation of observations into a regional Earth-system mrcury model, with the publication of annual indicator updates to support transparent monitoring of progress. Harmonization of methods across air, water, sediment, and biota is needed, ensuring comparability through consistent units, detection limits, and intercomparison exercises. Finally, the Mediterranean offers a unique opportunity to serve as a pilot region for evaluating the effectiveness of the Minamata Convention, where open data sharing and co-development of policy-relevant indicators with the Parties could set a global example.

6. Conclusion

The Mediterranean's message is consistent: while total Hg in open waters is ordinary, reactivity is high, yielding elevated MeHg availability, fish Hg, and diet-driven human exposure. With a focused observing system and aligned indicators, the region can demonstrate how Minamata measures translate into detectable environmental and health benefits—and how to keep pace with climate-sensitive change.

Key references:

AMAP/UN Environment Programme (2019). Technical Background Report for the Global Mercury Assessment 2018. Arctic Monitoring and Assessment Programme, Oslo, Norway / UN Environment Programme, Chemicals and Health Branch, Geneva, Switzerland, viii + 426 pp. ISBN 978-82-7971-108-7.

Cinnirella, S., Bruno, D. E., Pirrone, N., Horvat, M., Živković, I., Evers, D. C., Johnson, S., & Sunderland, E. M. (2019). Mercury concentrations in biota in the Mediterranean Sea, a compilation of 40 years of surveys. Scientific Data, 6(1), 205. https://doi.org/10.1038/s41597-019-0219-y

Cossa, D., Knoery, J., Bănaru, D., Harmelin-Vivien, M., Sonke, J. E., Hedgecock, I. M., Bravo, A. G., Rosati, G., Canu, D., Horvat, M., Sprovieri, F., Pirrone, N., & Heimbürger-Boavida, L.-E. (2022). Mediterranean Mercury Assessment 2022: An Updated Budget, Health Consequences, and Research Perspectives. Environmental Science & Technology, 56(7), 3840–3862. https://doi.org/10.1021/acs.est.1c03044

European Commission. (2023). Commission regulation (EU) 2023/915 of 25 April 2023 on maximum levels for certain contaminants in food and repealing Regulation (EC) No 1881/2006. Official Journal of the European Union. https://eur-lex.europa.eu/legal-content/EN/TXT/PDF/?uri=CELEX:32023R0915

Evers, D. C., Ackerman, J. T., Åkerblom, S., Bally, D., Basu, N., Bishop, K., Bodin, N., Braaten, H. F. V., Burton, M. E. H., Bustamante, P., Chen, C., Chételat, J., Christian, L., Dietz, R., Drevnick, P., Eagles-Smith, C., Fernandez, L. E., Hammerschlag, N., Harmelin-Vivien, M., … Wu, P. (2024). Global mercury concentrations in biota: their use as a basis for a global biomonitoring framework. Ecotoxicology, 33(4–5), 325–396. https://doi.org/10.1007/s10646-024-02747-x

Inoue M, Matsumura K, Hamazaki K, Tsuchida A, Inadera H. (2024) Maternal dietary intake of fish and child neurodevelopment at 3 years: a nationwide birth cohort—The Japan Environment and Children's Study. *Front. Public Health* 11:1267088.

Katsonouri, A., Gabriel, C., Esteban López, M., Namorado, S., et al., (2023). HBM4EU-MOM: Prenatal methylmercury-exposure control in five countries through suitable dietary advice for pregnancy – Study design and characteristics of participants. *International Journal of Hygiene and Environmental Health, 252*, 114213. https://doi.org/10.1016/j.ijheh.2023.114213

Kotnik, J., Sprovieri, F., Ogrinc, N., Horvat, M., & Pirrone, N. (2014). Mercury in the Mediterranean. Part 1: spatial and temporal trends. Environmental Science and Pollution Research, 21, 4063–4080.

Miklavčič Višnjevec, A., Kocman, D., & Horvat, M. (2014). Human mercury exposure and effects in Europe. Environmental Toxicology and Chemistry, 33(6), 1259–1270. https://doi.org/10.1002/etc.2482

Ogrinc, N., Hintelmann, H., Kotnik, J., Horvat, M., & Pirrone, N. (2019). Sources of mercury in deep-sea sediments of the Mediterranean Sea as revealed by mercury stable isotopes. Scientific Reports, 9, 11626. https://doi.org/10.1038/s41598-019-48061-z

Rajar, R., Četina, M., Horvat, M., & Žagar, D. (2007). Mass balance of mercury in the Mediterranean Sea. Marine Chemistry, 107(1), 89–102. https://doi.org/10.1016/j.marchem.2006.10.001

Rosati, G., Canu, D., Lazzari, P., & Solidoro, C. (2022). Assessing the spatial and temporal variability of methylmercury biogeochemistry and bioaccumulation in the Mediterranean Sea with a coupled 3D model. Biogeosciences, 19, 3663–3682. https://doi.org/10.5194/bg-19-3663-2022

Sprovieri, F., Hedgecock, I. M., Kotnik, J., Živković, I., Horvat, M., & Pirrone, N. (2025). Twenty years of studying the origins and fate of atmospheric mercury over the Mediterranean Sea. Science of the Total Environment, 964, 178278. https://doi.org/10.1016/j.scitotenv.2024.178278

Starling P, Charlton K, McMahon AT, Lucas C. (2015) Fish Intake during Pregnancy and Foetal Neurodevelopment—A Systematic Review of the Evidence. *Nutrients* 7(3):2001-2014.

UN Environment Programme (2019). Global Mercury Assessment 2018. UN Environment Programme, Chemicals and Health Branch, Geneva, Switzerland, 59 pp. ISBN 978-92-807-3744-8.

Žagar, D., Sirnik, N., Četina, M., Horvat, M., Kotnik, J., Ogrinc, N., Hedgecock, I. M., Cinnirella, S., De Simone, F., Gencarelli, C. N., & Pirrone, N. (2014). Mercury in the Mediterranean. Part 2: processes and mass balance. Environmental Science and Pollution Research, 21, 4081–4094. https://doi.org/10.1007/s11356-013-2055-5

Živković, I., Šolić, M., Kotnik, J., Žižek, S., & Horvat, M. (2017). The abundance and speciation of mercury in the Adriatic plankton, bivalves and fish – a review. Acta Adriatica, 58(3), 391–418. https://doi.org/10.32582/aa.58.3.2

Mercury Pollution from Artisanal Gold Mining in the southern Peruvian Amazon: A Cross-Media Case Study

Claudia Vega, Luis Fernandez
Centro de Innovacion Cientifica Amazonica (CINCIA), Madre de Dios, Peru

1. Description of the Case Study

Over the last 20 years, ASGM has deforested and degraded nearly 100,000 ha of high-biodiversity rainforest landscapes in the department of Madre de Dios, located in the southern Peruvian Amazon (Caballero Espejo et al., 2018), and created highly degraded landscapes that are pockmarked by thousands of hectares of mining ponds (Gerson et al., 2020). A 2018 study estimated that 181 tons of mercury are released to the region's waterways, soils, and air every year. As of this writing, Madre de Dios is considered the largest hotspot of ASGM activity and ASGM-related mercury pollution in Latin America (Cardo & Vargas, 2017).

This case study illustrates the causal link between mercury emissions from artisanal and small-scale gold mining (ASGM) activities—including amalgam burning in gold shops and mercury releases to soils and waters at mining sites—and elevated mercury levels in air, aquatic ecosystems, and terrestrial biodiversity. The objective is to demonstrate how ASGM contamination manifests across environmental media, with implications for both biodiversity and human exposure.

Between 2017 and 2019, The *Centro de Innovacion Cientifica Amazonica* (CINCIA) is a Peruvian non-profit scientific research centre, developed a framework to characterize the presence, magnitude, and spatial distribution of mercury pollution in and around ASGM sites. CINCIA focused on measuring mercury concentrations in biota, sediment, and air across an area that spanned more than 2,000 km^2 to evaluate mercury levels in different environments and media across the region to identify Hg hotspots.

ASGM and control sites were identified based on the presence and distance of mining activities. Control sites were selected to have very similar features to the impacted sites, but without ASGM. The sites defined as ASGM sites were initially located in rural environments, such as mining ponds formed during mining activity and subsequently abandoned after the cessation of the activity. In

urban areas, these sites included gold shops where amalgamated gold is burned, releasing mercury during the process.

Mercury in abandoned mining ponds: sediment and fish

The methodology to assess mercury levels in mining ponds included the sampling of bottom sediments and fish collected in mining ponds located in different ASGM areas of the Madre de Dios region. Natural oxbow lakes, upriver of mining activity were used as control sites.

Mercury around Mining ponds: Bird and bats

CINCIA's biomonitoring surveys were initially focused on fish because they were the predominant source of methylmercury dietary exposure for humans. However, it later expanded to include wildlife species, such as birds and bats, to develop a better understanding of the transfer of mercury along the food web (biomagnification) and the potential impact of mercury exposure on terrestrial biodiversity. In this case, bat fur and bird feathers from around mining ponds and natural oxbow lakes were sampled for mercury analysis.

Mercury levels in air: Amalgam burning gold shops

CINCIA, in joint effort with Toronto University monitored atmospheric mercury concentrations between 2017-2018 to determine the regional background of gaseous elemental mercury (GEM), and to assess the impact of local and regional ASGM sources on the overall mercury in the atmosphere in the Madre de Dios region. Passive air samplers were used for the collection of gaseous elemental mercury. The samples were analysed for total mercury and Hg isotopes to determine the sources of Hg emission.

2. Cross-media integration of observed levels/trends

- **Mining Ponds Assessment**

  Our results showed that with exception of the bottom sediments samples that didn't show any significant difference between ASGM and control sites (Fig), all the biota matrix (fish muscle, bird feather and bat fur) evaluated in and around mining ponds (impacted sites) and oxbows lakes (control sites), showed similar trend : *Mercury levels were consistently and significantly higher in biota from ASGM sites in comparison with control sites (fig1, 2 and 3)*. In birds, we reported the highest Hg level reported for bird feather in South America. We recorded in bats from ASGM sites the highest mercury levels in bat fur reported in the Neotropics. (Sayer et al 2023; Pisconte et al 2024; Portillo et al 2023).

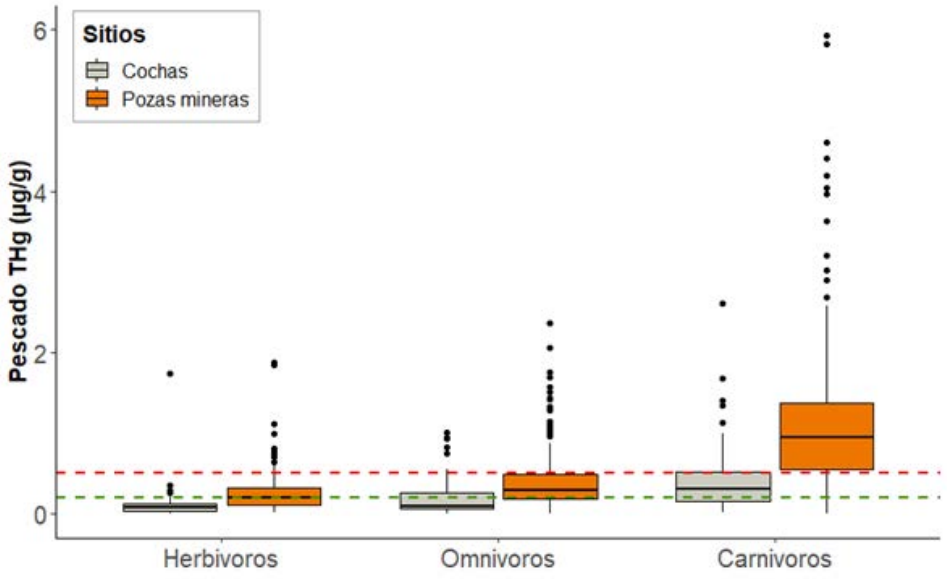

Fig. 1. Mercury concentrations in fish: ASGM ponds (*Pozas meneras*) vs. oxbow lakes (controls)(*Cochas*).

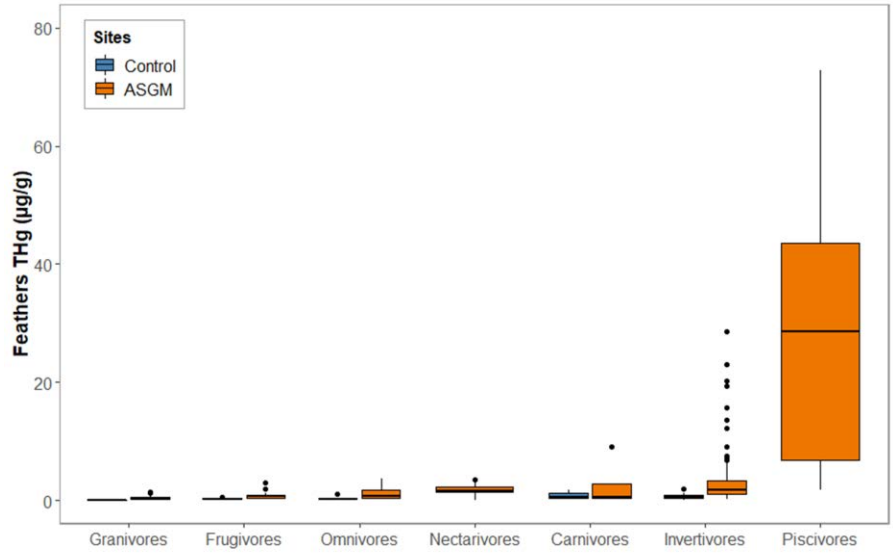

Fig. 2. Mercury concentrations in bird feathers: ASGM ponds vs. oxbow lakes (controls).

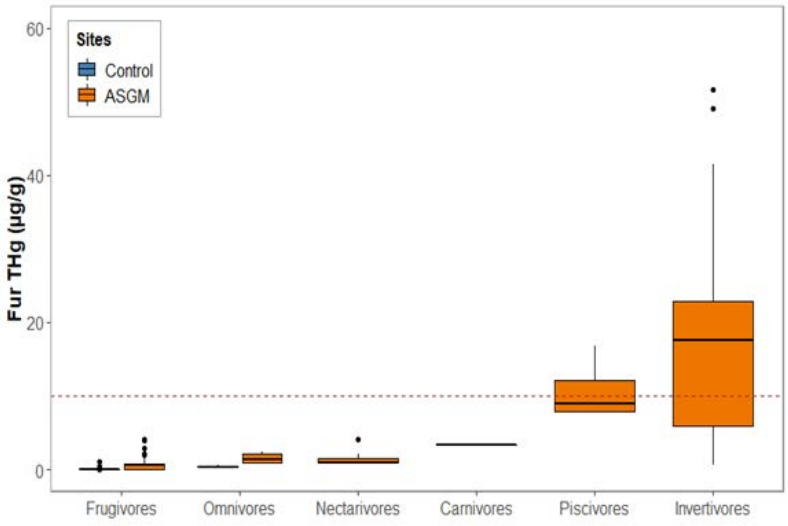

Fig. 3. Mercury concentrations in bat fur: ASGM ponds vs. oxbow lakes (controls).

- ***Mercury emissions from gold shops (air assessment)***

  Our data showed that there was a spatial variability of Hg emission (Gaseous elemental mercury GEM) in the air in Madre de Dios. Regional GEM concentrations were elevated (1.3 to 11 ng.m^3) compared to background levels (< 1 ng.m^3) and were even higher in areas near mining and gold shop activity * ~10 to >5000 ng m^3). And applying an isotope mixing model, it was estimated that about 70% of the mercury emitted to the air is derived from mining activity, which shows a distinct isotopic signature (Szponar et al 2025).

Taken together, these findings provide strong evidence of cross-media contamination, where mercury emissions from ASGM are simultaneously detectable in air, aquatic food webs, and terrestrial wildlife. The isotopic signatures reinforce that local ASGM is the dominant source, linking emissions directly to observed bioaccumulation.

3. Relevance to effectiveness evaluation

This case study is one of the few that directly examines mercury contamination from ASGM across multiple environmental matrices. The data provide clear evidence of how mercury from ASGM is distributed throughout mining regions and demonstrate the value of using cross-media

indicators to characterize contamination. While bottom sediment samples did not consistently differentiate between ASGM ponds and natural oxbow lakes, biota indicators told a different story: fish, birds, and bats in and around ASGM sites consistently showed significantly higher mercury concentrations than those from control sites. In urban areas, atmospheric monitoring of gold shops showed extremely elevated mercury emissions, further confirming the breadth of ASGM's impact across both aquatic and terrestrial systems.

These findings are directly relevant to the Minamata Convention's effectiveness evaluation, particularly under Article 7 (ASGM). They show that, despite ongoing national and international commitments, ASGM in Madre de Dios continues to release large amounts of mercury that are traceable across environmental media. This case underscores the urgent need to strengthen Peru's National Action Plan on ASGM, tighten controls on mercury trade and use, and develop targeted hotspot monitoring that can provide measurable evidence of the Convention's effectiveness.

4. Gaps, Limitations and Recommendations

While this case study provides clear evidence of cross-media mercury contamination from ASGM, several important gaps and limitations should be acknowledged. The monitoring period, conducted between 2017 and 2019, was relatively short and may not fully capture longer-term temporal trends. For example, sediment samples did not consistently differentiate between ASGM and control sites, likely reflecting time lags in mercury deposition. In addition, although mercury concentrations were measured in fish, birds, and bats, the study did not include direct human exposure assessments such as dietary surveys or biomonitoring of hair or blood. As a result, the link between observed environmental contamination and community health impacts remains indirect.

Geographically, the study focused exclusively on Madre de Dios, which is the largest ASGM hotspot in Latin America but does not represent the full diversity of mining contexts across the Amazon Basin. Similarly, atmospheric monitoring at gold shops was limited in duration and scope, restricting the ability to generalize results to regional or national scales.

These limitations point to several recommendations. Future work should expand biomonitoring to include human exposure pathways and extend geographic coverage to other ASGM regions in Peru and neighboring countries. Standardizing protocols across media—air, aquatic, and

terrestrial biota—would improve comparability across studies and strengthen regional assessments. Finally, the integration of isotope tracing into national mercury monitoring frameworks would provide a powerful tool to attribute sources more precisely and support enforcement of Minamata Convention commitments.

5. References

- Caballero Espejo, J., Messinger, M., Román-Dañobeytia, F., Ascorra, C., Fernandez, L. E., & Silman, M. (2018). Deforestation and forest degradation due to gold mining in the Peruvian Amazon: A 34-year perspective. *Remote Sensing*, 10(12), 1903.
- Gerson, J. R., Szponar, N., Zambrano, A. A., Bergquist, B., Broadbent, E., Driscoll, C. T., Vega, C & Bernhardt, E. S. (2022). Amazon forests capture high levels of atmospheric mercury pollution from artisanal gold mining. Nature communications, 13(1), 1-10.
- Cardo, M. A., & Vargas, P. M. (2017). *Proyecto: Plan nacional de acción sobre mercurio* en el sector de la minería de oro artesanal y de pequeña escala en el Perú. (Artisanal Gold Council 2017)
- Sayers, C. J., Evers, D. C., Ruiz-Gutierrez, V., Adams, E., Vega, C. M., Pisconte, J. N., ... & Fernandez, L. E. (2023). Mercury in Neotropical birds: a synthesis and prospectus on 13 years of exposure data. Ecotoxicology, 32(8), 1096-1123.
- Portillo, A., Vega, C. M., Mena, J. L., Bonifaz, E., Ascorra, C., Silman, M. R., & Fernandez, L. E. (2023). Mercury bioaccumulation in bats in Madre de Dios, Peru: implications for Hg bioindicators for tropical ecosystems impacted by artisanal and small-scale gold mining. Ecotoxicology, 1-13.
- Pisconte, J. N., Vega, C. M., Sayers, C. J., Sevillano-Ríos, C. S., Pillaca, M., Quispe, E., ... & Fernandez, L. E. (2024). Elevated mercury exposure in bird communities inhabiting Artisanal and Small-Scale Gold Mining landscapes of the southeastern Peruvian Amazon. Ecotoxicology, 33(4), 472-483.
- Szponar, N., Vega, C. M., Gerson, J., McLagan, D. S., Pillaca, M., Delgado, S., ... & Bergquist, B. A. (2025). Tracing atmospheric mercury from artisanal and small-scale gold mining. Environmental Science & Technology, 59(10), 5021-5033.

Case study Sweden: Integrated Analysis of Mercury Time-Trends in environmental media

Submitted to the OESG for Effectiveness Evaluation in the Minamata Convention

2025-12-01

Co-authors
Pianpian Wu, Swedish University of Agricultural Sciences/Dartmouth College

Kevin Bishop, Swedish University of Agricultural Sciences

Karin Eklöf, Swedish University of Agricultural Sciences

John Munthe, IVL Swedish Environmental Research Institute

Anne L. Soerensen, Swedish Museum of Natural History

Erik Björn, Umeå University

Claudia von Brömssen, Swedish University of Agricultural Sciences

Contents

Background and description of the integrated case study

Widespread mercury contamination in the biota of Fennoscandia was recognized already in the 1960s, during the same decade as the cause of the Minamata disease was becoming apparent in Japan. The first reports on mercury contamination were from birds (Westermark, Odsjö and Johnels, 1975), and fish (Berglund, 1971). Local contamination from industry as well as the use of mercury in agriculture were the original concerns, and the first bans on the use of mercury in agriculture came in the latter half of the 1960s. The discovery of unsafe mercury levels in birds and fish hundreds of kilometres from any local source raised concerns about long-range atmospheric transport of nature to remote areas. One manifestation of this concern was the first international conference on mercury as a global pollutant being held in Gävle, Sweden (Lindquist et al., 1991). Further, already in the 1960s, studies conducted in Sweden revealed that mercury in fish was predominantly present as methylmercury (often exceeding 90% of total mercury, Westöö, 1966) and that this compound could form in the environment through biological methylation of inorganic mercury (Jensen and Jernelöv, 1969). These discoveries spurred further studies on mercury's biogeochemical and bioaccumulation processes, research that remains highly active and critically important today. The Swedish concerns about mercury also led to comprehensive monitoring programs for mercury in the environment, and research focused on to determine both the causes of contamination and the effectiveness of countermeasures (Ammar et al. 2024).

This integrated case study centres around the Swedish monitoring program for contaminants in freshwater and marine (Baltic Sea) biota comprising 62 fish Hg time series with the longest time series starting in the late 1960s. By complementing this with long-term records of national mercury emissions, air concentrations, wet deposition, longer term proxies of environmental mercury (tree rings, peat, lake sediments) and mercury in birds, this study addresses the central question for the first effectiveness assessment of the UNEP Minamata Convention: Can reductions in the release of Hg to the environment reduce Hg in the biota?

Results and discussions

Mercury emissions and releases, including agriculture

Swedish emissions of mercury to air have decreased by almost 75% since the 1990s (Naturvårdsverket, 2025). In Europe, large emission reductions occurred in the early 1990s after the large-scale political changes in the former Soviet Union block. These emission reductions are undocumented but led to significant decreases in air concentrations in Sweden (Iverfeldt et al., 1995). In the period 2005 to 2022, emissions of mercury to air from the EU countries continued to decline by 55% (EEA, 2025). The use of mercury in agriculture to protect seeds from fungus was recognized as a source of mercury in birds already in the 1950s. Sweden restricted this use already in 1966, and any use in agriculture was banned by 1990 (Westermark, Odsjö and Johnels, 1975; Lindquist et al., 1991). Wood processing centres were also recognized as point sources of mercury contamination, since mercury was used in pulp and paper industries and in the production of chemicals in the chlor-alkali process. These uses were also restricted by the 1990s, and Sweden banned all use of mercury

and mercury-containing products in 2009, with similar legislation in the other Nordic countries (Hylander and Meili, 2005, Kemi 2025).

Discharges from municipal wastewater treatment plants have also decreased in Sweden since the 1980s. For discharge to water, the releases have decreased with >90% since the early 1990s (29 kg or <0.05 ug/L in 2022), while concentrations for sewage sludge have decreased with >85% since 1987 (0.4 mg/kg dry matter in 2022) (SCB 2022, Naturvårdsverket, 2016).

Atmospheric mercury deposition

Long-term monitoring by the Swedish Environmental Protection Agency (Naturvårdsverket) shows that atmospheric Hg deposition in rural Sweden has declined by over 50% since the 1990s (Naturvårdsverket, 2024).This decline is attributed to international emission reductions following the large-scale political and industrial changes in Europe in the early 1990s and continuing with policy driven agreements such as CLRTAP and the EU air quality directives.Despite improvements, background deposition persists and will continue to constrain the influence of national and regional emission reductions. In addition, remobilization from soil and sediments continues to impact surface waters.

Mercury in surface waters

Trends in Hg concentration were evaluated between 2000 and 2010 from 19 watercourses in the Swedish monitoring data (Eklöf et al 2012). Data show no significant trend for most sites (n = 18 of 19), only one site had increasing trends of Hg concentrations. A decade later, trend analyses were conducted for both Swedish monitoring data and long-term data measure within the International Cooperative Programme on Integrated Monitoring of Air Pollution Effects on Ecosystems (ICP IM). Eklöf et al. (2024) show a decline by average 1.5% in total Hg concentrations in surface waters from 2000 to 2020 in three of the sites. Using generalized additive mixed models (GAMM) it was found that trends were not monotonic. In the first five years (2000-2005) there was a general decline in Hg concentrations in many sites, while in the last five years (2015-2020) increasing trends outnumbered the decreasing trends. These variations are most likely due to other factors that may influence the mobility of mercury such as recovery from acidification, reduced atmospheric deposition, local land use, organic matter transport, and hydrological regimes.

Mercury in environmental archives (tree rings, peat and marine/lake sediment).

Environmental archives in the form of tree rings (Peng et al., 2024), tree litter fall (Zhang et al., 2025), and peat profiles (Li et al., 2023) have proven successful at tracking atmospheric mercury concentrations. These archives track both the increase in atmospheric Hg over the Nordic countries during much of the 1900s, and the decline of regional atmospheric Hg levels after they culminated ca 1980, followed by stabilization at a lower level after ca 2000. A study on sediment from a lake in Northern Sweden found steady Hg levels from the 1950s to the end of the record in 2007 (Rydberg et al. 2008), thus deviating from the other terrestrial archives. More extensive work on sediment records is found in Baltic offshore waters near

Sweden. These cores show a peak in Hg concentration in the ~1970s followed by declining concentrations to ~2010 (Leipe, 2013). In the last two decades (2003 to 2020), 16 monitoring stations show no clear declining concentrations in offshore sediment along the Swedish coast (Josefsson, 2022). The different environmental archives thus show similar long term trends while the trends deviate in recent decades (decreasing or no trend). Stable mercury isotope measurements of surface sediments (0–2 cm; n = 29) from the Baltic Sea and Kattegat indicate that the pool of mercury from recent inputs reflects a variable mixture of sources, dominated by a terrestrial and an industrial end-member, with a smaller contribution from direct atmospheric deposition (Bouchet et al., 2023). Differences in source composition are likely an important factor contributing to the varying recovery rates observed among locations. In general, understanding the source composition of mercury is important for evaluating and comparing time trends across locations.

Mercury in fish

Diverse temporal trends in fish Hg have been observed since 1965. Åkerblom et al. (2014) looked into >40000 Hg observations from a mix of fish species collected from >2800 Swedish freshwater sites over 50 years. An overall analysis of the normalized dataset showed that the temporal development did not follow any consistent decreases or regional patterns. However, restricting the dataset to locations with long term monitoring, they found an overall decline of ~20 % between the two periods 1965-1990 and 1991-2012. Braaten et al. (2019; 2020) examined temporal trends in Hg concentrations from perch and pike in a pan-Nordic study on freshwater lakes. They found that Hg levels in fish across the Nordic countries had decreased with 20% for pike, 50% for perch between 1970 and 2015 and linked it to reduced atmospheric deposition and changes in water chemistry (e.g., sulphate and DOC). However, they suggested biota Hg recovery lags behind atmospheric decreases due to the remobilization of legacy Hg and continued in-situ methylation. Swedish monitoring of perch Hg concentrations from 27 lakes (reference lakes) across Sweden showed that during the period 2011-2020, 19% of time series were decreasing significantly (3-6%/y, $p<0.05$), while the remaining lakes showed no significant trend (Faxneld and Soerensen 2022). For the Swedish coastal environment, 30% of 30 fish (herring, perch, cod, eelpout) stations showed significant decreases from the monitoring start year (1972 to 2008) to 2020 while 10% of the stations showed significant increases (Soerensen and Faxneld 2022). For the 2011-2020 period, an equal occurrence (20%) of significantly increasing and decreasing trends were found at the 30 stations. Temporal trends from the Swedish monitoring are shown in Figure 2. Concentration of Hg in monitored perch still exceeds the EU environmental threshold (20 ng/g muscle ww, EQS secondary poisoning) for all lakes and most Baltic Sea fish (Faxneld and Soerensen 2022; Soerensen and Faxneld 2022).

Mercury in birds

Two decadal time series exist for Hg in Swedish birds, one based on white-tailed sea eagle feathers from the area around the central Swedish east coast (1966-2011; Sun et al. 2019) and one based on guillemot eggs from Gotland, a Swedish island in the Baltic Sea (1968-2023; Ammar et al. 2024). Both these time series start around the time when early work by Berg et

al. (1966) and Johnels et al. (1979) showed peak Hg concentrations in white-tailed sea eagle, marsh harrier and eagle owls likely due, for a large part, to use of Hg as seed dressing, a practice that was forbidden from 1966. For the white-tailed sea eagle, Sun et al. (2019) found a 70% decrease between 1967 and 2011. For the guillemot eggs, a decrease of 1.9%/y (resulting in a similar total decrease of 70%) was found between 1968 and 2023, while the decrease during the period 2011-2020 was smaller (0.47%/y; Soerensen et al. 2025).

Synthesis and outlook

Figure 1 shows the long term trends of three historic environmental archives from Sweden or the nearby Baltic Sea. While there are minor differences, all three matrices show a similar pattern with low concentrations until the early 1900s where concentrations begin to increase, and peak within a short period between 1960-1975. After the peak, Hg concentrations start to decline and only the tree ring record shows a potential levelling off in the last years of the time series. These long term records present a uniform picture of the anthropogenic influence in Sweden since industrialization.

Since the peak in the 1960s, more biota data have become available to supplement the decreasing trends in the few long term records, and since the 1990s, also data from more volatile compartments such as air and water has become available (Figure 2). These shorter term records do not present a picture as uniform as the long-term environmental archives. Air concentrations, wet deposition, releases from wastewater treatment plants and concentrations in Swedish streams and rivers are all decreasing ~40-60% during the period but with different consistency and variability. These decreases are on a scale similar to the decrease seen during the period from the 1970s to the present day in the historic archives (Figure 1) and the time series on guillemot (bird) eggs (Figure 2). However, we also see that both Swedish freshwater perch and Baltic Sea herring do not follow the same tendency as seen for the other matrices. Here the records show a limited decline in the freshwater environment (<20%, 1995-2023) and no significant decline in the Baltic Sea (marine) environment (Figure 2). These long term fish trends, based on Swedish monitoring data, aligns with the result from the same monitoring data during the recent 2011-2020 period and the results on Swedish freshwater fish from Åkerblom et al. (2014) of a 20% overall decrease between the periods 1965–1990 and 1991-2012. The study by Braaten et al. (2019) shows a different trend with a 50% pan-Nordic decrease in perch (see discussion in section 5 Mercury in fish).

The smaller response for both freshwater and marine fish than for other compartments, both sources and sinks, indicate that fish can be a difficult matrix for capturing anthropogenically driven trends because many other variables and processes also influence Hg levels in fish. These include net methylmercury formation, uptake and accumulation processes and also changes in fish stocks, growth and condition, fish age at collection, and changes in nutrients driving Hg sedimentation rates (Soerensen et al. 2016, Soerensen et al. 2017, Braaten et al. 2020). Such changes are driven by factors including climate and fishing pressure on aquatic ecosystems. Forest harvest in catchments has also been identified as a practice which can increase the concentration of mercury in fish of a particular lake for some years (Wu et al., 2018), due to the increase of mercury into runoff waters (Porvari et al., 2003, Bishop et al.,

2009). Since forest harvest has been a feature of the Swedish landscape for over a century, this is likely to be a source of variation more than a long-term trend.

We show here that even if significant decreases in Hg sources and environmental concentrations have taken place, other types of pressures and changes in the environment can result in a lack of clear or proportional response in both freshwater and marine fish populations. Thus it is important to keep sources of local variation, and the potential for delayed responses when using biota time series to evaluate the effect of the convention.

Mercury cycling in the environment is complex. Nonetheless, the results from both historic archives and over 60 years of environmental Hg monitoring and research in Sweden indicate that controlling Hg releases into the environment will reduce Hg in the environment (as seen for sediment, tree rings and birds), although the picture is less clear for freshwater and marine fish. Improvements can be rapid, as in the case of how quickly banning the use of Hg in agriculture led to reductions in the body burdens of Hg in birds that ate the seed treated with Hg (Westermark, Odsjö, Johnels, 1975; Figure 2). Mercury in the atmosphere is also linked to contamination of fish, but this link is less direct and modulated via a large number of biogeochemical, microbial and ecological processes, and the rate of response here has been slower in freshwater and even more blurred in the Baltic Sea but long term and in the 2011-2020 period.

The response of biota to decreased mercury emissions is proceeding over the course of decades but with many confounding factors (Munthe et al., 2007; Braaten et al. 2020). The concentrations in most fish remain below levels safe for human consumption but above the environmental target level used in the EU Water Framework Directive. Both the challenges of harmonizing the fish data from monitoring programs, and confounding influences (e.g. changes in land use and climate) contribute to variation in the fish Hg levels and make trend analysis difficult. The availability of Hg in environmental archives and surface waters, provides important evidence that supports the interpretation of linkages between emissions, different environmental media, and the biota. In summary, reducing emissions to the atmosphere and local releases of Hg into the environment have proven their worth in reducing Hg in the environment, but it requires diligent follow-up, often over decades, to observe the benefits when it comes to reduced atmospheric Hg levels and fish.

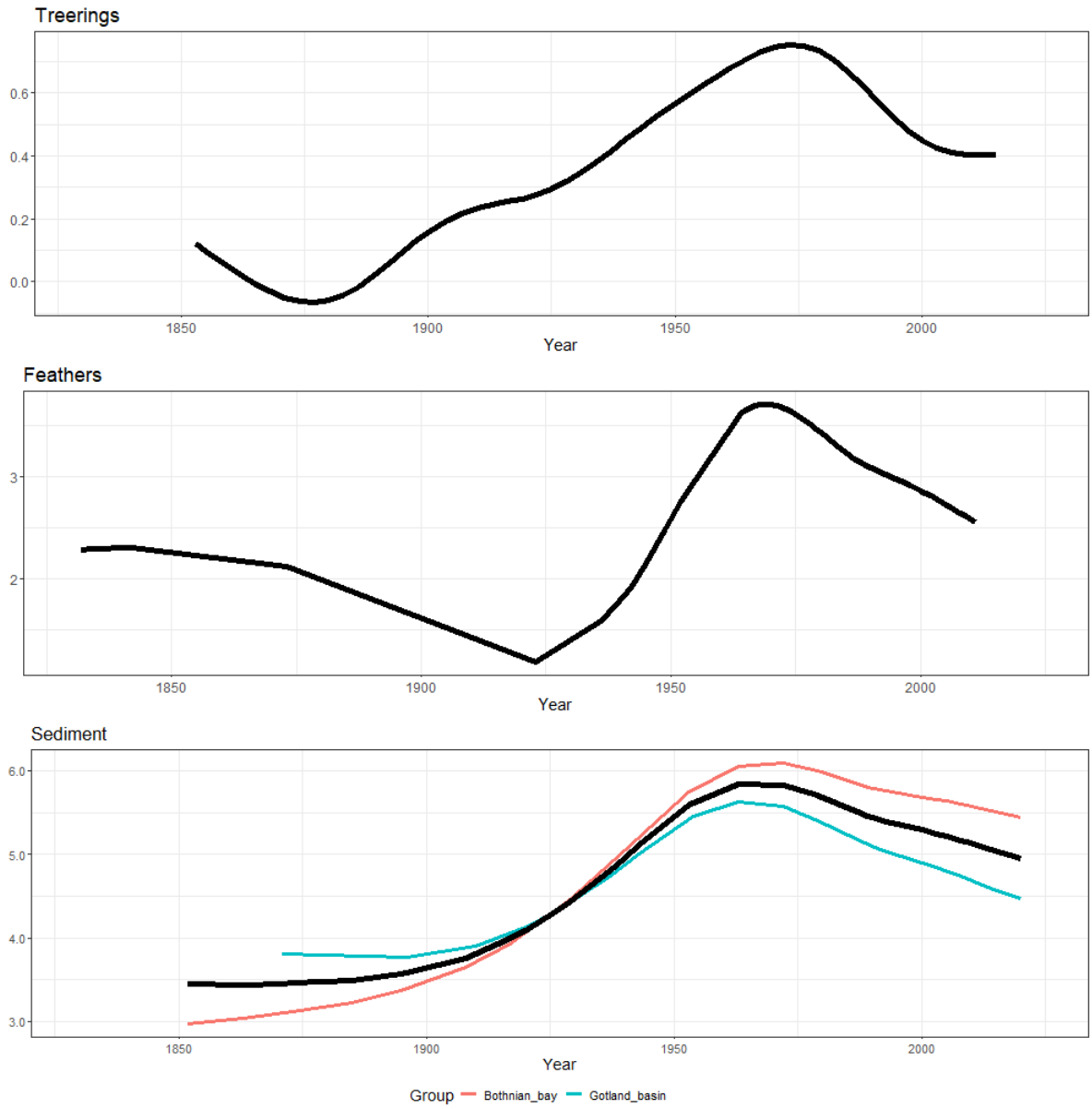

Figure 1. Long-term trend of Swedish environmental mercury observations since 1850 or earlier, collected from tree rings (top panel, Zhang et al., 2025), white tailed sea eagle feathers (middle panel, ug/g), and sediment (bottom panel, ug/kg). Generalised additive models are used for single series (Hastie and Tibshirani, 1986; Wood, 2017) and hierarchical generalised additive models for plots with several series (Pedersen et al., 2019). Data sources: The trend for bird (white tailed sea eagle) feather is based on two datasets, Berg et al. (1966) covering the period 1832-1965 and Sun et al. (2019; data from figure 2) covering the period 1967-2011; Baltic Sea sediment data is from dated cores in the Bothnian Bay and Gotland Basin presented in Leipe et al. (2013; data from figure 4) covering the period 1871-2009 and surface sediments from Josefsson et al. (2022) covering approximately the same location during the period 2003-2020.

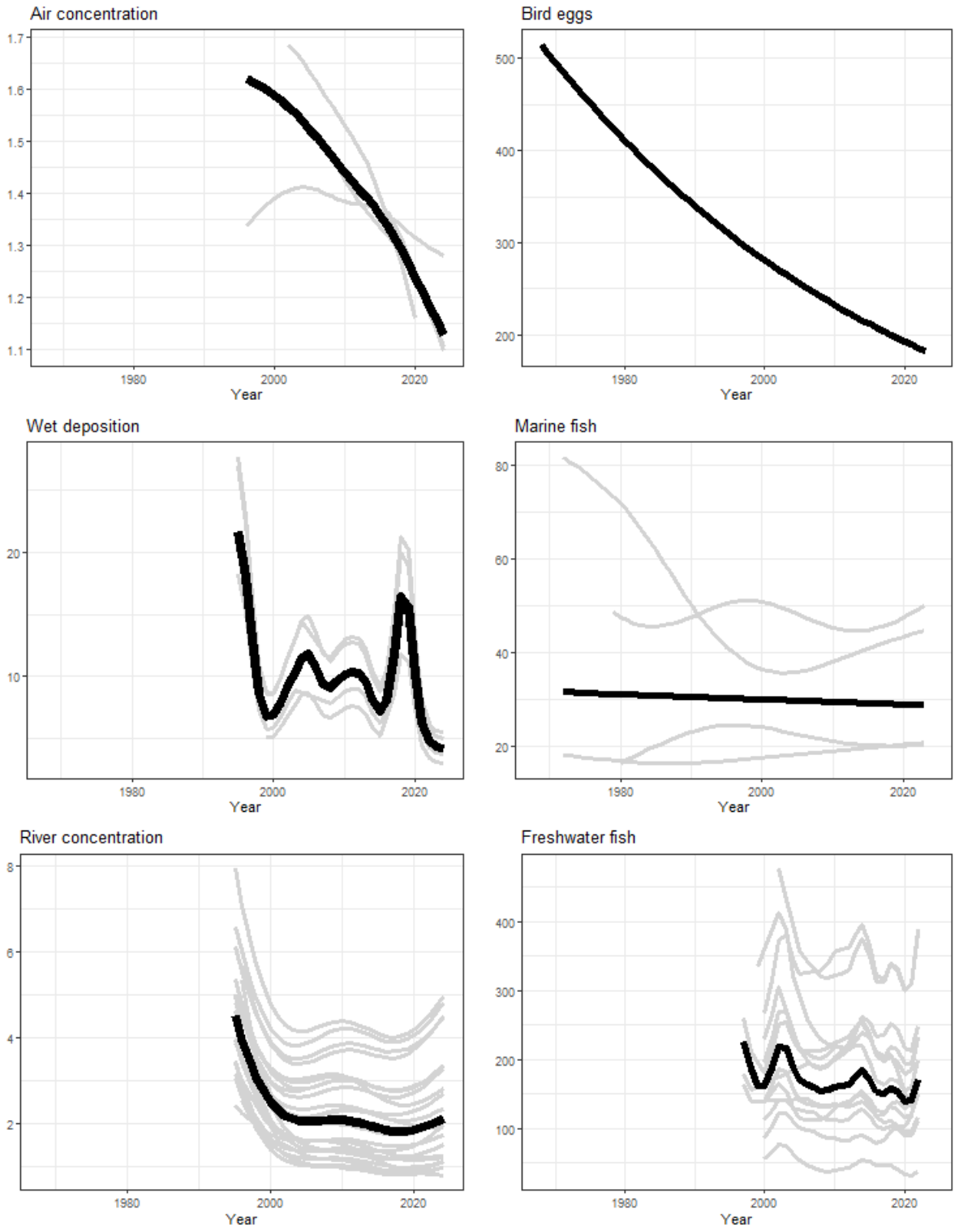

Figure 2. Short-term trend of Swedish environmental mercury observations from around 1980s until now. Left top panel: Air mercury concentrations; Left middle panel: Wet deposition of mercury concentrations; Left bottom panel: River water mercury concentrations; Right top panel: Guillemot (bird) egg mercury concentrations (ng/g ww); Right middle panel: Herring (marine) mercury concentrations (ng(g ww); Right bottom panel: Perch (freshwater) mercury concentrations (ng/g ww). Generalised additive models are used for single series (Hastie and Tibshirani, 1986; Wood, 2017) and hierarchical generalised additive models for plots

with several series (Pedersen et al., 2019). The fish data is further normalized for length differences. Data sources: Guillemot (bird) eggs and marine fish data are presented in Ammar et al. (2024), freshwater fish data are presented in Faxneld et al. (2025). Air concentrations and wet deposition downloaded from the national data-host at SMHI: https://datavardluft.smhi.se/portal/. River water mercury concentrations downloaded from the national and regional environmental monitoring of freshwater at SLU: https://miljodata.slu.se/MVM/.

Relevance to effectiveness evaluation

High relevance: Reductions in Hg emissions to the environment are directly associated with decreased Hg burdens in biota. In certain cases—such as the prohibition of Hg use in agriculture (where the link between the Hg source and exposure to biota was direct and short)—measurable effects have been observed within a decade: The response can take much longer and be highly variable in the case of fish higher in the food web where the link between the Hg source and biota exposure is indirect and modulated by multiple processes.

Gaps and limitations

Extensive as the work in Sweden has been to follow the mercury levels in biota and their causes, as well as the effectiveness of countermeasures, much more remains to be done to define causal linkages and rates. Further studies that cross traditional system boundaries between different media (air, vegetation, soils, water and biota) are of particular value in this regard (Bishop and Eklöf, 2022).

The importance of local legacy point sources (such as sediment contaminated from previous pulp and paper industrial activities) as well as the influence of changing land-use (e.g. forestry) and climate change on the recovery rates remain uncertain. The spread of Hg from different sources and its contribution to the Hg load to aquatic ecosystems and food chains in surrounding environments are challenging to quantify. Environmental change processes can mobilise Hg from soils and influence Hg biogeochemical processes which may cause confounding effects on the recovery.

General conclusions

Sweden and the Baltic Sea region demonstrate that there is a long-term linkage between reduced mercury emissions, exposure and levels in biota. This can provide a model for assessing Hg policy effectiveness, but continued monitoring and mechanistic studies are needed. The legacy Hg pool in soils and sediments, combined with climate-driven shifts in DOC and hydrology, poses challenges for achieving further reductions in aquatic MeHg exposure.

To allow future assessment of trends of Hg in different media, future monitoring activities should be harmonised and designed for comparison and integrated assessment. This would include parameters such as location of monitoring sites, time period and frequency of monitoring as well as methodology for e.g. field sampling and chemical analyses and statistical treatment.

References

Ammar, Y., Faxneld, S., Sköld, M., & Soerensen, A. L. (2024). Long-term dataset for contaminants in fish, mussels, and bird eggs from the Baltic Sea. *Scientific Data*, *11*(1), 400. https://www.nature.com/articles/s41597-024-03216-0

Berg, W., A. Johnels, B. Sjöstrand, and T. Westermark (1966), Mercury content in feathers of Swedish birds from the past 100 years, *Oikos*, 71-83.

Berglund, F. (1971). Methyl mercury in fish: A toxicologic-epidemiologic evaluation of risks: Report from an expert group. *Nordisk Hygienisk Tidskrift*, *4*, 19-364.

Bishop, K., Allan, C., Bringmark, L., Garcia, E., Hellsten, S., Högbom, L., Johansson, K., Lomander, A., Meili, M., Munthe, J. and Nilsson, M., 2009. The effects of forestry on Hg bioaccumulation in nemoral/boreal waters and recommendations for good silvicultural practice. AMBIO: A Journal of the Human Environment, 38(7), pp.373-380.

Bishop, Kevin, and Karin Eklöf. "Boundary-Crossing Field Research Marks the Way to Evidence-Based Management of Mercury in Forest Landscapes." Journal of Geophysical Research: Biogeosciences 127, no. 8 (2022): e2022JG007065.

Bouchet, S., A.L. Soerensen, E. Björn, E. Tessier, D. Amouroux, Mercury sources and fate in a large brackish ecosystem (the Baltic Sea) depicted by stable isotopes, Environ. Sci. Technol., 2023, 57, 14340-14350

Braaten, H. F. V., Åkerblom, S., Kahilainen, K. K., Rask, M., Vuorenmaa, J., Mannio, J., ... & de Wit, H. A. (2019). Improved environmental status: 50 years of declining fish mercury levels in boreal and subarctic Fennoscandia. *Environmental science & technology*, *53*(4), 1834-1843.

Braaten, H. F. V., Lindholm, M., & de Wit, H. A. (2020). Five decades of declining methylmercury concentrations in boreal foodwebs suggest pivotal role for sulphate deposition. Science of the Total Environment, 714, 136774.

EEA, 2025. Information downloaded from https://www.eea.europa.eu/en/analysis/indicators/heavy-metal-emissions-in-europe 2025-07-29.

Eklöf, K. et al. (2024). *Declining mercury concentrations in European rivers: A multi-decadal perspective*. Environmental Pollution, 345, 124761. https://doi.org/10.1016/j.envpol.2024.124761

Eklöf, K., Fölster, J., Sonesten, L. and Bishop, K. 2012. Spatial and temporal variation of THg concentrations in run-off water from 19 boreal catchments, 2000-2010. Environmental Pollution 164, 102-109. https://doi.org/10.1016/j.envpol.2012.01.024

Faxneld S., Anne L. Soerensen. 2022.The Swedish National Monitoring Programme for Contaminants in Freshwater Biota (until 2020 year's data). Report 7:2022, Swedish Museum of Natural History, Stockholm Sweden

Faxneld, S., C. Jonsson, A. Forsberg, N. Stjärnkvist, Soerensen, A.L. (2025), Graphic and statistical overview of temporal trends and spatial variations in the Swedish National Monitoring Programme for Contaminants in Freshwater Biota (including data through 2023), Report, Swedish Museum of Natural History, Stockholm, Sweden. https://urn.kb.se/resolve?urn=urn:nbn:se:nrm:diva-5963

Hastie, T., Tibshirani, R., 1986. Generalized Additive Models. Stat. Sci. 1, 297–310. https://doi.org/10.1214/ss/1177013604

Hylander, L.D. and Meili, M., 2005. The rise and fall of mercury: converting a resource to refuse after 500 years of mining and pollution. *Critical Reviews in Environmental Science and Technology*, *35*(1), pp.1-36.

Iverfeldt, Å., Munthe, J., Brosset, C. and Pacyna, J. Long-term changes in concentration and depositon of atmospheric mercury over Scandinavia. Water, Air, Soil Pollution 80, 227-233, 1995.

Jensen S. and Jernelöv A. (1969), Biological methylation of mercury in aquatic organisms, Nature, 223, pp. 753-754.

Johnels, A., G. Tyler, and T. Westermark (1979), A history of mercury levels in Swedish fauna, *Ambio*, 160-168.

Josefsson, S. (2022). *Contaminants in Swedish offshore sediments 2003–2021*. SGU Rapport 2022:08. https://urn.kb.se/resolve?urn=urn:nbn:se:naturvardsverket:diva-10289

KEMI (2025). *Brief facts about the regulations for mercury*. https://www.kemi.se/en/rules-and-regulations/additional-eu-rules/mercury/brief-facts-about-the-regulations-for-mercury, accessed on 12 Aug 2025

Leipe, T., M. Moros, A. Kotilainen, H. Vallius, K. Kabel, M. Endler, N. Kowalsi (2013), Mercury in Baltic Sea sediments - Natural background and anthropogenic impacts. Chemie der Erde 249-259.

Li C, Jiskra M, Nilsson MB, Osterwalder S, Zhu W, Mauquoy D, Skyllberg U, Enrico M, Peng H, Song Y, Björn E. Mercury deposition and redox transformation processes in peatland constrained by mercury stable isotopes. Nature Communications. 2023 Nov 15;14(1):7389.

Lindqvist, O., Johansson, K., Bringmark, L., Timm, B., Aastrup, M., Andersson, A., … & Meili, M. (1991). Mercury in the Swedish environment—recent research on causes, consequences and corrective methods. *Water, Air, and Soil Pollution*, *55*(1), xi-261.

Munthe, J., Bodaly, R.A., Branfireun, B.A., Driscoll, C.T., Gilmour, C.C., Harris, R., Horvat, M. Lucotte, M and Malm O. 2007. Recovery of mercury-contaminated fisheries. AMBIO: A Journal of the Human Environment, 36(1), 33-44.

Naturvårdsverket (2024). *Nedfall av metaller i regional bakgrund – årsdeposition*. Online, accessed on 16 July 2025

Naturvårdsverket 2025. Information downloaded from https://www.naturvardsverket.se/data-och-statistik/luft/utslapp/utslapp-av-kvicksilver-till-luft/. Accessed on 2025-07-29

Naturvårdsverket (2016), Wastewater treatment in Sweden 2016, report available at: https://naturvardsverket.diva-portal.org/smash/record.jsf?pid=diva2:1503600, Naturvårdsverket, Stockholm, Sweden

Pedersen, E.J., Miller, D.L., Simpson, G.L., Ross, N., 2019. Hierarchical generalized additive models in ecology: an introduction with mgcv. PeerJ 7, e6876. https://doi.org/10.7717/peerj.6876

Peng, H., Zhang, X., Bishop, K., Marshall, J., Nilsson, M.B., Li, C., Bjorn, E. and Zhu, W., 2024. Tree Rings Mercury Controlled by Atmospheric Gaseous Elemental Mercury and Tree Physiology. *Environmental Science & Technology*, *58*(38), pp.16833-16842.

Porvari, P., Verta, M., Munthe, J. and Haapanen, M., 2003. Forestry practices increase mercury and methyl mercury output from boreal forest catchments. Environmental science & technology, 37(11), pp.2389-2393.

Rydberg, J., V. Gälman, I. Renberg, R. Bindler (2008), Assessing the stability of mercury and methylmercury in a varved lake sediment deposit, Environmental Science and Technology 42, 4391-4396.

SCB (2022), Discharges to water and sewage sludge production in 2022 Municipal wastewater treatment plants, pulp and paper industry and some other industries, report available at: https://www.scb.se/publikation/58299, Naturvårdsverket and Statistic Central Byrån, Stockholm, Sweden

Soerensen and Faxneld (2022). Graphic and statistical overview of temporal trends and spatial variations within the Swedish National Monitoring Programme for Contaminants in Marine Biota (until 2020 year's data), 5:2022, Swedish Museum of Natural History, Stockholm, Sweden.

Soerensen, A.L., C. Jonsson, A. Forsberg, J. Eliassen, N. Stjärnkvist and S. Faxneld (2025), The Swedish National Monitoring Programme for Contaminants in Marine Biota (until 2023 year's data) - temporal trends and spatial variations, Report, Swedish Museum of Natural History, Stockholm, Sweden

Soerensen, A.L., A.T. Schartup, A. Skrobonja, E. Björn (2017), Organic matter drives high interannual variability in methylmercury concentrations in a subarctic coastal sea, Environmental Pollution, 229, 531-538, doi: 10.1016/j.envpol.2017.06.008

Soerensen, A.L., A. Schartup, E. Gustafsson, B. G. Gustafsson, E. Undeman, E. Björn (2016), Eutrophication increases plankton methylmercury concentrations. Environmental Science and Technology, 50, 11787–11796, doi:10.1021/acs.est.6b02717

Sun, J., R. Bossi, J. O. Bustnes, B. r. Helander, D. Boertmann, R. Dietz, D. Herzke, V. L. Jaspers, A. L. Labansen, and G. Lepoint (2019), White-tailed eagle (Haliaeetus albicilla) body feathers document spatiotemporal trends of perfluoroalkyl substances in the northern environment, *Environ. Sci. Technol.*, *53*(21), 12744-12753.

Westermark, T., Odsjö, T. and Johnels, A.G., 1975. Mercury content of bird feathers before and after Swedish ban on alkyl mercury in agriculture. Ambio, pp.87-92.

Westöö, G. (1966), Determination of Methylmercury Compounds in Foodstuffs, Acta Chimica Scandinavica 20, pp. 2131-2137.

Wood, S.N., 2017. Generalized additive models: an introduction with R, Second edition. ed, Chapman & Hall/CRC texts in statistical science. CRC Press/Taylor & Francis Group, Boca Raton.

Wu, P., Bishop, K., von Brömssen, C., Eklöf, K., Futter, M., Hultberg, H., Martin, J. and Åkerblom, S., 2018. Does forest harvest increase the mercury concentrations in fish? Evidence from Swedish lakes. Science of the Total Environment, 622, pp.1353-1362.

Zhang, X., Peng, H., Osterwalder, S., Bishop, K., Nilsson, M.B., Peichl, M., Björn, E. and Zhu, W., 2025. Limited response of boreal forest litterfall mercury deposition to declines in atmospheric mercury concentrations (1987–2000). *Environmental Pollution*, *383*.

Åkerblom, S., Bignert, A., Meili, M. et al. Half a century of changing mercury levels in Swedish freshwater fish. *AMBIO 43 (Suppl 1), 91–103 (2014).* https://doi.org/10.1007/s13280-014-0564-1

Integrated Analysis of Mercury in the Derwent Estuary, Australia

Authors:

Olha Furman (OESG member- Australia)

Akira Weller-Wong (the Derwent Estuary Program Scientist)

1. Description of the case study

The Derwent Estuary covers an area of about 200 km^2 and is an integral part of Tasmania's natural, cultural and economic heritage (Macleod & Coughanowr, 2019) in Australia. It supports diverse urban, industrial, and recreational uses (Macleod & Coughanowr, 2019). Historically, the estuary has been impacted by the operations of a large zinc smelter (in operation since 1917) and a paper mill (established in 1941). Although modern environmental management practices have significantly improved, the legacy of past industrial activity continues to affect the estuary and is likely to persist for decades.

Several environmental issues affect the Derwent Estuary, including contamination by metals, loss of habitats and species, introduced pests, weeds, altered river flow regimes, blocked migratory pathways for fish and eels, elevated nutrients, algal growth and hypoxia in localised areas (Macleod & Coughanowr, 2019).

The Derwent Estuary Program, initiated in 1999, plays a central role in advancing the understanding and management of these issues. Cooperative monitoring arrangements with the State Government, industries, local governments and the scientific community have generated a wealth of information on water and sediment quality, seafood safety and estuarine habitats and species (DEP, 2020, 2021). Metal levels in the Derwent sediments, water column, fish and some invertebrates have been monitored for several decades (Bloom & Ayling, 1977; Macleod & Coughanowr, 2019; Ratkowsky et al., 1975; Whitehead, 2013) (Figures 1a, b and c). Additional data on mercury emissions and releases is available through both the Australia's National Pollutant Inventory and industry reports (NPI, 2025; Nyrstar, 2025).

These monitoring datasets represent one of the rare long-term environmental data series from the Southern Hemisphere, a region often underrepresented in global data collection efforts. Moreover, these datasets reflect a commitment to responsible management, collaboration, and the generation of knowledge.

2. Cross-media integration of observed levels/trends

The Derwent Estuary contains some of the highest recorded concentrations of mercury, zinc, lead, and cadmium in sediments compared to other estuaries worldwide (Jones, 2013; Macleod & Coughanowr, 2019). While the primary source of these metals is historical industrial activity, ongoing contributions from fugitive dust, diffuse groundwater inflows, and point-source discharges from current operations may continue to influence both bound and soluble metal levels in the estuary (Nyrstar, 2025).

Modern control measures

Zinc metal production in Hobart involves several key stages: ore concentration (crushing and flotation), roasting, leaching, purification, and electrolysis. The zinc ore, primarily a sulfide

mineral, is roasted to convert zinc sulfide to zinc oxide, releasing sulfur dioxide (SO_2) and other impurities, including mercury, in the process.

In Tasmania, emissions from the Hobart zinc smelter are regulated under the *Environmental Management and Pollution Control Act (1994)* through an environmental permit issued by Environment Protection Agency of Tasmania (EPA Tasmania, 2024). The facility implements a range of control measures to reduce emissions of both legacy and current contaminants to the Derwent Estuary.

The implementation of modern control measures began in the 1980s, marking a significant shift in environmental management practices. To control air emissions, the zinc smelter uses electrostatic mist precipitators, wet scrubbers, chemical absorption systems, and filters to remove particulate matter and pollutants from the gas stream before atmospheric release (Nyrstar, 2025). These systems are generally effective at capturing particle-bound mercury and some oxidised divalent mercury species, but they are less effective at removing elemental mercury vapour (UNEP, 2021). To address this, the gas scrubbing process at the Hobart zinc smelter also includes a specific mercury removal step, utilising the Boliden-Norzink process which converts elemental mercury into mercury(I) chloride (calomel) via reaction with mercury(II) chloride. The calomel is then treated with sodium hypochlorite to regenerate the scrubbing solution. Minor amounts of excess calomel are stored onsite for reuse when required, or if necessary, stabilised and disposed of with other site mercury bearing wastes.

Mercury containing wastewater is treated via a dedicated mercury removal plant. The process generates mercury filter cake, which is currently managed through chemical stabilisation and disposal at an approved facility (Nyrstar, 2025).

The refinery also generates significant quantities of process wastewater, stormwater and recovered groundwater. These are treated using lime neutralisation, flocculation, reverse osmosis and dilution before being discharged to the Derwent River (Nyrstar, 2025).

A comprehensive environmental monitoring program is currently in place to track mercury concentrations across multiple compartments (Nyrstar, 2025).

Emissions/releases

Mercury and its compounds are reported under the Australian National Pollutant Inventory (NPI, 2025). Environmental monitoring indicates that total mercury is primarily released to surface waters, with smaller quantities emitted to the atmosphere (Figure 2). Historically, atmospheric mercury emissions from the smelter, in the absence of effective control measures, were likely a significant source of mercury contamination in the Derwent Estuary.

Between 2007 and 2022, annual mercury emissions to air decreased significantly from 21.3 kg to 1.52 kg reflecting the effectiveness of multiple control measures implemented during this period (Figure 2).

In contrast, annual mercury releases to the Derwent Estuary via discharge outfalls—which receive flows from the effluent treatment plant and tail gas scrubber—ranged from 9.42 kg to 39.17 kg between 2007 and 2022 (Figure 2). Between 2019 and 2024, total mercury concentrations in water, discharged via the outfall to the Derwent Estuary, remained elevated (minimum: 0.15 µg/L, mean: 0.9 µg/L, maximum: 6.1 µg/L) compared to concentrations

recorded during 2016–2018(Nyrstar, 2025). This increase is attributed to ongoing maintenance of the electrostatic mist precipitators and the tail gas scrubbing system (Nyrstar, 2025).

Groundwater is not considered a primary source of mercury contamination in the Derwent Estuary (personal communication with the Derwent Estuary Program scientist).

Mercury observations in ambient water and sediments

Estuarine waters adjacent to the Hobart smelter exhibit low total mercury concentrations, a pattern commonly observed in receiving estuaries where metals tend to partition into sediments, thereby reducing levels in the water column. Between 2000 and 2024, most monthly mercury measurements in ambient water were below the laboratory reporting limit of 0.05 µg/L (DEP, 2020). However, during this period, 51 exceedances of the laboratory reporting limit were reported, including 16 instances where mercury concentrations exceeded the Australian and New Zealand 99% species protection guideline of 0.1 µg Hg /L for marine waters. These exceedances occurred in the industrialised section of the estuary, near the smelter.

Most sediments in the estuary do not meet national sediment quality guidelines for mercury, with highly contaminated sediments extending approximately 40 km downstream from the zinc smelting operations (Whitehead, 2013) (Figure 3). At most sites in proximity to the smelter, mercury concentrations exceeded the upper national sediment quality guideline value of 1.0 mg Hg (inorganic)/kg dry weight (Raes et al., 2022). Mercury concentrations in surface sediments vary spatially throughout the estuary, with the highest concentrations observed near the zinc smelter (Raes et al., 2022; Whitehead, 2013). Data from the annual New Town Bay Sediment Quality Monitoring Program indicate some variability in metal concentrations, including total mercury. However, no consistent trends were observed near the zinc smelter over the 2000–2024 period (Figure 4) (Nyrstar, 2025).

Mercury observations in invertebrates

To monitor bioavailability to organisms, oysters have been deployed annually to surface waters throughout the estuary and then retrieved to measure the concentration of accumulated metals including mercury (Nyrstar, 2025). Wild oysters and mussels were also collected on a triennial basis to determine possible human health risks of exposure to metals through collection of wild shellfish (Nyrstar, 2025). Oysters and mussels are exposed to both particulate-bound and dissolved mercury through filter feeding and direct absorption from the water column. As effective bioindicators, they exhibited changes in mercury concentrations influenced by anthropogenic inputs and environmental factors such as sediment resuspension and water quality.

Deployed oysters at nine impacted sites in the middle estuary accumulated higher concentrations of mercury than those deployed to the control site (Mickey's Bay) and showed the highest loads from sites nearest to the zinc smelter (Nyrstar Wharf) (DEP, 2020, 2021) between 2014 and 2024 (Figure 5a).

Wild oysters and mussels collected in the middle (near the zinc smelter) and lower zones of the Derwent Estuary showed higher concentrations of mercury than those from sites furthest from zinc smelting activities (the D'Entrecasteaux Channel and Mickey's Bay) (Figures 5b and c).

Within the estuary, the highest concentrations were typically recorded in the middle estuary and Ralphs Bay, whilst the western shore exhibited the lowest levels. These spatial patterns likely reflect the influence of estuarine circulation, ambient water metal concentrations, proximity to contaminant sources, estuarine processes and longer water and sediment retention times at Ralphs Bay. Sites in the middle estuary are closest to the zinc smelter, whereas marine-influenced regions, such as the western shore, are generally exposed to lower concentrations of metals in the water column.

In 2025, the Derwent Estuary Program scientists assessed mercury temporal trends in deployed oysters using the Harmonised Regional Seas Assessment Tool (HARSAT) being developed as a collaboration between AMAP (Arctic Monitoring and Assessment Programme), HELCOM (Baltic Sea Regional Seas Convention) and OSPAR (NE Atlantic Regional Seas Convention) (Ltd., 2025) (see Annex 2 for further details). Between 2004 and 2024, four sampling sites, including the control site, showed no statistically significant trends in mercury concentrations in deployed oysters. In contrast, six impacted sites within the estuary exhibited significant linear or nonlinear trends. At three of these sites, mercury concentrations increased annually by 1.6% to 3.4% over the 2004-2024 period (Figure 6a).

Mercury observations in fish

Environmental organisms at higher trophic levels are primarily exposed to organic mercury through dietary sources. Sand flathead (*Platycephalus bassensis*) were selected as bio-indicators of metal contamination because of their high site fidelity, abundance and regular consumption by humans (Jones et al., 2013; Ratkowsky et al., 1975). Sand flathead are benthic carnivores, most likely exposed to mercury through dietary intake of epibenthic fauna such as crabs, which in turn feed at the sediment surface where methyl mercury can be produced(Jones, 2013). Sand flathead also show high site fidelity and a relatively small home range (~5-10 km) with limited migration downstream during the spring/summer, presumably for spawning purposes(Tracey et al., 2020).

The control region (Mickey's Bay) mercury concentrations in fish (0.20 ± 0.02 mg kg^{-1}) were significantly lower than mercury concentrations in fish from within the Derwent Estuary (0.49 ± 0.01 mg kg^{-1}) between 1975 and 2011(Jones et al., 2013).

In 2025, the Derwent Estuary Program scientists plotted current mercury concentrations in fish (Figure 5d). Mercury concentrations in fish from the control site (Mickey's Bay) were lower than those measured in fish collected from within the Derwent Estuary during 2014–2024. The observed spatial variability in mercury concentrations across impacted sites is likely influenced by differences in fish growth rates(Jones, 2013) and potentially greater mercury bioavailability and longer water and sediment retention times in Ralphs Bay (Ralphs Bay Spit and Richardson Beach)(Jones et al., 2014).

Assessing the temporal change of Hg bioaccumulation in fish is complicated by shifts in habitat, fish length, growth rates, prey preferences and the potential for seasonal movements or migration (Jones, 2013). Jones et al 2013 used linear and non-linear models to examine spatial and temporal variations between regions. The authors concluded that calculating length-standardized mercury concentrations are important to accurately evaluate spatial and temporal trends. Both linear (data from 1974-2011) and non-linear models (data from 1991-2011) that

take into consideration the fish biometrics, showed no significant change in mercury concentrations over sampling time despite reductions of mercury inputs (Jones et al., 2013).

In 2025, the Derwent Estuary Program scientists used the Harmonised Regional Seas Assessment Tool (HARSAT) to assess long-term trends in mercury concentrations in fish across sampling sites. No statistically significant trends were detected across all sites between 2002 and 2024, consistent with the findings of Jones et al. (2013) (Figure 6b). In the current study, length standardisation was not applied due to lack of log-linear relationship between mercury concentration and fork length. However, applying the length-standardisation method described by Jones et al. (2013) may be appropriate for adjusting mercury concentrations for fish size in future trend analyses.

Mercury observation in birds

Methylmercury is absorbed largely through the diet, and birds which feed on fish and other aquatic organisms are most at risk of exposure (Einoder et al., 2018). Biomagnification of mercury has been observed in the piscivorous birds residing in the Derwent Estuary, with concentrations reaching levels considered toxic (Einoder et al., 2018). For example, feathers collected near the refinery showed mercury concentrations of 24.8 ± 4.8 mg Hg/kg dry weight in White-bellied Sea-Eagles and 19.3 ± 6.9 mg Hg/kg dry weight in Black-faced Cormorants (Einoder et al., 2018).

Human consumption advice

Understanding mercury concentrations in fish and invertebrates remain crucial as a mechanism for monitoring and in protecting humans who consume seafood. Observed mercury concentrations in deployed oysters and wild oysters and mussels are significantly lower than Food Standards Australia and New Zealand national guidelines for mercury (Maximum Permitted Limit; 0.5 mg kg^{-1}) over last two decades (DEP, 2020, 2021; Nyrstar, 2025).

Of all the legal sized flathead sampled from the Derwent in the 2014-2022 period (n=325), 68.5% had a mercury concentration exceeding Food Standards Australia and New Zealand national guidelines for mercury (Maximum Permitted Limit; 0.5 mg kg^{-1})(DEP, 2020, 2021).

The following advice has been published by the Director of Public Heath (DEP 2021):

- Do not eat fish from the Derwent more than twice a week and the following people should further limit their consumption to once a week:
    - Pregnant and breastfeeding women
    - Women who are planning to become pregnant
    - Children aged six years and younger
- When eating fish from the Derwent, it is best to avoid eating fish from other sources in the same week.

Key Findings

The Derwent Estuary case highlights complex and persistent mercury contamination issues. Modern control measures have substantially reduced mercury emissions from industrial activities over recent decades. However, elevated mercury concentrations in fish and invertebrates at impacted sites, compared to control sites, indicate that historical contamination remains a major source of exposure.

Metal concentrations in all biota were consistently lower at the control site (Mickeys Bay) compared to impacted sites within the Derwent Estuary. Mercury spatial patterns in biota likely reflect the influence of proximity to contaminant sources, estuarine circulation, and estuarine processes. For example, elevated mercury concentrations in biota from Ralphs Bay, despite its greater distance from the zinc smelter, suggest additional environmental factors influencing mercury bioavailability and bioaccumulation in this region. Ralphs Bay has been previously characterised by longer water and sediment retention times and greater mercury bioavailability.

There were some differences in temporal trends between deployed oysters and resident benthic fish, likely reflecting distinct exposure pathways and bioaccumulation mechanisms. Despite reductions in total anthropogenic mercury inputs over the past two decades, no significant temporal decline in mercury concentrations in fish has been observed between 2002 and 2024. In comparison, mercury concentrations in deployed oysters showed either no significant changes or increased annually by 1.6% to 3.4% over 2004-2024. Although these concentrations in deployed oysters remain well below thresholds of concern for human health, further investigation and predictive modelling are required to better understand the processes driving these observed changes. An assessment of the mercury discharge from industrial activities, environmental and biogeochemical drivers, such as climatic conditions (wind and rainfall), sediment geochemistry, co-contaminants, mercury methylation, and food-web dynamics is suggested as all these processes and inputs may influence mercury bioavailability in surface deployed oysters.

Overall, the results suggest that significant reductions in anthropogenic mercury inputs achieved to date have not translated into corresponding decreases in mercury concentrations in fish and oysters. This highlights the complexity of mercury cycling processes and interactions within the Derwent Estuary, as well as the need for long-term monitoring and targeted management strategies.

3. Relevance to effectiveness evaluation

The Minamata Convention has elevated global awareness of mercury as an environmental hazard, prompting regulatory action across jurisdictions. In response, many zinc smelters have implemented control measures, including mercury removal technologies (UNEP, 2021).

This case study provides a rare and detailed examination of mercury cycling within an estuarine environment impacted by modern and historical zinc smelting activities. The site's current environmental permit sets discharge and emission limits for mercury and mandates ongoing monitoring of estuarine water, sediment, and biota. This enables timely and effective responses to any increases in environmental mercury exposure.

Over the past two decades, modern control measures have effectively reduced mercury emissions. However, elevated mercury concentrations in fish and invertebrates at impacted sites suggest that historical contamination, resulting from the absence of earlier regulatory controls, remains a significant source of exposure.

These findings are directly relevant to the effectiveness evaluation under the Minamata Convention, particularly Articles 8 and 9, which address emissions and releases. The metal

production and processing sector is a large anthropogenic source of mercury emissions and releases globally, and its contribution is likely to grow (UNEP, 2021). To mitigate associated mercury risks, the adoption of best available techniques (BAT) and best environmental practices (BEP) is essential to help minimise mercury emissions and releases. Without appropriate control measures, elevated mercury levels in impacted environment and biota are likely to persist for multiple decades, posing potential ecological and human health risks.

3. Gaps, Limitations and Recommendations

While this case study provides clear evidence of cross-media mercury contamination resulting from historical and potentially current industrial activities, several important gaps and limitations should be acknowledged.

First, sediment coring could offer valuable insights into mercury deposition rates and help assess the effectiveness of mercury reduction measures implemented over last few decades.

Second, key factors influencing methylation potential and bioaccumulation remain poorly understood. A strong correlation between total mercury and selenium in both sediments and fish suggests that selenium may play a significant role in modulating the ecological impacts of mercury contamination (Jones, 2013; Jones et al., 2014). This highlights the importance of including selenium dynamics in future scientific assessments of mercury methylation and bioaccumulation.

Third, integrating isotope tracing within the Derwent Estuary could yield critical information on mercury sources, transport pathways, speciation and bioavailability, thereby enhancing our understanding of mercury cycling in estuarine systems.

Finally, predictive models that link changes in anthropogenic inputs and environmental factors to mercury species accumulation in the food web are needed to evaluate the effectiveness of pollution control measures. Such models would support evidence-based decision-making and guide future remediation and management efforts.

Annex 1. Figures

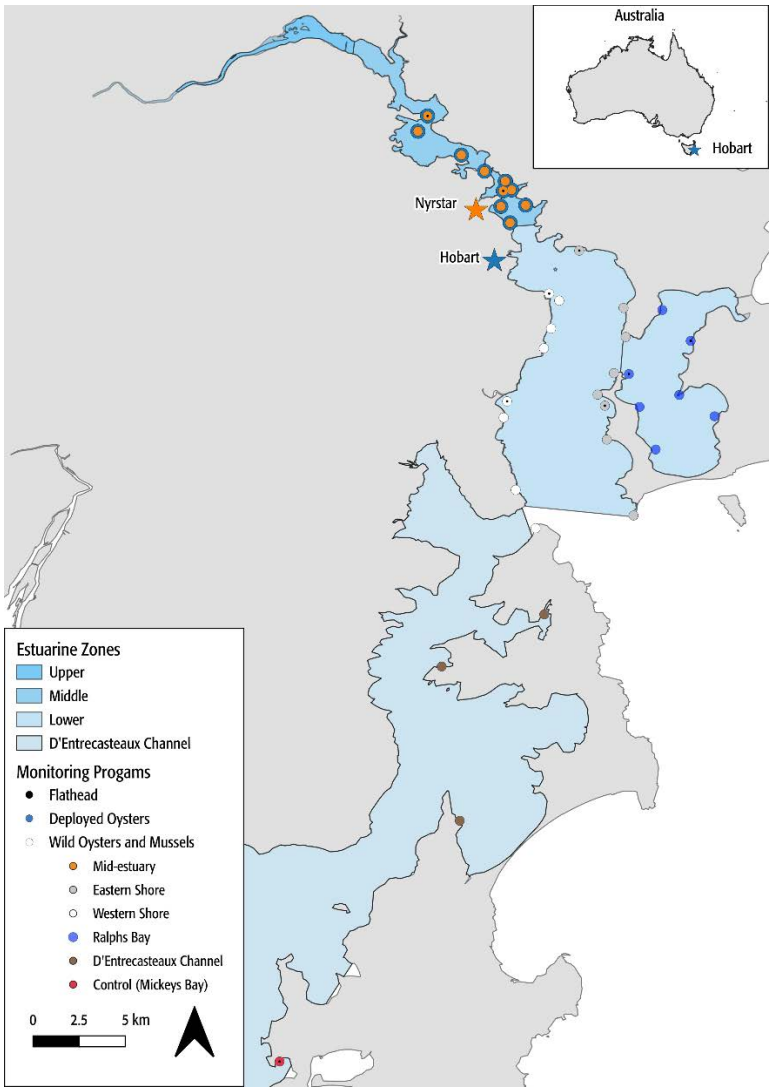

Figure 1a. Derwent Estuary Program fish (flathead), deployed oysters, wild oysters and mussels sampling locations.

Figure 1b. Derwent Estuary Program fish (flathead) and deployed oysters sampling locations.

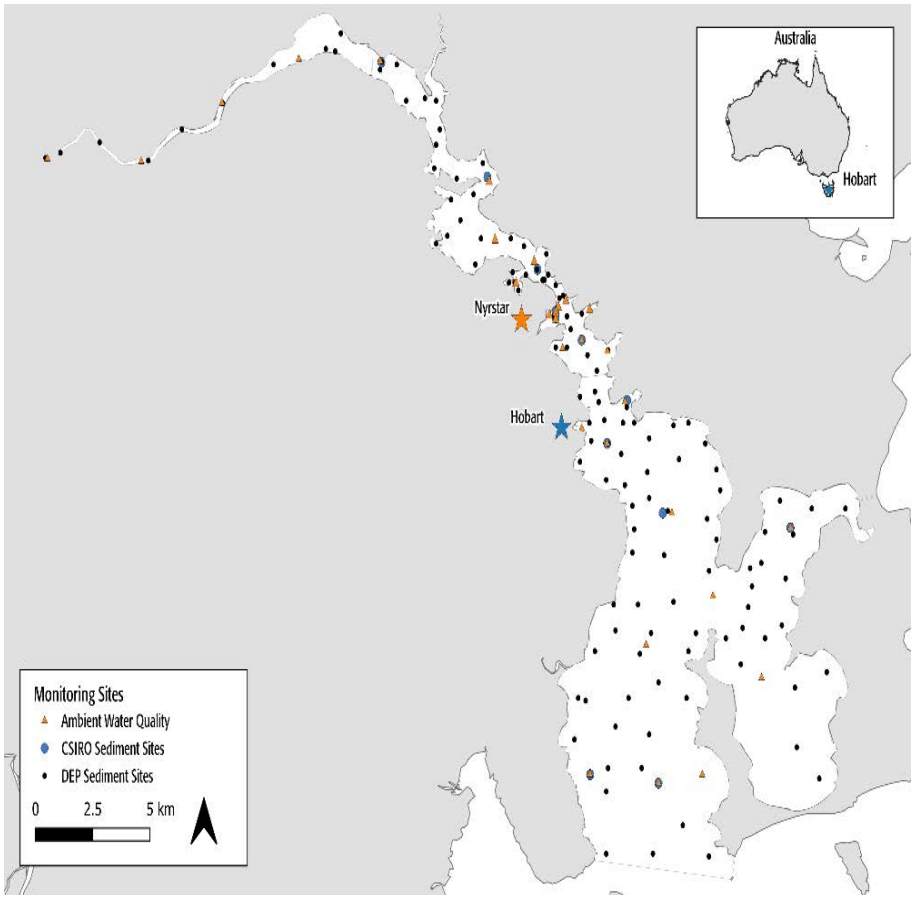

Figure 1c. Derwent Estuary Program water quality and sediment and CSIRO sediment sampling locations.

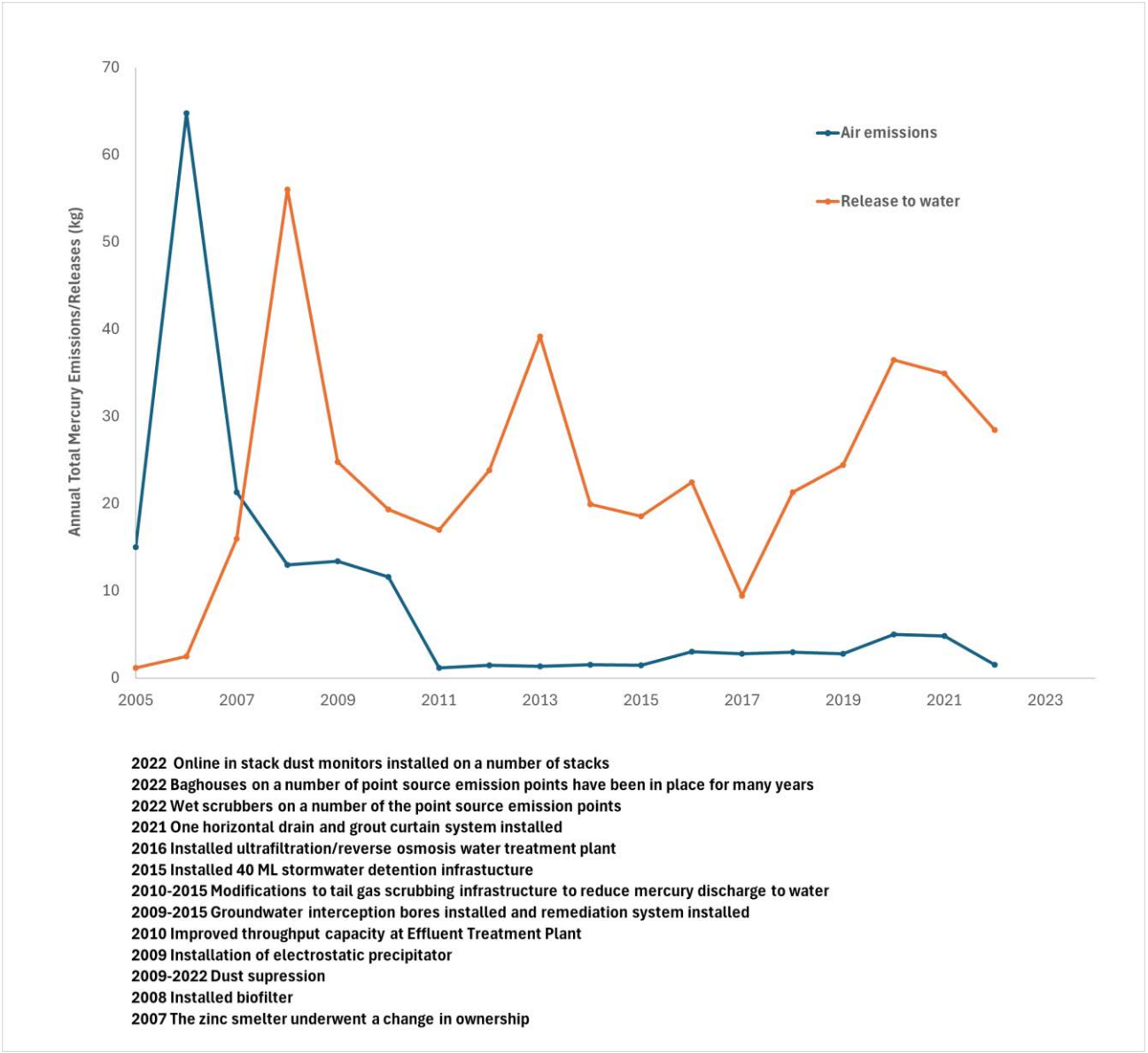

Figure 2. Annual total mercury emissions to the air and releases to the surface water at the Hobart Zinc Smelter. Total air emissions are calculated with a combination of direct measurements and emission factors. Mercury emissions and releases from point sources are based on direct measurements. A monitoring program at the facility is conducted to quantify emissions/releases from multiple point emission/discharge points to determine compliance with Environmental Licence and the National Pollutant Inventory Reporting requirements. Stack monitoring is conducted by an independent NATA accredited organisation. Additionally, two daily 24-hour composite samples taken from discharge outfall (which receives flows from the effluent treatment plant and tail gas scrubber) are analysed for pH, iron, sulphate, copper, cadmium, mercury, lead and zinc and the flow rate is measured for reporting purposes. Sources: Australia's National Pollutant Inventory data and Nyrstar Hobart Triennial Public Report 2022-2024.

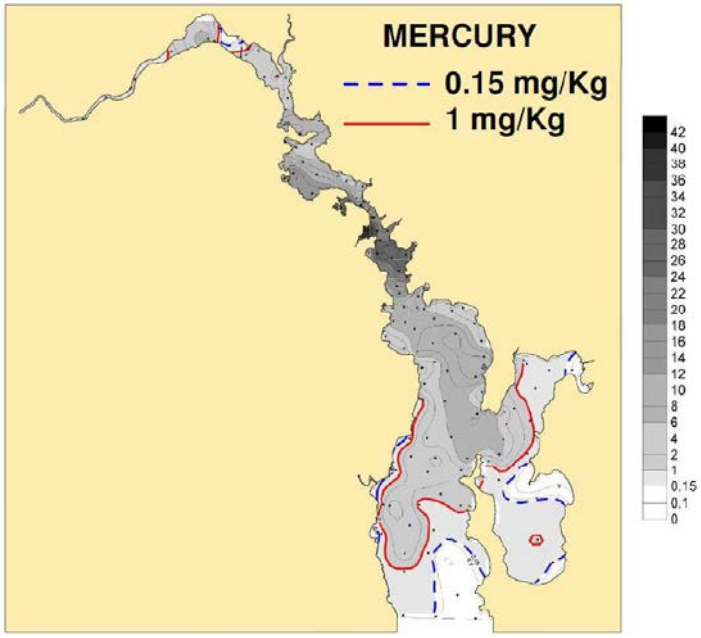

Figure 3. Total Mercury (Hg) distribution in surface sediments from the Derwent Estuary 2011 survey (Whitehead, 2013).

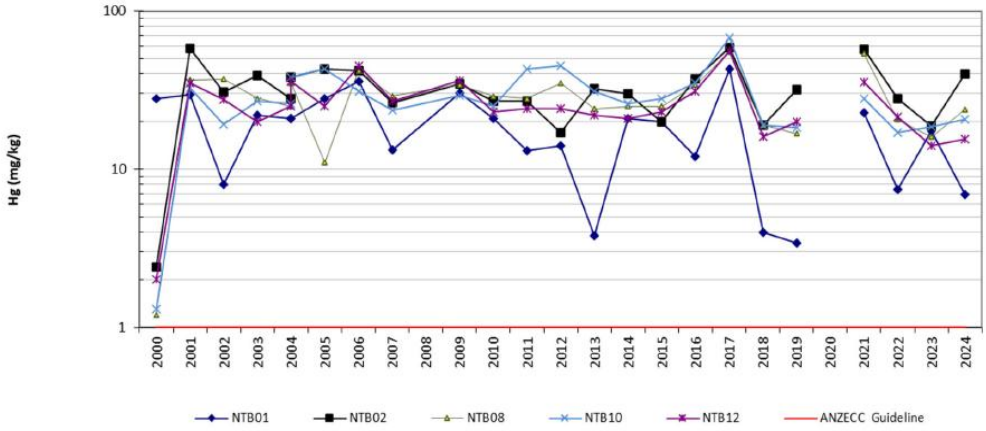

Figure 4. Total mercury concentrations in New Town Bay sediments. Source: Nyrstar Hobart Triennial Public Report 2022-2024.

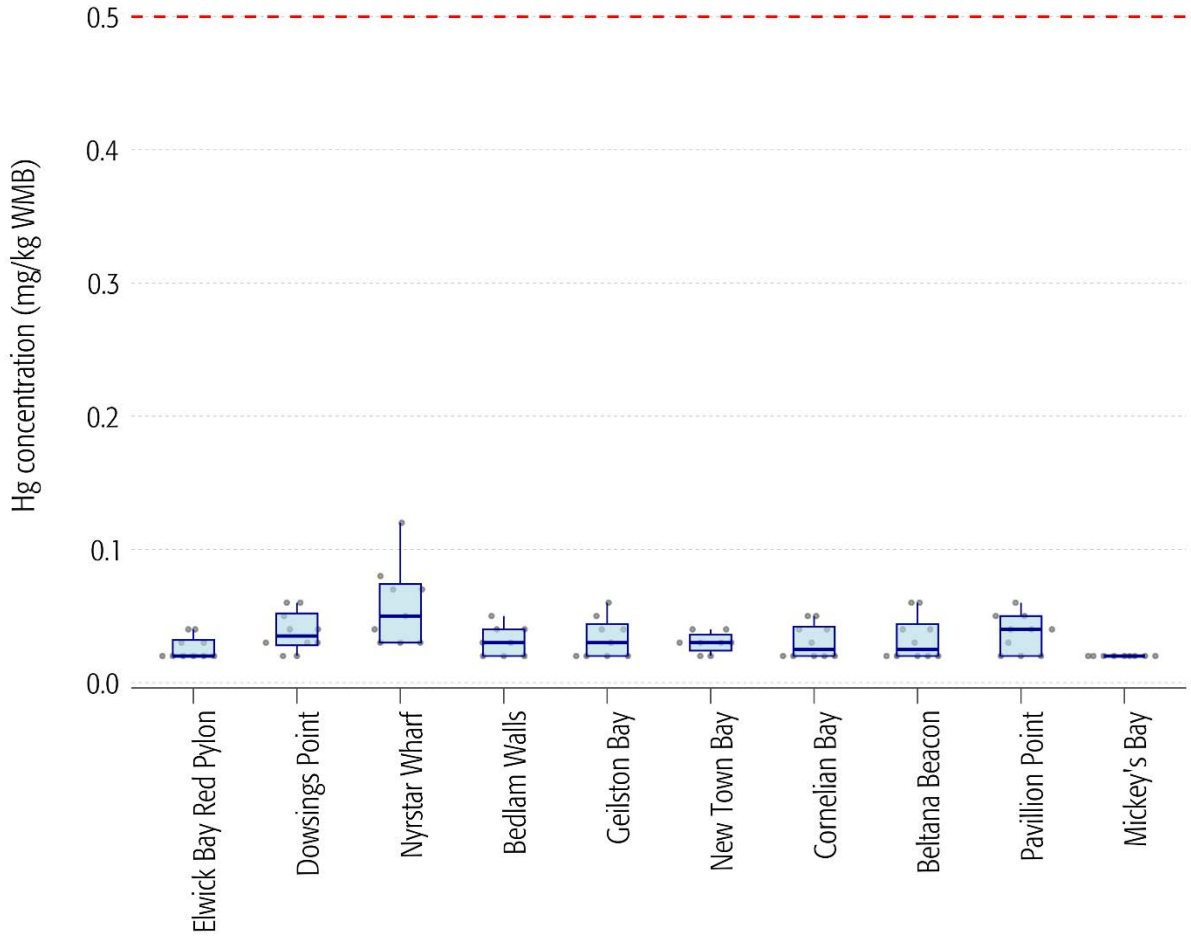

Figure 5a. Total mercury concentrations in surface-deployed Pacific Oysters' soft tissues (2014-2024). Box plots show the minimum, 20th percentile, median, 80th percentile and maximum concentrations at nine impacted sampling sites in the middle estuary and a control site in Mickey's Bay. Grey dots show the raw data. Horizontal red line represents Food Standards Australia and New Zealand national guideline for mercury (Maximum Permitted Limit; 0.5 mg kg^{-1}). Mercury concentrations are expressed in mg/kg wet matter basis (WMB). Outliers were removed using the interquartile range (IQR) method. Values that were more than 1.5 times the IQR below the first quartile or above the third quartile were excluded.

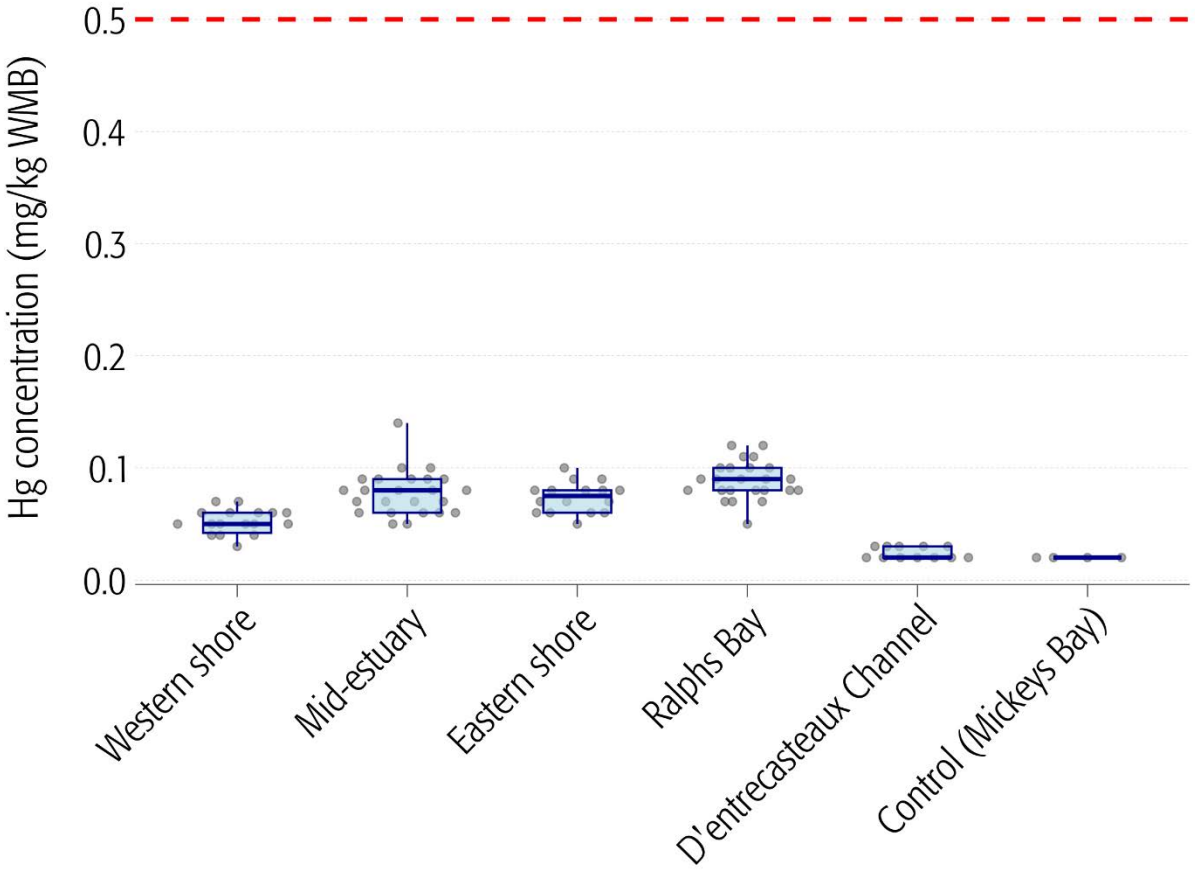

Figure 5b.

Total mercury concentrations in wild mussels' soft tissues (2014-2024). Box plots show the minimum, 20th percentile, median, 80th percentile and maximum concentrations at five regions and a control site in Mickeys Bay. Grey dots show the raw data. Horizontal red line represents Food Standards Australia and New Zealand national guideline for mercury (Maximum Permitted Limit; 0.5 mg kg^{-1}). Mercury concentrations are expressed in mg/kg wet matter basis (WMB). Outliers were removed using the interquartile range (IQR) method. Values that were more than 1.5 times the IQR below the first quartile or above the third quartile were excluded.

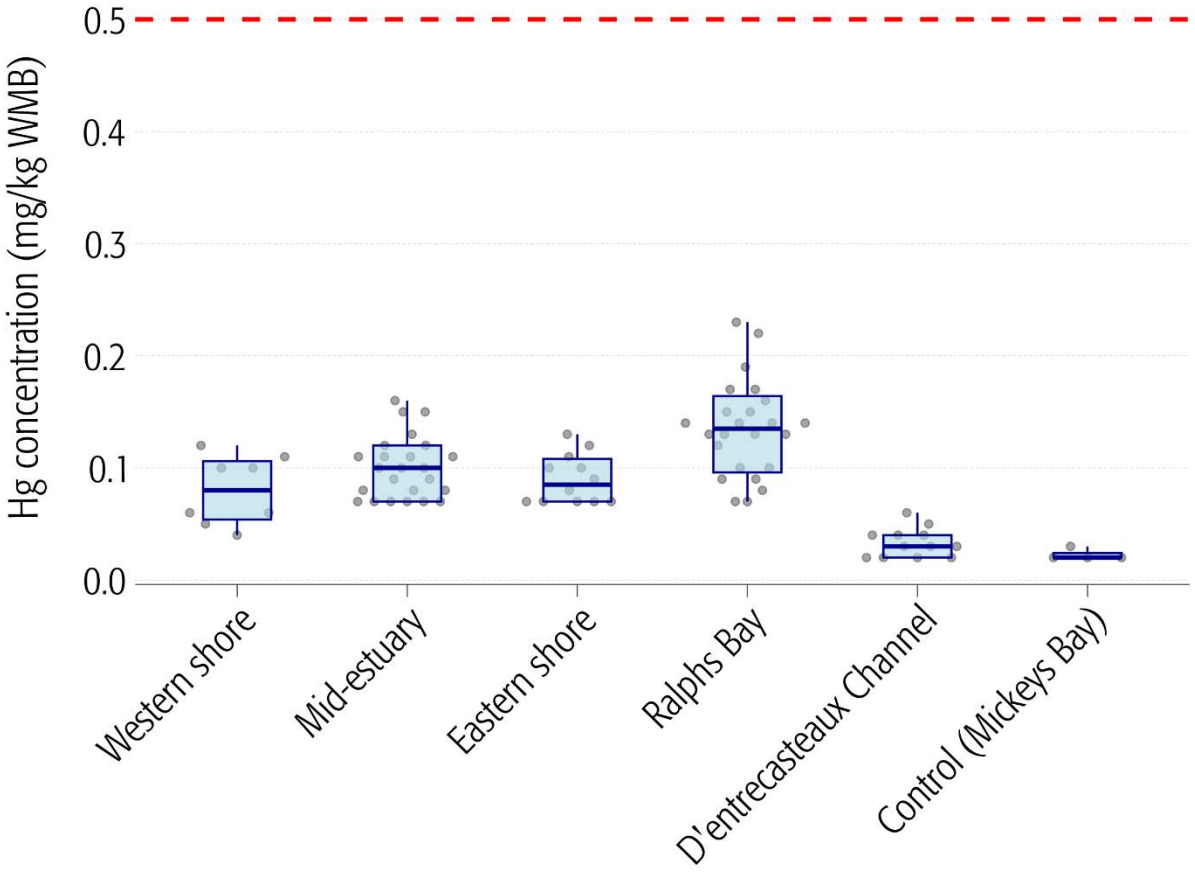

Figure 5c.

Total mercury concentrations in wild oysters' soft tissues (2014-2024). Box plots show the minimum, 20th percentile, median, 80th percentile and maximum concentrations at five regions and a control site in Mickeys Bay. Grey dots show the raw data. Horizontal red line represents Food Standards Australia and New Zealand national guideline for mercury (Maximum Permitted Limit; 0.5 mg kg^{-1}). Mercury concentrations are expressed in mg/kg wet matter basis (WMB). Outliers were removed using the interquartile range (IQR) method. Values that were more than 1.5 times the IQR below the first quartile or above the third quartile were excluded.

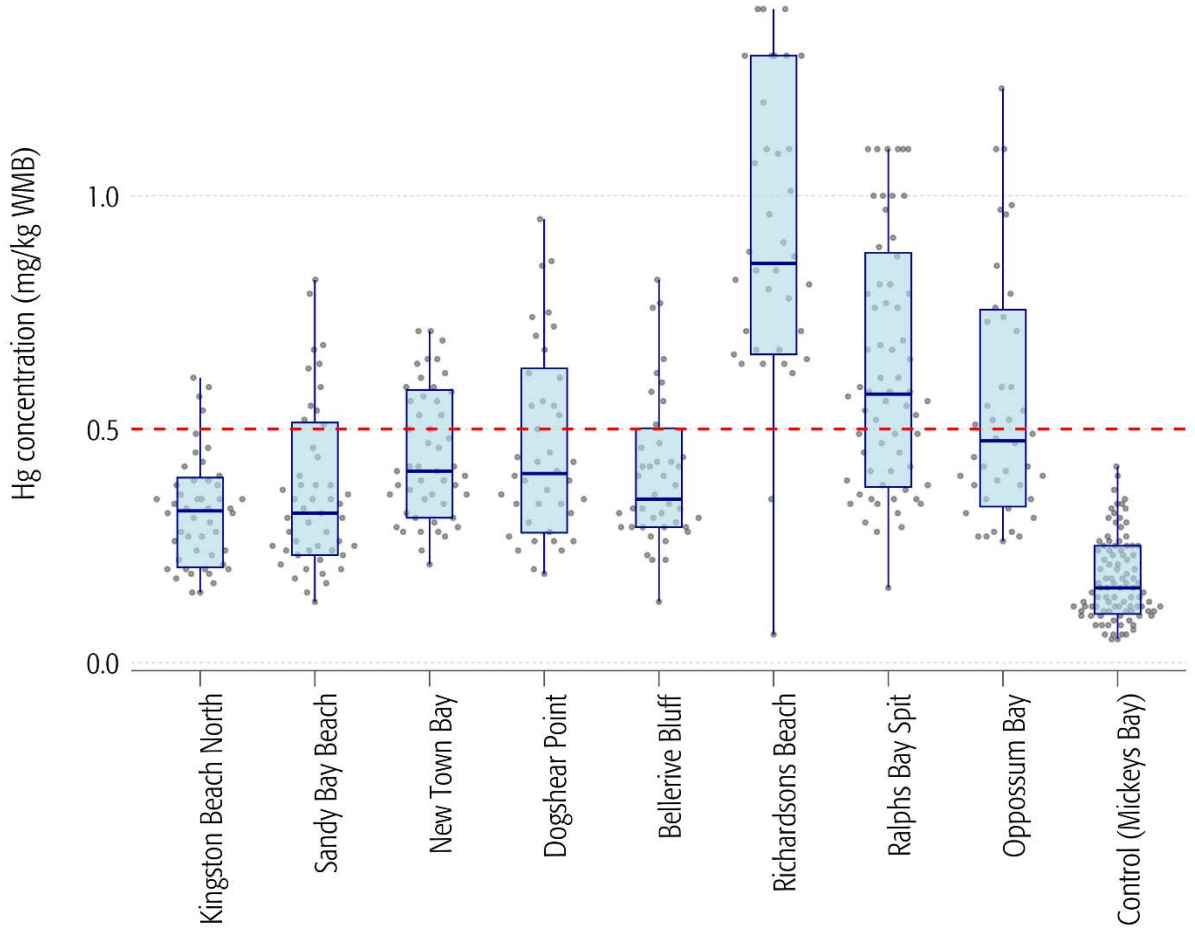

Figure 5d.

Total mercury concentrations in fish (flathead) muscle tissues (2014-2024). Box plots show the minimum, 20th percentile, median, 80th percentile and maximum concentrations at eight impacted sampling sites and a control site in Mickeys Bay. Grey dots show the raw data. Horizontal red line represents Food Standards Australia and New Zealand national guideline for mercury (Maximum Permitted Limit; 0.5 mg kg^{-1}). Mercury concentrations are expressed in mg/kg wet matter basis (WMB). Outliers were removed using the interquartile range (IQR) method. Values that were more than 1.5 times the IQR below the first quartile or above the third quartile were excluded. 2018 data points were removed because the skin was left on and data was erroneous. Mercury concentrations were not length-standardised.

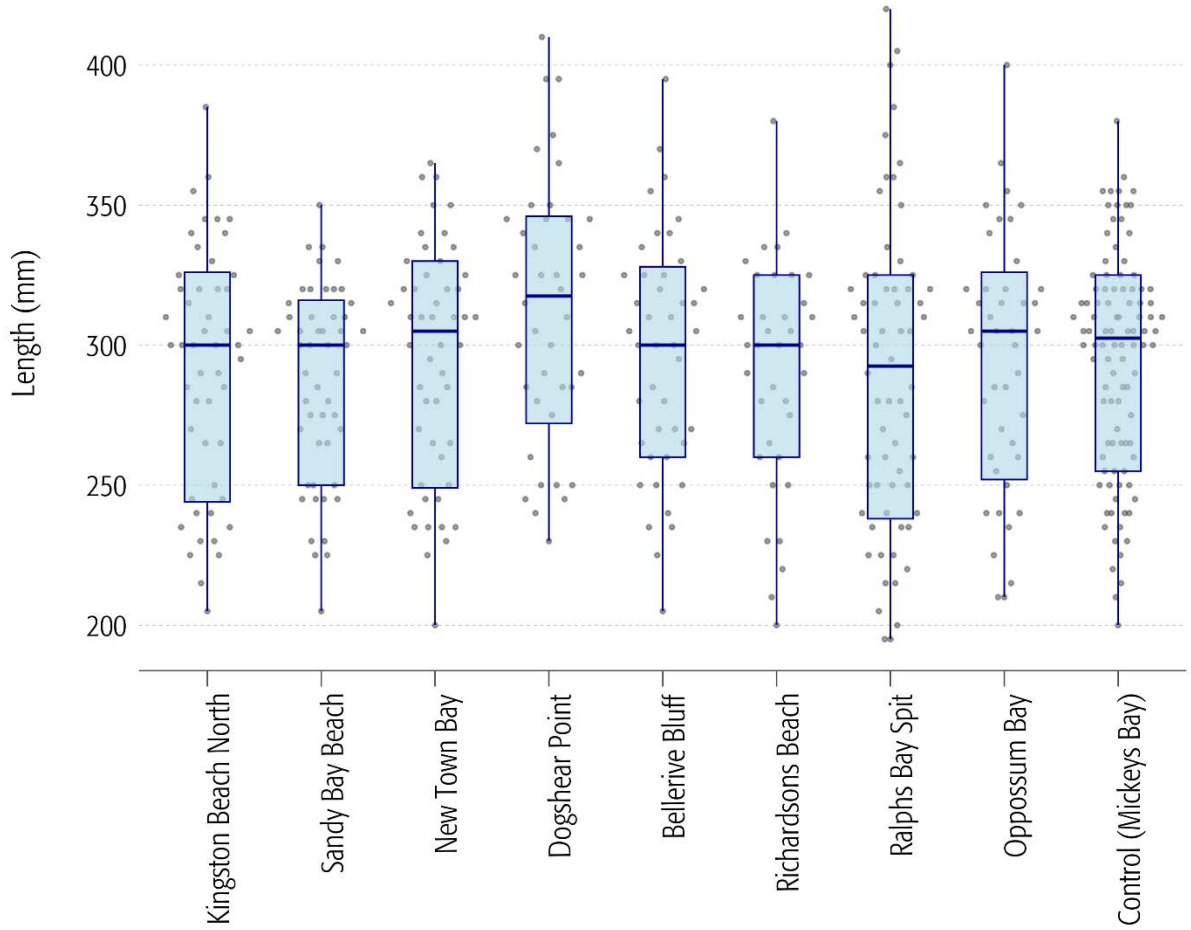

Figure 5e.

The fork length of fish (flathead) caught between 2014 and 2024. Box plots show the minimum, 20th percentile, median, 80th percentile and maximum concentrations at eight impacted sampling sites and a control site in Mickeys Bay. Grey dots show the raw data. Outliers were removed using the interquartile range (IQR) method. Values that were more than 1.5 times the IQR below the first quartile or above the third quartile were excluded.

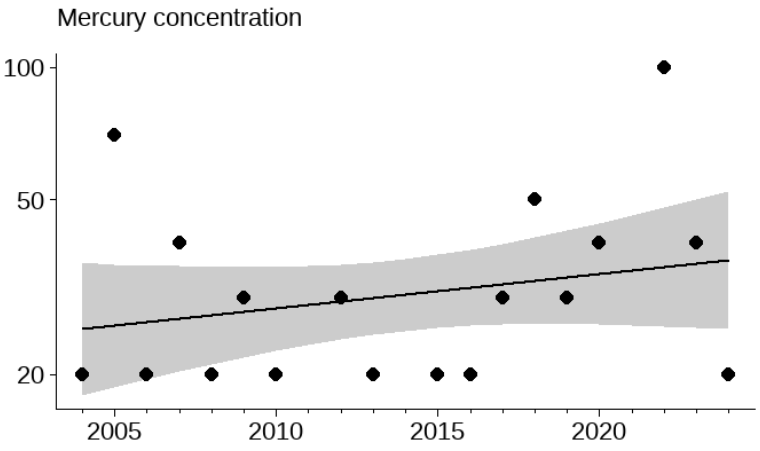

Compartment: Biota (Pacific oyster soft body)
Station: Bedlam Walls
Units : $\mu g\ kg^{-1}$ wet weight
Data extraction:

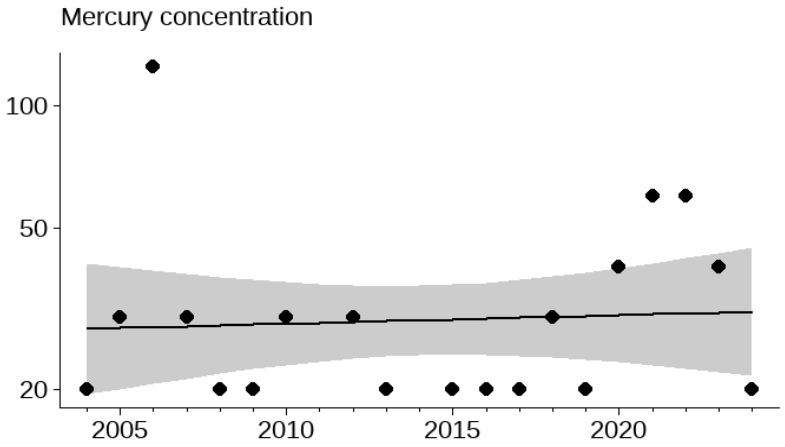

Compartment: Biota (Pacific oyster soft body)
Station: Beltana Beacon
Units : $\mu g\ kg^{-1}$ wet weight
Data extraction:

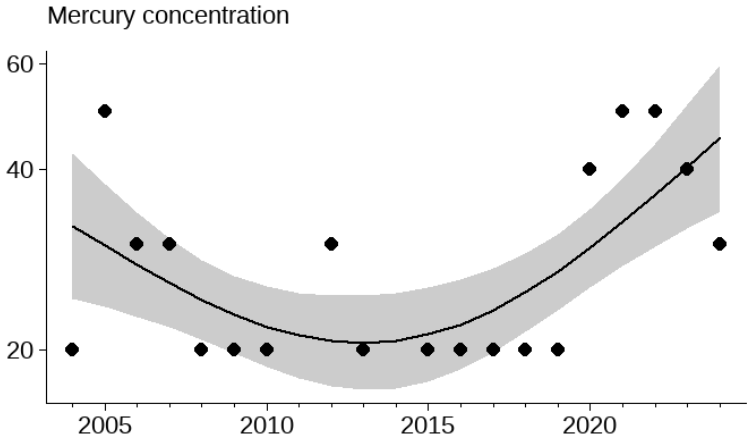

Compartment: Biota (Pacific oyster soft body)
Station: Cornelian Bay
Units : $\mu g\ kg^{-1}$ wet weight
Data extraction:

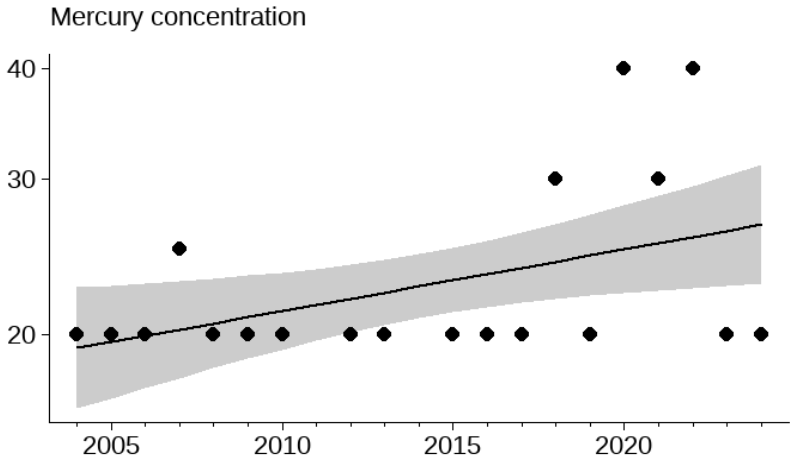

Compartment: Biota (Pacific oyster soft body)
Station: Elwick Bay Red Pylon
Units : $\mu g\ kg^{-1}$ wet weight
Data extraction:

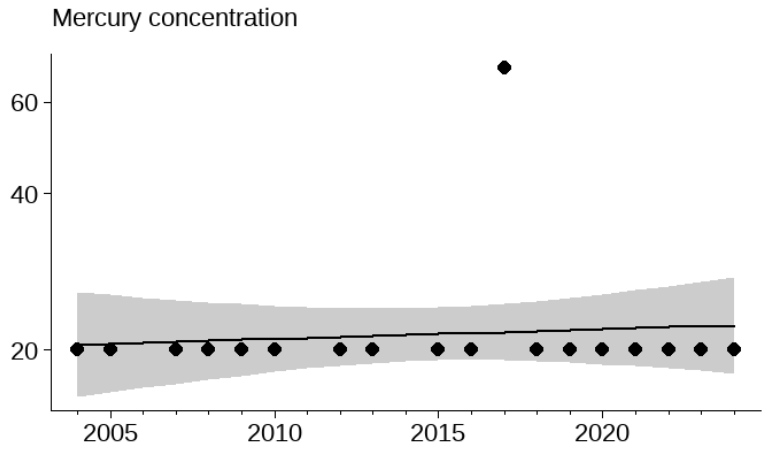

Compartment: Biota (Pacific oyster soft body)
Station: Mickey's Bay
Units : µg kg^{-1} wet weight
Data extraction:

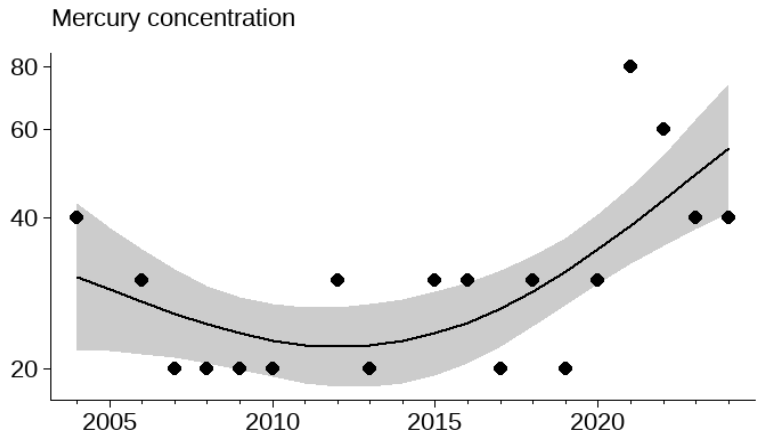

Compartment: Biota (Pacific oyster soft body)
Station: New Town Bay
Units : µg kg^{-1} wet weight
Data extraction:

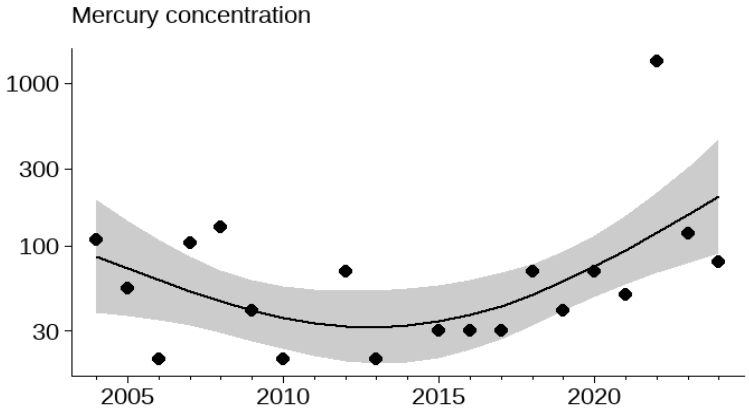

Compartment: Biota (Pacific oyster soft body)
Station: Nyrstar Wharf
Units : µg kg^{-1} wet weight
Data extraction:

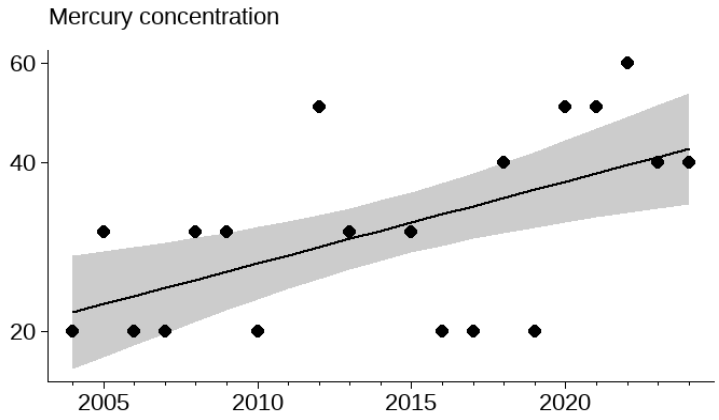

Compartment: Biota (Pacific oyster soft body)
Station: Pavillion Point
Units : µg kg^{-1} wet weight
Data extraction:

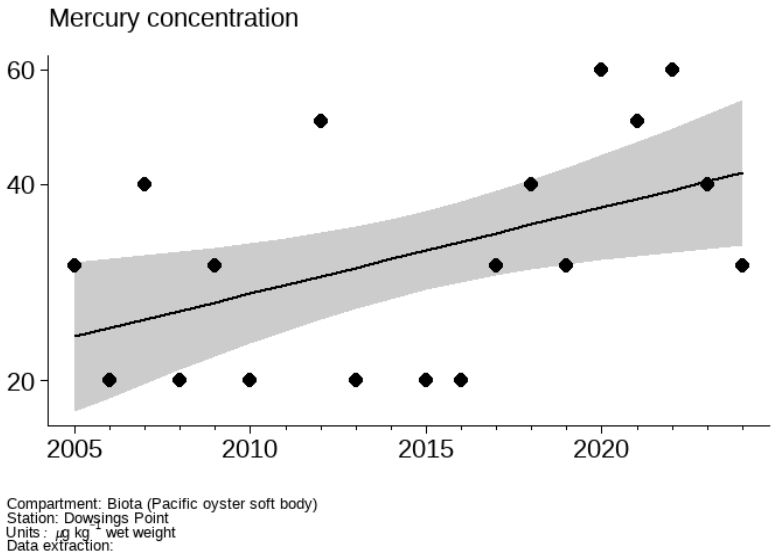

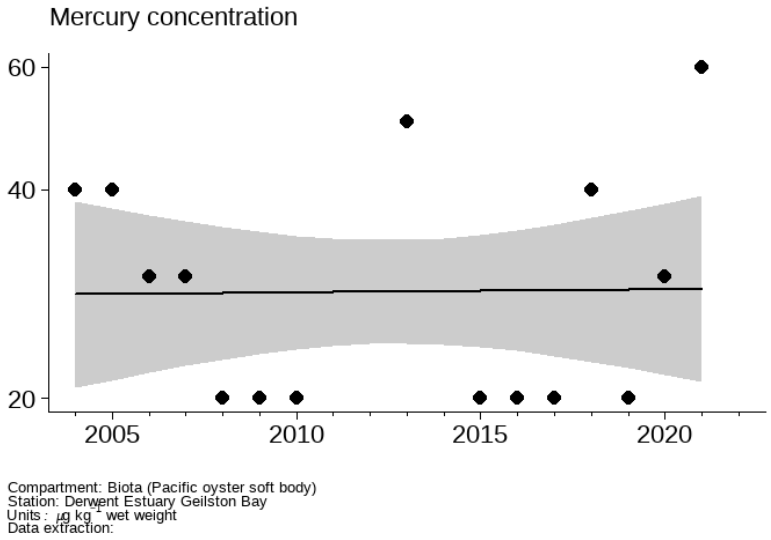

Sampling Site	**Trend**	**p-value** (the significance of the trend)	**Concentrations change over 2004-2024**
Bedlam Walls	No significant temporal trend	0.298	Concentrations at the end of the time series were not significantly different from those at the start of the time series.
Beltana Beacon	No significant temporal trend	0.783	Concentrations at the end of the time series were not significantly different from those at the start of the time series.
Cornelian Bay	**Significant nonlinear trend**	0.005	Concentrations at the end of the time series were not significantly different from those at the start of the time series.

Sampling Site	**Trend**	**p-value** (the significance of the trend)	**Concentrations change over 2004-2024**
Elwick Bay	**Significant log-linear trend in the time series**	0.045	Concentrations have increased by an estimated 1.6% per year over the course of the time series.
Mickey's Bay (control)	No significant temporal trend	0.691	Concentrations at the end of the time series were not significantly different from those at the start of the time series.
New Town Bay	**Significant nonlinear trend**	0.011	Concentrations at the end of the time series were significantly higher than those at the start of the time series.
Nyrstar Wharf	**Significant nonlinear trend**	0.018	Concentrations at the end of the time series were not significantly different from those at the start of the time series.
Pavillion Point	**Significant log-linear trend**	0.007	Concentrations have increased by an estimated 3.4% per year over the course of the time series.
Dowsing Point	**Significant log-linear trend**	0.032	Concentrations have increased by an estimated 3% per year over the course of the time series.
Geilston Bay	No significant temporal trend	0.950	Concentrations at the end of the time series were not significantly different from those at the start of the time series.

Figure 6a. Trend analysis of total mercury in surface-deployed oysters across nine impacted sites in the Derwent Estuary and one control site (Mickey's Bay) from 2004 to 2024, using the HARSAT tool. To account for variability in control oyster sources, baseline correction was applied by subtracting control oyster values from retrieved oyster measurements. This approach ensures that observed changes reflect environmental influences rather than differences in source oyster conditions. Where this correction resulted in values below the limit of reporting (LOR), data were adjusted to equal the LOR. The figures show the fitted trend along with pointwise 90% confidence bands (grey shaded areas). Individual points represent composite mercury concentration measurements (see methodology for further details). Outliers were retained in the analysis; their exclusion did not significantly affect the results.

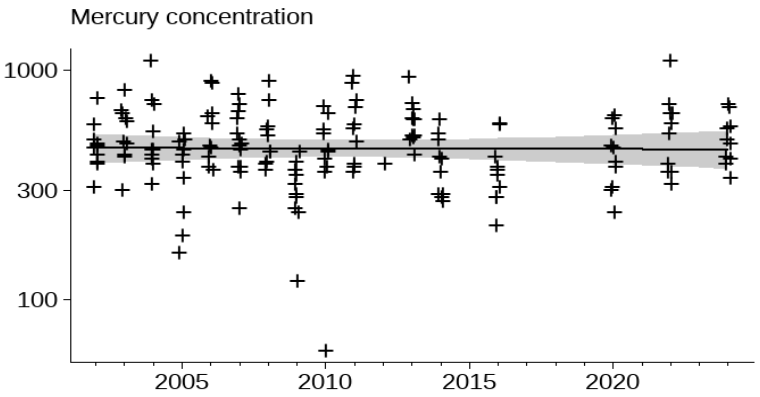

Compartment: Biota (Sand flathead muscle)
Station: New Town Bay
Units : $\mu g\ kg^{-1}$ wet weight
Data extraction:

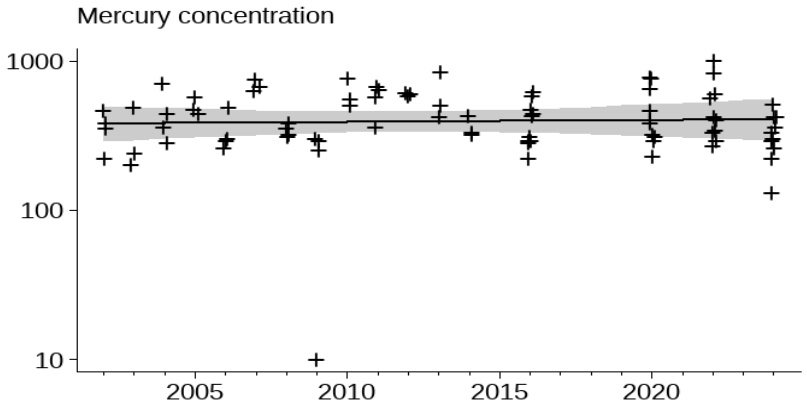

Compartment: Biota (Sand flathead muscle)
Station: Bellerive Bluff
Units : $\mu g\ kg^{-1}$ wet weight
Data extraction:

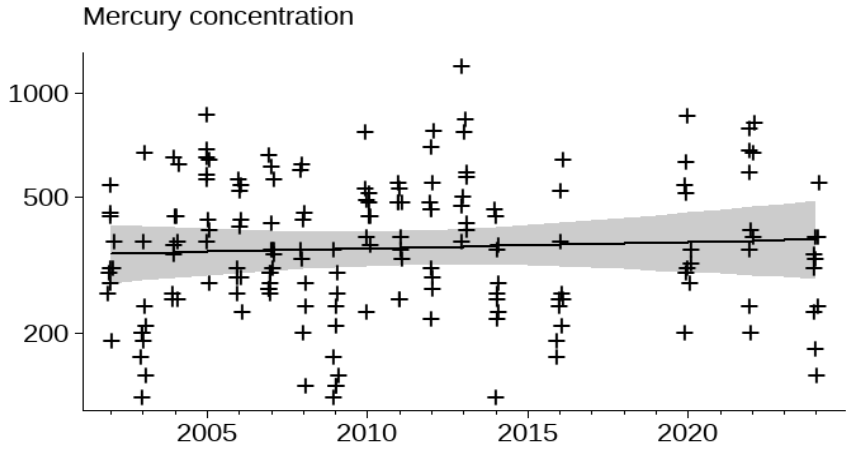

Compartment: Biota (Sand flathead muscle)
Station: Sandy Bay Beach
Units : $\mu g\ kg^{-1}$ wet weight
Data extraction:

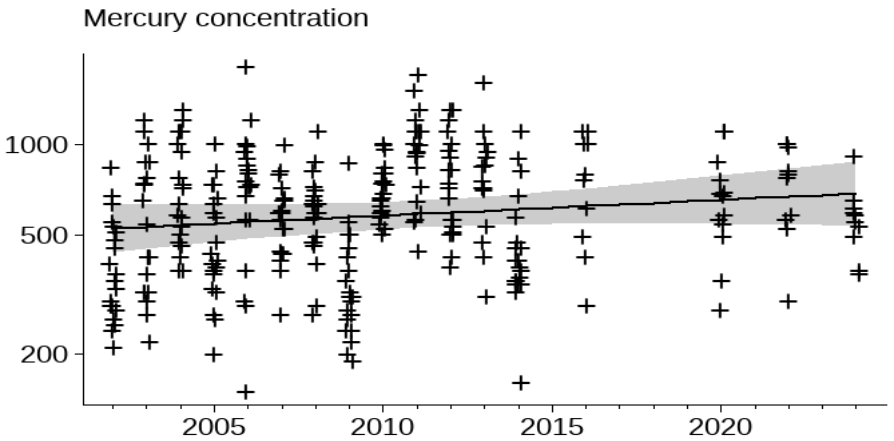

Compartment: Biota (Sand flathead muscle)
Station: Ralphs Bay Spit
Units : $\mu g\ kg^{-1}$ wet weight
Data extraction:

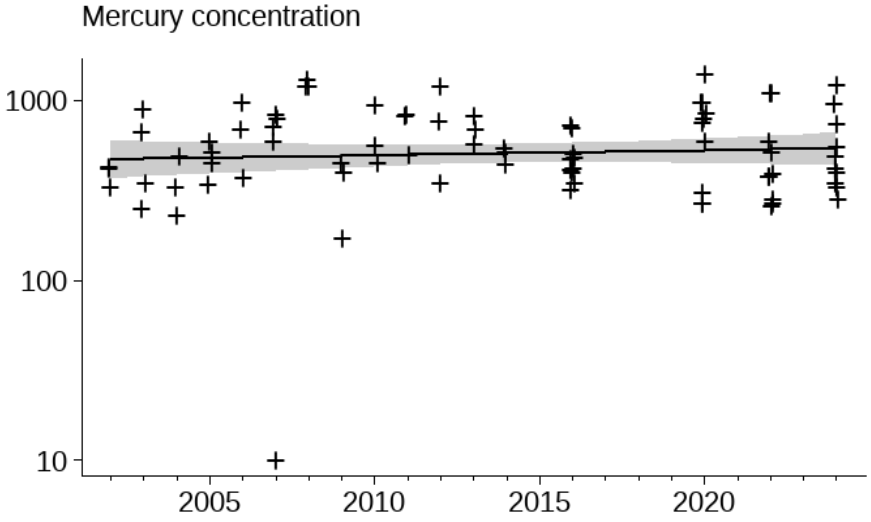

Compartment: Biota (Sand flathead muscle)
Station: Opossum Bay
Units : $\mu g\ kg^{-1}$ wet weight
Data extraction:

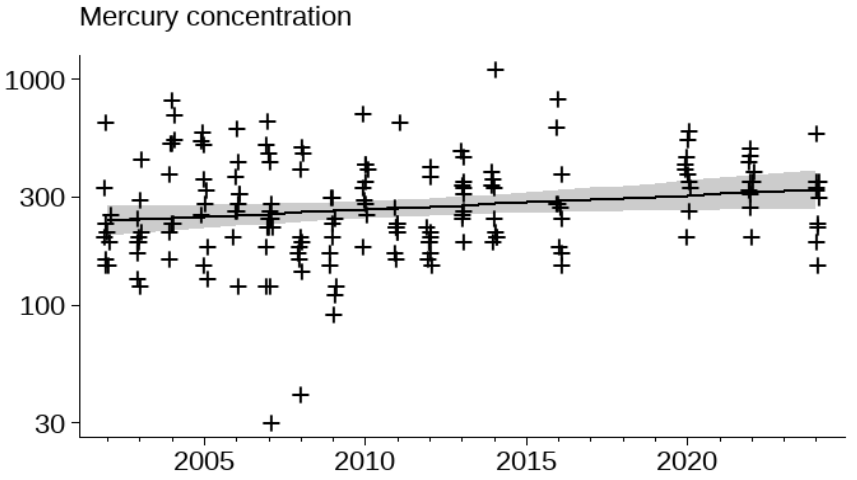

Compartment: Biota (Sand flathead muscle)
Station: Kingston Beach North
Units : $\mu g\ kg^{-1}$ wet weight
Data extraction:

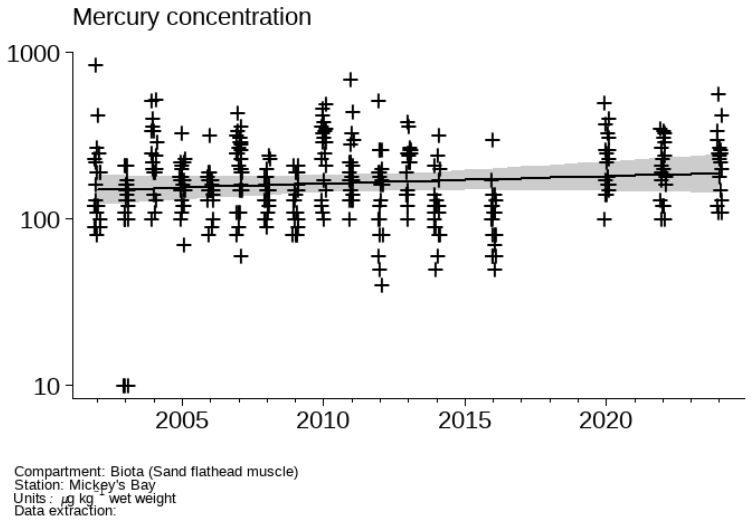

Sampling Site	**Trend**	**p-value** (significance of the trend)	**Concentrations change over 2002-2024**
New Town Bay	No significant trend	0.930	Concentrations at the end of the time series were not significantly different from those at the start of the time series.
Bellerive Bluff	No significant trend	0.822	
Sandy Bay Beach	No significant trend	0.673	
Ralphs Bay Spit	No significant trend	0.214	
Oppossum Bay	No significant trend	0.518	

Sampling Site	**Trend**	**p-value** (significance of the trend)	**Concentrations change over 2002-2024**
Kingston Beach North	No significant trend	0.076	
Mickey's Bay (control)	No significant trend	0.326	

Figure 6b. Trend analysis of total mercury in wild caught fish (flathead) across six impacted sites in the Derwent Estuary and one control site (Mickey's Bay) from 2002 to 2024, using the HARSAT tool. 2018 data points were removed because the skin was left on and data was erroneous. Figures show the fitted trend with pointwise 90% confidence bands (grey shaded areas). Individual points represent the individual mercury concentration measurements. Outliers were retained in the analysis; their exclusion did not significantly affect the results.

Annex 2. Methodology

Sampling sites

Several sites within the Derwent Estuary were being sampled; whilst Mickey's Bay (MB) serves as a reference and control region and was included to provide comparative data from a region that has not been contaminated with mercury and other pollutants (located 48 km south of the estuary).

Ambient water quality

The Derwent Estuary Program coordinates monthly ambient water quality monitoring of 29 sites throughout the Derwent estuary as a cooperative initiative between the Tasmanian Government, Nyrstar Hobart and Boyer (DEP, 2020). Physicochemical parameters are sampled throughout the water column using handheld multiprobes that are calibrated immediately prior to each sampling event.

Sediments

2011 DEP sampling survey

Seabed surface sediment samples were collected at 123 sites throughout the estuary in November 2011. Sample sites were selected to include good overlap with the 2000 sampling survey (77 sites in common). At most sites a multi-corer (with 3 cm diameter core tubes) was used to obtain triplicate cores in a single deployment. The upper 5cm of core material was extruded with a plunger pushed into the core tube and mixed into a glass container to become an integrated sample. As triplicate cores were collected, these provided a sample for: i) metals and % organic carbon analysis, ii) grainsize and iii) archived samples for future analyses. At sandier locations the multi-core recovery was not always successful, so in this instance an Ekman or VanVeen grab sample was obtained. The depth and coherency of the grab samples was not always constrained to the upper 5cm of the sediment surface. Triplicate samples were taken from the grab samples for the same purpose as those taken from the multi-corer. All samples were kept cool and then frozen within several hours of collection.

All sediments were analysed for concentrations of metals (aluminium (Al), arsenic (As), cadmium (Cd), copper (Cu), iron (Fe), lead (Pb), zinc (Zn), manganese (Mn) and mercury (Hg)) and percentage of organic carbon at the Analytical Services Tasmania (AST) Laboratory in Hobart, Tasmania following AST Methods 2301 and 2304.

CSIRO sampling survey

Monthly sediment surveys were conducted between May 2018 and February 2020 at the same 11 sites where the DEP collected physico-biochemical water-column data. Over the span of 2.5 years, 160 sediment samples were collected for abiotic and genomic bacterial DNA analyses from the lower to the upper basin of the estuary. At each site, three sediment cores were collected using a triangular configured sediment corer with polyethylene sample tubes (4.5-cm internal diameter) located at each corner. The top 1 cm of three sediment cores were homogenously mixed in glass jars, and subsamples were taken for genomic DNA (gDNA) extractions, TN, TOC, including analyses of the d15N and d13C, total phosphorus (P) as phosphate from sediment digests (referred to as total PO43- dry weight) and metals, which included As, Cd, Cu, iron (Fe), Pb, Zn and mercury (Hg).

Sediment metal concentrations and total phosphorus were analysed by inductively coupled plasma-atomic emission spectroscopy (ICP-AES; Method 2301). Sediment Hg analyses were performed by cold- vapour atomic fluorescence spectroscopy (CV-AFS; Method 2304). Stable isotope analysis was used to determine the fractionation and potential source of C and N in the estuary. The isotopic composition of the total N and organic C in the sediments (d15N and d13C) were analysed at the CSIRO laboratories in Hobart, Tasmania. A Carlo Erba NA1500 CNS analyser was interfaced with a Conflo IV to a Thermo Scientific Delta V Plus isotope ratio mass spectrometer and operated in the continuous-flow mode during sample analyses.

Deployed Pacific Oysters

In 2004, Nyrstar Hobart commenced annual deployment of cultured oysters of consistent age to various locations throughout the estuary. The goal was to enable better comparison of accumulated metal loads between different sites. Oysters of the same known age were sourced from a commercial shellfish operation around Tasmania (to ensure sound baseline conditions). A minimum of 20 individuals were analysed prior to estuarine deployment to give a baseline for accumulation of metals at source locations.

Thirty-two oysters were placed into oyster baskets and deployed into surface waters at nine sites in the middle estuary and one control site (Mickeys Bay) at Bruny Island. Baskets were deployed in December and retrieved in January, as per previous surveys. The oysters were secured sub-tidally to existing structures as close to the bottom as possible.

Upon retrieval, oysters were shucked and placed on ice in the field and transported directly to a freezer. Oysters from each basket were combined, homogenised and analysed as a single sample at Analytical Services Tasmania.

Baseline-corrected data was calculated by subtracting concentrations measured in non-deployed oysters from post-deployed oyster concentrations.

Wild oysters and mussels

Wild Pacific Oysters were sampled from 26 locations and Blue Mussels from 30 locations. Sites are categorised into four Derwent Estuary regions (middle estuary, eastern shore, western shore, and Ralphs Bay), a D'Entrecasteaux Channel and a control site (Mickeys Bay).

The contractor navigated to each site using a vessel-mounted GPS, then anchored onsite and dived using scuba, aiming to collect mussels and oysters of all sizes. Wild oysters were sampled by randomly taking twenty individuals from the species *Ostrea angasi* or *Crassostrea giga* at each sampling location specified and combining them to form a single sample for each location. Similarly, twenty individuals of the mussel species *Mytilus galloprovincialis* were taken from each specified sampling location and combined to give a single sample for each site.

Twenty mussels and oysters were collected from each site, shucked, rinsed in deionized water then placed in a labelled sampling bag and frozen prior to submission to the laboratory, Analytical Services Tasmania. Flesh was dried, pulverised and analysed using CV-AFS for mercury.

Wild Southern Sand Flathead

Total metal loads in flathead (*Platycephalus bassensis*) were assessed by the current and former owners of the Hobart zinc smelter. Southern Sand Flathead were sampled annually from 2002 to 2015 and biennially from 2016 to 2024, targeting up to 10 fish above legal size (>320 mm) from seven locations in the Derwent estuary and 20 fish from a reference site at Mickey's Bay, Bruny Island. Fish from each site were measured, weighed, gutted, rinsed in deionized water, and submitted to Analytical Services Tasmania. A representative sample of flesh was extracted, dried, ground and analysed by cold vapour atomic fluorescence spectroscopy (CV-AFS) for mercury concentrations. Metal concentrations are expressed in mg/kg wet matter basis (WMB).

Temporal trends

The Derwent Estuary Program scientists analysed temporal trends of mercury in biota by using Harmonised Regional Trend Analysis Tool - HARSAT tool. Statistical time-trend analysis was performed in R version 4.5.1 using the HARSAT package version 1.0.3 (https://harsat.amap.no/).

HARSAT is applied for data analysis by the Arctic Monitoring and Assessment Programme (AMAP), the Baltic Marine Environment Protection Commission (HELCOM) and the Convention for the Protection of the Marine Environment of the North-East Atlantic (OSPAR) for assessment of data concerning contaminants and their effects in the marine environment

Metal concentrations were log-transformed and changes in the log concentrations over time were modelled using linear mixed models. When there are more than 15 years of data, both a linear model and a smoother on 2,3 and 4 degrees of freedom (df) were fitted to the data. Model selection was based on the lowest Akaike Information Criterion (AICc). The primary metric used to summarise changes over time was the change in total Hg concentrations from 2002(4) to 2024, with significance assessed at the 5% level. The significance of each fitted trend—whether linear or non-linear—was assessed using a likelihood ratio test. Further methodological details are available in Morris et al. 2022.(Morris et al., 2022)

References

Bloom, H., & Ayling, G. M. (1977). Heavy metals in the Derwent Estuary. *Environmental Geology*, *2*(1), 3-22. https://doi.org/10.1007/BF02430661

DEP (2020). *State of the Derwent Estuary 2020 - An update and review of environmental data and activities*.

DEP (2021). *Metal contamination in fish and shellfish of the Derwent estuary - A summary of results to December 2020*.

Einoder, L. D., MacLeod, C. K., & Coughanowr, C. (2018). Metal and Isotope Analysis of Bird Feathers in a Contaminated Estuary Reveals Bioaccumulation, Biomagnification, and Potential Toxic Effects. *Arch Environ Contam Toxicol*, *75*(1), 96-110. https://doi.org/10.1007/s00244-018-0532-z

EPA Tasmania. (2024). Environment Protection Notice (EPN) No. 7043/6. In. Tasmania, Australia.

Jones, H. J. (2013). *Accumulation of mercury in estuarine food webs: biogeochemical and ecological considerations.* University of Tasmania].

Jones, H. J., Swadling, K. M., Butler, E. C. V., & Macleod, C. K. (2014). Complex patterns in fish – sediment mercury concentrations in a contaminated estuary: The influence of selenium co-contamination? *Estuarine, Coastal and Shelf Science*, *137*, 14-22. https://doi.org/https://doi.org/10.1016/j.ecss.2013.11.024

Jones, H. J., Swadling, K. M., Tracey, S. R., & Macleod, C. K. (2013). Long term trends of Hg uptake in resident fish from a polluted estuary. *Marine Pollution Bulletin*, *73*(1), 263-272. https://doi.org/https://doi.org/10.1016/j.marpolbul.2013.04.032

Ltd., A. H. O. I. A. (2025). *HARSAT: Harmonized Regional Seas Assessment Tool. R package version 1.0.3.1008*. In Arctic Monitoring and Assessment Programme (AMAP); Helsinki Commission (HELCOM); OSPAR Commission (OSPAR); International Council for the Exploration of the Sea (ICES); AmbieSense Ltd (2025).

Macleod, C., & Coughanowr, C. (2019). Heavy metal pollution in the Derwent estuary: History, science and management. *Regional Studies in Marine Science*, *32*, 100866. https://doi.org/https://doi.org/10.1016/j.rsma.2019.100866

Morris, A. D., Wilson, S. J., Fryer, R. J., Thomas, P. J., Hudelson, K., Andreasen, B., Blévin, P., Bustamante, P., Chastel, O., Christensen, G., Dietz, R., Evans, M., Evenset, A., Ferguson, S. H., Fort, J., Gamberg, M., Grémillet, D., Houde, M., Letcher, R. J., . . . Rigét, F. F. (2022). Temporal trends of mercury in Arctic biota: 10 more years of progress in Arctic monitoring. *Science of The Total Environment*, *839*, 155803. https://doi.org/https://doi.org/10.1016/j.scitotenv.2022.155803

NPI. (2025). *National Pollutant Inventory data within Australia - Mercury and mercury compounds from Hobart Zinc Smelting Source*.

Nyrstar. (2025). *Nyrstar Hobart Triennial Public Environment Report 2022 – 2024*.

Raes, E. J., Holmes, B. H., Karsh, K., Hillyer, K. E., Green, M., van de Kamp, J., Bodrossy, L., Whitehead, S., Proemse, B., Taylor, U., Weller-Wong, A., Revill, A. T., Brewer, E. A., & Bissett, A. (2022). Organic matter and metal loadings influence the spatial gradient of the benthic bacterial community in a temperate estuary. *Marine and Freshwater Research*, *73*(4), 428-440. https://doi.org/https://doi.org/10.1071/MF21225

Ratkowsky, D. A., Dix, T., & Wilson, K. (1975). Mercury in fish in the Derwent Estuary, Tasmania, and its relation to the position of the fish in the food chain. *Marine and Freshwater Research*, *26*, 223-231.

Tracey, S. R., Hartmann, K., McAllister, J., & Lyle, J. M. (2020). Home range, site fidelity and synchronous migrations of three co-occurring, morphologically distinct estuarine fish species. *Science of The Total Environment*, *713*, 136629. https://doi.org/https://doi.org/10.1016/j.scitotenv.2020.136629

UNEP. (2021). *UNEP Global Mercury Partnership Study report on mercury from non-ferrous metals mining and smelting*.

Whitehead, J. C., Christine; Rushton, Michael;. (2013). *Derwent Estuary surface sediments comparison between 2000 & 2011 surveys: - metals, clay/silt ratio & % organic carbon*.

Integrated Analysis Study of Mercury in Tropical Tuna Species

Team:

Robert Mason, Department of Marine Sciences, University of Connecticut, Groton, CT, USA, robert.mason@uconn.edu

Anaïs Médieu, IRD, University of Brest, CNRS, Ifremer, Plouzané, France, anais.medieu@ird.fr

Raphael Lavoie, Wildlife Research Center, Ottawa, Ontario, Canada, raphael.lavoie@ec.gc.ca

Mi-Ling Li, School of Marine Science and Policy, College of Earth, Ocean & Environment, University of Delaware; milingli@udel.edu

Background

The team has expertise in mercury biogeochemical cycling and transformations of mercury (Hg) within the ocean waters and atmosphere, and on the sources and sinks for Hg species in the open ocean. The expertise also extends to the understanding of the bioaccumulation of methylmercury (MeHg) at the base of the marine food web and the factors influencing the trophic transfer and bioaccumulation of MeHg through the marine food web. Overall, the team has the capability to assess the impacts of mercury exposure on humans and wildlife. The focus of the study is tropical tuna species – skipjack (*Katsuwonus pelamis*), yellowfin (*Thunnus albacares*) and bigeye (*T. obesus*) globally but with a focus on the Pacific Ocean and the integrated analysis of temporal trends that will aim to investigate the factors that influence MeHg levels in seawater food web and how that impacts the MeHg concentration in tuna, and potential human exposure. Finally, an assessment of how the activities of the Minamata Convention have changed the levels of exposure of humans and wildlife in the Pacific region to MeHg and its importance relative to other factors (the so-called Effectiveness Evaluation).

Case Study Focus: Factors influencing the concentration of mercury in ocean tuna species with a specific focus on the Pacific Ocean

The case study was used to examine the following questions that are contained within the OESG report.

1. *How do temporal trends of Hg levels observed in species that display different degrees of site fidelity (fish, invetebrates, plants, mammals, birds) vary with emissions/release data in impacted areas by point sources?*
2. *What is the contribution of changes in primary anthropogenic emissions and releases to changes in Hg levels observed in biota over the period circa 2010 to present? (local environment, lower trophic levels)*
3. *What is the contribution of environmental processes and pressures (including climate, habitat changes) to the trends observed in Hg levels in biota over the period circa 2010 to present (does not include anthropogenic inputs)?*
4. *Are the spatial patterns and temporal trends in Hg oserved in air, soil, sediment, surface and ocean waters consistent with trends in biota or humans?* Focus is on ocean concentrations.

The questions are addressed in the order listed above.

1. How do temporal trends of Hg levels observed in species that display different degrees of site fidelity (fish, invetebrates, plants, mammals, birds) vary with emissions/release data in impacted areas by point sources?

Case study Focus: Tropical tuna species in the global ocean

Tuna are among the most widely consumed marine fish globally, but are also known to accumulate high Hg concentrations as they are top predators. In white muscle tissue, the most edible part, MeHg represents the major chemical form of total Hg, making tunas a major route of human exposure to MeHg. Some species do not migrate substantially making them a good indicator species for examining the regional expsoure and trends in ocean Hg concentration. In the open ocean, total Hg concentrations at depths of <1,000 m are thought to have tripled globally following anthropogenic Hg uses and emissions (Lamborg et al., 2014; Outridge et al., 2018), yet it is still unclear how these anthropogenic Hg inputs are converted into MeHg and biomagnified in marine food webs. Understanding temporal MeHg trends in highly consumed marine top predators such as tuna remain therefore crucial as a mechanism for monitoring and anticipating changes in human exposure and evaluating the effectiveness of the Minamata Convention in protecting humans who consume seafood.

Médieu et al. (2024) revisited existing and newly-acquired Hg concentrations in tropical tuna species to investigate the temporal variability of tuna Hg concentrations from 1971 to 2022 in six regions of the Pacific, Atlantic, and Indian Oceans (Fig. 1). Tropical tuna – skipjack *(Katsuwonus pelamis*), yellowfin (*Thunnus albacares*), and bigeye (*T. obesus*) – are globally distributed and highly exploited (constituing 94% of the global tuna catches) and therefore hold significant importance for human health (FAO, 2022). They exhibit distinct growth rates, life spans (Murua et al., 2017), and foraging habitats – skipjack and yellowfin primarily feeding on epipelagic prey and bigeye generally relying on mesopelagic species (Olson et al., 2016). Moreover, they display relatively limited movements and show site fidelity (Fonteneau and Hallier, 2015; Houssard et al., 2017) contrary to bluefin tunas that undertake large transoceanic migrations (Block et al., 2005; Hobday et al., 2015; Madigan et al., 2014), and are therefore expected to reflect MeHg patterns in surface and subsurface waters. Thus, they should strongly reflect the local concentrations and the impacts of anthopogenic releases of Hg given their feeding in the upper ocean.

Once standardized by fish size (Houssard et al., 2019), tuna Hg concentrations are highly variable among years but generally stable in the various locations and over the course of the study outlined here, except in the northwestern Pacific where yellowfin, bigeye, and skipjack tuna Hg concentrations increased significantly in the late 1990s (Fig. 2) (Médieu et al., 2024). This apparent global stability of tuna Hg concentrations over multiple decades aligns with previously reported stable Hg levels in tropical tuna species from the southwestern Pacific over the past 20 years (Médieu et al., 2021), and with earlier observations of stable Hg concentrations in yellowfin from the central north Pacific, based on a comparison of data from 1971 and 1998 (Kraepiel et al., 2003). Yet, this multi-decadal and global stability differs from studies that have suggested increasing trends in yellowfin (n = 5 years of data) and bigeye tuna (n = 4 years) from Hawaii between 1998 and 2008 (Drevnick and Brooks, 2017). The global stability also disagrees with the reported mean annual decrease of 2.4% between 2004 and 2012 (n = 9 years) in bluefin tuna (Lee et al., 2016). By reanalyzing regional trends using both historical and recent data, along with a wider range of tuna body sizes, Médieu et al. (2024) also found apparent stability in tuna Hg concentrations where these species reside. These comparisons highlight the operational difficulty of obtaining robust and continuous datasets over the long periods of time

needed to determine sensitive and accurate Hg trends in biota. In the framework of AMAP, several metrics of performance have been developed to describe and discuss the statistical power of Hg time series, and ensure statistically powerful Hg biomonitoring through time in the Arctic (AMAP, 2021). Among them, the "adequacy" parameter, defined as the number of actual monitoring years in a time series divided by the number of years required to detect a 5% annual change in Hg levels, was developed to indicate whether trend detection is justified for a specific time series (Bignert et al., 2004). Using this parameter, Médieu et al. (2023) found that only half of the regional published Hg time series in tropical tunas were adequate to demonstrate a statistical trend, highlighting the need for collecting long and continous temporal data on tuna

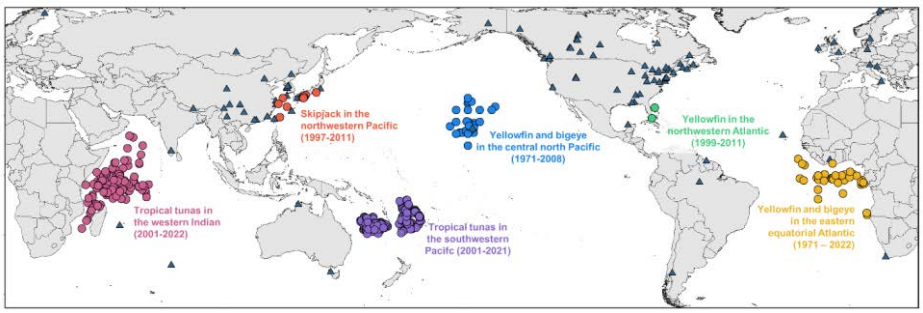

Hg concentrations to accurately explore temporal trends.

Figure 1. *Spatial distribution of tropical tunas analyzed for Hg (colored circles) and atmospheric Hg level observation sites (blue triangles), adapted from Médieu et al. (2024).*

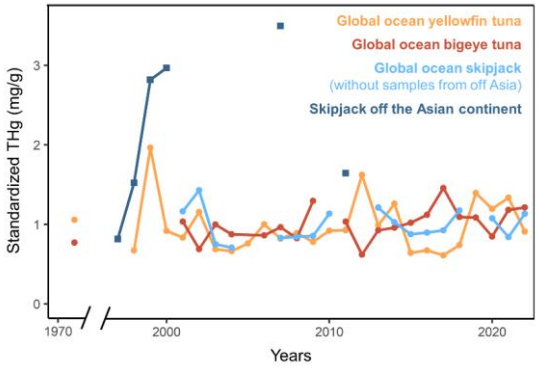

Figure 2. *Temporal variability of standardized Hg concentrations (mg/g) in tropical tunas: yellowfin (orange), bigeye (red), and skipjack (blue), adpated from Médieu et al. (2024). The colored dots represent average annual concentrations measured in the global ocean, except in the northwestern Pacific, off Asia. In that area, average annual concentrations are represented by dark blue squares.*

In the northwestern Pacific Ocean, the significant increase of standardized Hg concentrations in skipjack in the late 1990s mirrored increasing Hg emissions to the atmosphere from Asia over the same period (Streets et al., 2019), suggesting a significant contribution of anthropogenic Hg releases to marine Hg in this particular region (Fig. 2) (Médieu et al., 2024). Such results are in accordance with enriched Hg concentrations found in sediments (Fu et al.,

2010; Kim et al., 2019: Sun et al., 2023), seawater (Laurier et al., 2004), and tunas (Médieu et al., 2022; Tseng et al., 2021) from the same area. A regional modeling study further confirmed the local impact of Hg emissions and releases to the coastal oceans in this region (Liu et al., 2016). Overall, the analysis of the tuna data suggest that in regions of significant regional anthropogenic inputs such as the northwest Pacifc Ocean close to Asia that the impact on fish concentrations are evident and can be demonstrated but for many open ocean regions more removed from point source inputs that a changing anthropogenic signal can be masked by other factors such as mixing of ocean waters and Hg transport with ocean currents. This if further examined below.

2. What is the contribution of changes in primary anthropogenic emissions and releases to changes in Hg levels observed in biota over the period circa 2010 to present? (local environment, lower trophic levels)

Case study: Tropical tunas in the global ocean

In the northwestern Pacific Ocean, skipjack Hg concentrations in 2011 were significantly lower than in 1999, 2000, and 2007 (Médieu et al., 2024), which may reflect the documented reduction in Hg emissions and atmospheric concentrations in East Asia since the 2010s, and/or changes in emitted Hg speciation in China (Marumoto et al., 2019; Nguyen et al., 2019; Shi et al., 2022; Tang et al., 2018; Zhang et al., 2023; Zheng et al., 2018). Yet, more recent tuna Hg data in this particular region is needed to gain a more accurate understanding of how changing local anthropogenic Hg emissions affect the marine Hg cycle.

In the global ocean, the stability of Hg concentrations in tropical tunas in all oceans between 1971 and 2022 was revealed by the Médieu et al. (2024) study, which contrasts with the significant decrease in global primary anthropgenic Hg emission, concentration and deposition trends (AMAP and UNEP, 2019) and natural archived-based reconstructed deposition since the 1970s (Li et al., 2020). Such contrast has already been documented in other aquatic ecosystems (Wang et al., 2019), and authors hypothesized it likely resulted from: i) multicausal and local processes controlling MeHg net production, bioavailabilty, and biomagnification; and ii) the large amount of legacy Hg. In particular, these studies concluded that the stability in tuna Hg concentration is due to subsurface (between 50 and 1,500 m) and deep (below 1,500 m) ocean inertia, and the resulting upward mixing of legacy Hg from deep ocean layers into surface waters (the uppermost 50 m of the water column). Mercury that was emitted within the last century still continues to circulate between the different parts of the biosphere (i.e., atmopshere, vegetation, surface ocean and deep ocean), and still be present in the subsurface ocean (Amos et al., 2013). While surface waters rapidly equilibrate with the atmosphere, deeper oceanic waters have a longer residence time, so that Hg accumulated there takes longer to be redistributed to shallower waters where tunas live and feed. In those waters, Hg emitted decades or centuries ago may still be present, and thus these waters may not yet reflect the effects of the reduction in Hg emissions into the atmopshere.

To better understand how emission reductions could impact Hg concentrations in the different ocean layers and in marine biota, Médieu et al. (2024) used the circulation model of Amos et al. (2013), featuring three emission reduction scenarios based on varying degrees of stringency (Angot et al., 2018; Pacyna et al., 2016). Such modelling illustrated that even if Hg emissions into the atmosphere were drastically reduced, it would take almost 10 years to detect a fall in Hg concentrations in surface waters, and approximately 25 years in subsurface waters; therefore a dataset of at least that long is needed to demonstrate a decline in tuna MeHg concentrations. If emissions of Hg continue as they are today, the model did not predict any decrease in the various ocean layers between now and 2100. Overall, this analysis suggests that

the greater the reduction in emissions, the more rapidly there will be a decline in Hg concentrations in tuna. Far from suggesting that the Minamata Convention is ineffective, Médieu et al. (2024) concluded that there is a need to continue the global effort to reduce Hg emissions more energetically.

In support of this conclusion based on the tuna data of little change in concentration over time, data from models included in the current OESG analysis of ocean data can be used to further examine the notion of changes in concentration over time. The trends since 2010 in the mean MeHg (MMHg in Figure 3) concentrations for the tropical Pacific Ocean surface waters (30 ºN to 30 ºS) show no obvious trend. While there is seasonal variability and a large spread in the modeled data, there is no consistent trend in concentration over the time period (Bieser, pers. comm.). There could be latitudinal or longitudinal differences in surface water MeHg but the data from the Bowman et al. (2016) (GEOTRACES GP16) and Starr et al. (2025) (GEOTRACES GP15) cruises in the Pacific Ocean show little latitudinal or longitudinal variation except for regions where upwelling was occurring (equatorial or off Peru). These data suggest that there are not strong differences in surface water MeHg concentrations except for locations close to shore or in regions with enhanced local anthropogenic inputs. Thus, the fish data are consistent with the model output and measurements.

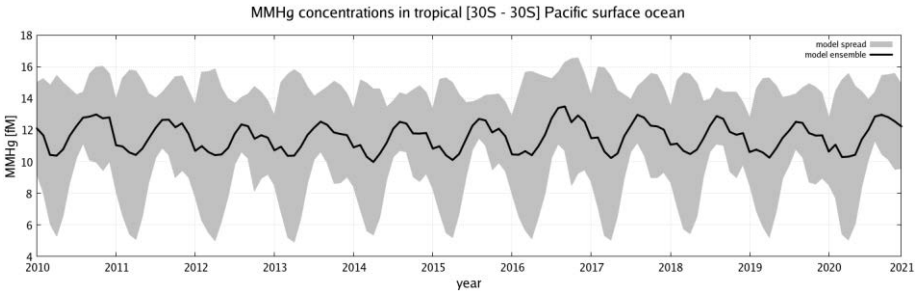

Figure 3: Model output for surface layer methyl-mercury (MMHg) concentrations (fM) for the period 2010 to 2021 for the tropical regions of the Pacific Ocean (30 ºN to 30 ºS; Bieser, pers. comm.)

3. What is the contribution of environmental processes and pressures (including climate, habitat changes) to the trends observed in Hg levels in biota over the period circa 2010 to present (does not include anthropogenic inputs)?

Case study: Tropical tunas and albacore in the Pacific Ocean

Mercury concentrations significantly differ among tropical tunas and albacore (*T. alalunga*), following the general pattern: bigeye > albacore > yellowfin and skipjack (Médieu et al., 2023). Tuna Hg concentrations also vary spatially, as highlighted regionally in the eastern Pacific (Ferriss and Essington, 2011) and the western Indian (Chouvelon et al., 2017), and across 12 locations in the global ocean (Nicklisch et al., 2017). These studies relied on spot samples acquired at a low spatial resolution, and did not examine the potential drivers of concentration differences. Recent collaborations under the international framework of the IMBeR regional program Climate Impacts on Oceanic Top Predators (CLIOTOP) and through the access to tuna samples from extensive tuna tissue banks (e.g., Pacific Marine Specimen Bank coordinated by the Pacific Community) has enabled a study to produce broad-scale and high-resolution maps of Hg concentrations in bigeye, yellowfin, and albacore from the western

central Pacific region (Houssard et al., 2019), and in skipjack for the entire Pacific Ocean (Médieu et al., 2022). Such maps allow for the refinement of the risk assessments of Hg exposure from tuna consumption by species and catch areas, and to explore the processes driving tuna Hg variability.

Fish body size (or weight) is one of the main drivers of intra-species variability of tuna Hg (e.g., Besada, 2006; Cai et al., 2007; Kojadinovic et al., 2006), reflecting the natural MeHg bioaccumulation in individuals through time. Yet, this parameter is not often considered when comparing Hg levels across locations (Nicklisch et al., 2017) and is rarely reported in the literature (Médieu et al., 2023). To remove bias associated to fish size differences and explore other processes leading to tuna Hg variability, such as tuna trophic ecology, ocean biogeochemistry or anthropogenic emissions, Houssard et al. (2019) developed a size-standardization method of Hg concentrations and were able to reveal higher standardized Hg concentrations around New Caledonia and Fiji compared to the equator in yellowfin, albacore, and bigeye (Fig. 4A-C). Strong spatial variability of standardized Hg concentrations in skipjack was also found in the Pacific Ocean (Fig. 4D), likely resulting from changes in: i) tuna diet; ii) seawater MeHg concentrations at the base of marine food webs; and/or iii) amounts of surface ocean inorganic Hg loadings from the atmosphere (Médieu et al., 2022).

Identifying and evaluating the relative importance of ecological, biogeochemical, and anthropogenic processes to explain tuna Hg variability can be complicated given the difficulty with quantifying these processes and disentangling possible interplay among them. Tuna foraging depth is considered as a key driver to explain higher Hg concentrations in mesopelagic species like bigeye (Choy et al., 2009); yet it is still unclear what the relative importance of both food chain length and/or baseline MeHg variations as possible causal effects (Ferriss and Essington, 2011). The recent exploration of standardized Hg concentrations in tunas alongside ecological data (e.g., tuna trophic position estimates), biogeochemical (e.g., dissolved O_2 concentrations), physical (e.g., thermocline depth), and anthropogenic (e.g., atmospheric elemental Hg concentrations) model outputs through quantitative models (e.g., generalized additive models) offers new perspectives to disentangle the relative importance of the possible drivers. In the western central Pacific, this transdisciplinary approach revealed that spatial variability of standardized Hg concentrations in bigeye, yellowfin and albacore was mainly explained by both tuna foraging depth, and local biogeochemistry driving variability of seawater MeHg concentrations (Houssard et al., 2019). The higher Hg concentrations in bigeye compared to the two other species are most likely due to its ability to forage deeper in ocean layers where MeHg concentrations are generally highest (Fig. 5b). Such links between MeHg concentrations and bioavailability in seawater and Hg concentrations in marine top predators is expected but rarely observed due to scarce MeHg data in the water column as they require scientific campaigns at sea and specialized equipment for collection. Around New Caledonia and Fiji, a significant positive trend between tuna Hg levels and dissolved MeHg levels from the surface to down to 600 m confirmed the importance of both marine biogeochemical processes leading to variable MeHg in seawater, and tuna foraging depth (Fig. 5) (Barbosa et al., 2022).

At the Pacific Ocean scale, large spatial patterns of standardized Hg concentrations in the epipelagic skipjack were also mainly explained by the natural functioning of the ocean, specifically in relation to the depth at which MeHg concentrations peak in the water column. The relatively higher standardized Hg concentrations in the eastern Pacific and northwestern Pacific (Fig. 4D) are likely related to low oxygen levels in the ocean, especially in the eastern region, owing to methylation in association with bacterial degradation of sinking organic matter (Médieu et al., 2022). Such specific conditions in these areas are expected to cause MeHg concentrations to peak in water closest to the surface (< 100 m) (Bowman et al., 2020), where

skipjack live and feed, as compared to the western Pacific where the MeHg peak occur in deeper waters, between 400 and 800 m (Fig. 5) (Barbosa et al., 2022).

The highest skipjack Hg concentrations in the northwestern Pacific, however, may also be due to major sources of anthropogenic emissions located nearby and associated to the heavy use of fossil fuels for power generation in Asia (Médieu et al., 2022). Such anthropogenic sources add to natural biogeochemical processes that are conducive to surface MeHg bioavailability in marine food webs. These results in tropical tunas and albacore align with findings in bluefin tunas where Hg levels were found to reflect global patterns of Hg bioavailability and pollution in ocean basins (Tseng et al., 2021).

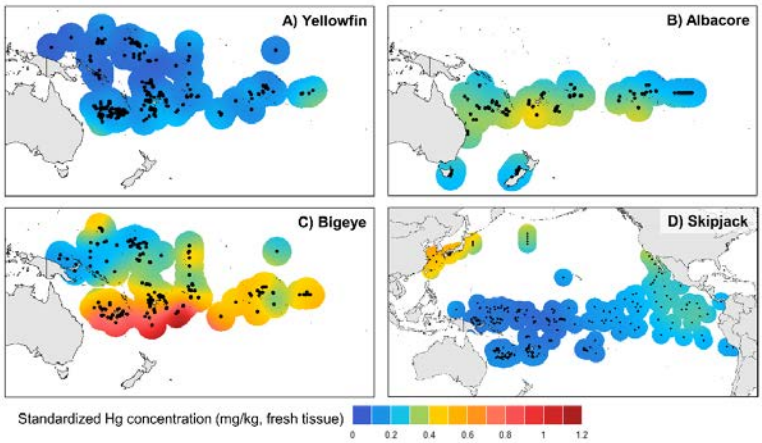

Figure 4. *Spatial distribution of standardized Hg concentrations (mg/kg, fresh tissue) in* ***A)*** *yellowfin,* ***B)*** *albacore,* ***C)*** *bigeye, and* ***D)*** *skipjack, adapted from Houssard et al. (2019) and Médieu et al., (2022). Black dots show the catch location of the sampled fish.*

These recent broad-scale and transdisciplinary studies lead to the hypothesis that the spatial variability in tuna Hg concentrations is mainly explained by both tuna foraging depth and the variability of MeHg formation and bioavailability in the ocean. By revealing the importance of ecological and biogeochemical processes, these studies support the assumption that climate change will likely affect MeHg concentrations in marine food webs. First, the already-observed expansion of the oxygen-minimum zone in the eastern Pacific is forecast to continue over the next few decades (Schmidtko et al., 2017; Stramma et al., 2008) and may be conducive to forming MeHg and increasing its bioavailability at the base of food webs. On the other hand, changes to primary productivity and organic matter export may also counter this trend. Current ocean circulation models cannot accurately predict such biogeochemical changes, specifically in tropical areas such as the eastern Pacific Ocean (Laufkötter et al., 2016; Tagliabue et al., 2020), and our understanding of the climate-induced regional changes is therefore insufficient to quantify their impacts in conjunction with changes in Hg emissions and cycling in the environment. Second, although tropical tuna species in the global ocean have displayed relatively high site fidelity (Fonteneau and Hallier, 2015) and had no major changes in foraging depth or diet (Médieu et al., 2024) in the past decades, seawater warming is expected to lead to a shift in foraging habitat toward higher latitudes or deeper in the water column, and possibly to increased MeHg concentrations in marine top predators (Schartup et al., 2019). Also, the effect of temperature on tuna migration and therefore tuna catch in the Pacific Ocean has been examined and there is evidence that increasing temperature has lead to an increase in the tuna

catch by those using purse seine nets (Mediodia, 2021). Overall, there is a need for continuous and long-term global monitoring of Hg levels in tunas, combined with Hg concentrations and speciation in seawater, phytoplankton and zooplankton to explore how climate-driven biogeochemical and ecological processes will impact MeHg accumulation in marine food webs, and ultimately offset or enhance measures at reducing emissions.

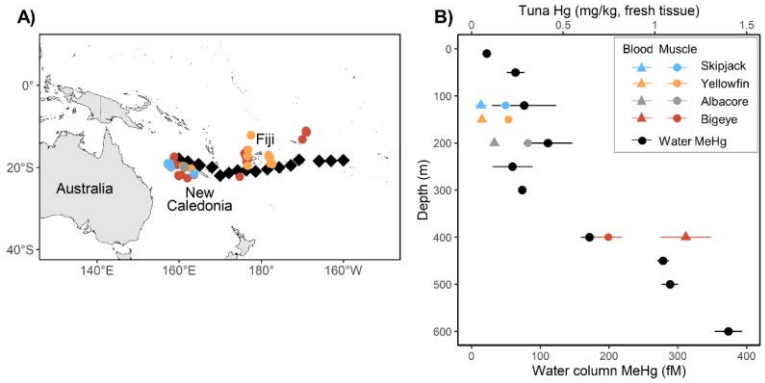

Figure 5. *The importance of tuna foraging depth in the context of marine methylmercury (MeHg) depth profiles in the southwestern Pacific Ocean.* ***A)*** *Location of seawater (black diamonds) and tuna (colored dots) blood and muscle samples used to investigate the link between tuna Hg concentrations and dissolved MeHg levels in water.* ***B)*** *Relationship between total Hg concentrations (mg/kg, fresh tissue) in tuna species exhibiting different foraging depths, and concentration-depth profile of dissolved MeHg (fM), concentration-depth profiles were averaged from all locations), adapted from Barbosa et al., (2022).*

4. Are the spatial patterns and temporal trends in Hg observed in air, soil, sediment, surface and ocean waters consistent with trends in biota or humans?

Case Study: Spatial distribution of mercury in yellowfin tuna concentration in ocean waters and the potential impact on human exposure

The examination in this case is with reference to concentrations in tuna relative to their environmental concentrations, and to the potential for these changes to influence human exposure. Two approaches are considered. This first involves the analysis and comparison of tuna concentrations to that of modeled concentrations of MeHg is seawater, with this analysis taking into account discrepancies in MeHg concentration that may be present due to coastal and local factors. The information that is used for this case study comparative analysis comes from the simulations of Li et al. (2024). The second approach is to compare trends in Hg levels in tuna since 2010 with modeled or measured data for seawater MeHg concentration, assuming that this proxy is a valid approximation of the resultant concentration in tuna, given that other potential influencing variables will have a relatively small effect, as discussed above. Finally, the information on tuna Hg trends over time is used to discuss the potential impact on subsistence fisher people in the Pacific Ocean. Both island and other countries are examined based on their seafood consumption and the impact that changes in MeHg concentration over time might have. Coastal subsistence fishing populations'catch data is

taken from the Sea Around Us database (https://www.seaaroundus.org/). The analysis examines the relative importance of tuna in the diet of subsistence fisher people in the region (tropical Pacific Ocean) and how the changes or lack thereof in tuna MeHg concentration could impact their level of exposure to MeHg.

Approach #1: The methodology for the first evaluation comes from Li et al. (2024) who used a model to simulate MeHg levels in yellowfin tuna caught in 24 distinct marine regions (Fig. 6). In order to capture the regional variability in MeHg exposure, these authors scaled a global mean MeHg concentration for yellowfin tuna - bounded by empirically defined ranges - according to seawater MeHg concentrations at each harvesting location and feeding depth (1–250 m). These seawater MeHg concentrations were drawn from prior simulations using the Massachusetts Institute of Technology general circulation model (MITgcm). Because the MITgcm has a relatively coarse spatial resolution (1°×1°), it does not resolve fine-scale variability in nearshore hydrodynamics or inputs from polluted coastal discharges. This spatial averaging can lead to underestimates of seawater MeHg in continental margin and shelf regions. To correct for these potential confounding factors, the authors incorporated measured MeHg concentrations from shelf and marginal seas and used empirically derived values to adjust the modeled concentrations in these areas. As a result of this approach, regions with higher seawater MeHg concentrations are predicted to yield higher MeHg levels in yellowfin tuna. This method directly links spatial variability in seawater MeHg to MeHg levels in biota, enabling regional estimates that reflect environmental differences in MeHg exposure.

The spatial modeling approach showed good predictive performance based on a weighted linear regression of observed and modeled yellowfin tuna mercury concentrations ($R^2 = 0.80$; Fig. 6b). Most of the modeled values are within the empirical concentration range for common market sizes of yellowfin tuna (5 - 20 kg) (Table 1). Li et al. 2024 found however a lower predictive performance for yellowfin tuna caught in certain coastal regions. This likely reflects the spatial heterogeneity that is not well captured by the global modeling approach, possibly due to local coastal emission sources that aren't included in the model. The coastal scaling included in this study was limited to regions with available observational data. Li et al. (2024) also excluded seawater values from the literature that were collected in small, enclosed or semi-enclosed coastal systems (e.g., lagoons, bays) that are heavily influenced by point sources as these would be unrepresentative. Future studies that generate additional empirical or modeled seawater MeHg data in coastal regions will be important for further assessing the consistency between seawater and biota MeHg levels. This is an area that could be further explored by addressing other OESG questions and tasks related to emission sources.

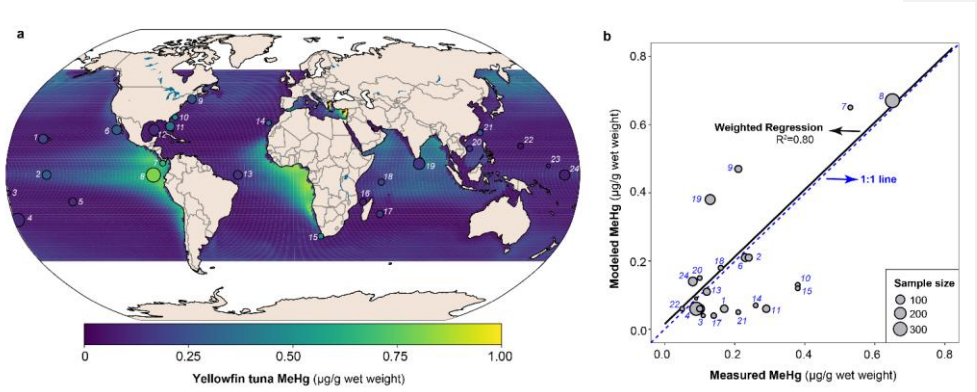

Figure 6. Comparison of empirical and modeled methylmercury (MeHg) concentrations in 1482 yellowfin tuna from 24 ocean locations. Panel (a) shows the modeled yellowfin tuna MeHg concentrations as the background color over its distribution range (59°N - 48°S). Circles show observed MeHg concentrations for size normalized yellowfin (length = 90 cm; weight=15 kg) (Houssard et al. 2019). Circle size and color represent the sample size of each study and the average MeHg concentration of yellowfin tuna (see data in Table 1). The site number is indicated next to each circle. Panel (b) shows a weighted linear regression of measured versus modeled yellowfin tuna MeHg concentration (black line; y=1.0x+0.01; R^2=0.80). The weight is the sample size of each study, indicated by circle size. Site numbers are shown on both panels. Taken from Li et al. 2024.

Approach #2: As discussed above and detailed in Figs. 2 & 3, the trends in concentration of Hg in tuna from the tropical Pacific Ocean and the trends in the modeled concentration of MeHg in the ocean mixed layer from the modeling effort that has been part of the OESG analysis demonstrate a similar conclusion of no significant change in concentration over time. Overall, it is clear that the concentration of MeHg in the surface waters of the tropical Pacific Ocean, while showing distinct seasonal trends, and regions of elevated concentration due to enhanced local anthropogenic inputs or in relation to specific phenomena such as upwelling, have not changed significantly since 2010. Overall, the annual variation is substantially larger than any potential trend over time (Fig. 3). Such a lack of trend is also demonstrated through the analysis of tuna Hg concentrations over time for the tropical Pacific Ocean and for other regions in that there is also no trend in fish concentrations as discussed in Médieu et al. (2024) besides those locations with enhanced regional anthropogenic inputs. Furthermore, the lack of substantial change does not correlate with either the changes in global anthropogenic emissions of Hg over this time period, or the regional emissions that are more reflective of the various study regions (Fig. 6).

Human Health Impacts: In terms of the impact on human health of these results, it is worth examining a few countries, focusing on the Pacific Ocean, that consume tuna and other seafood (Table 2). As noted above, the data in Table 2 is for subsistence fishers and not for the overall population that are likely exposed to fish from many locations. The consumption of tuna is high for some island states, being highest in the Cook Island (62% of the total mass), the Marianas (55%) and Kiribati (39%). A variety of tuna species are consumed. These 3 countries also consume a high fraction of seafood that is low in MeHg concentration. Thus, it is reasonable to conclude for these populations that their exposure to MeHg has not changed significantly since 2010. The same conclusion cannot be reached for the countries in Table 2

that do not consume much tuna or other large predatory fish and mostly consumed seafood with low MeHg (e.g. Tuvalu, Indonesia, Marshall Islands and Australia; all >50% consumption of low MeHg seafood). Their exposure is most likely linked to regional anthropogenic inputs rather than global sources and while the magnitude of these inputs have likely changed, this cannot be ascertained from the examining at the trends in open ocean MeHg concentrations or in the change in concentrations in tuna. Thus, the cases studies reported here cannot characterize in detail changes in human exposure given the focus of the studies.

Table 1. Comparison of simulated and empirical MeHg concentrations (μg/g wet weight) of yellowfin tuna of a common market size (90 cm or 15 kg) and range (5-20 kg) across 24 ocean regions.

Site	**Sample size**	**Longi-tude** [a]	**Lati-tude** [a]	**Empirical conc. (range)** [b]	**Model conc.** [c]
Indian (Reunion Is.)	19	55	-22	0.14 (0.05, 0.17)	0.04
Indian (Mozambique Channel)	20	44	-15	0.08 (0.03, 0.09)	0.06
Indian	15	55	-4	0.16 (0.06, 0.21)	0.18
Indian (Sri Lanka)	140	79	6	0.13 (0.04, 0.16)	0.38
Atlantic (New England)	47	-70	42	0.21 (0.07, 0.26)	0.47
Atlantic (N. & S. Carolina)	10	-78	3	0.38 (0.14, 0.47)	0.13
Atlantic (Northeast)	10	-16	29	0.26 (0.09, 0.33)	0.07
Atlantic (Florida)	56	-80	27	0.29 (0.10, 0.36)	0.06
Atlantic (Southeast)	9	18	-34	0.38 (0.14, 0.48)	0.12
Atlantic (Brazil)	52	-35	0	0.12 (0.04, 0.15)	0.11
Atlantic (Gulf of Mexico)	112	-90	25	0.10 (0.04, 0.13)	0.06
Pacific (South China Sea)	10	111	15	0.10 (0.04 ,0.13)	0.15
Pacific (North China Sea)	10	120	23	0.21 (0.07, 0.26)	0.05
Pacific (Hawaii)	60	-160	20	0.17 (0.06, 0.21)	0.06
Pacific (Northwest)	10	144	16	0.05 (0.02, 0.06)	0.0
Pacific (ARCHm/WCPO)	292	-178	-25	0.09 (0.03, 0.12)	0.06
Pacific (NPTG/WCPO)	2	160	5	0.09 (0.03, 0.11)	0.09
Pacific (PEQD/WCPO)	5	180	-10	0.11 (0.04, 0.13)	0.04
Pacific (SPSGm/WCPO)	32	-140	-15	0.10 (0.04, 0.13)	0.06
Pacific (WARMm/WCPO)	96	170	0	0.08 (0.03, 0.10)	0.14
Pacific (Ecuador)[d]	347	-88	0	0.65 (0.23, 0.81)	0.67
Pacific (California)	68	-114	25	0.23 (0.08, 0.28)	0.21
Pacific (Central Equatorial)	50	-155	0	0.24 (0.08, 0.30)	0.21
Pacific (East)	10	-82	7	0.53 (0.19, 0.66)	0.65

Notes: a: If not explicitly included in the publication, capture location is estimated based on the description of the study site; b: Normalized observed MeHg concentrations is to a common size (90 cm or 15 kg) and range (62-98 cm or 5-20 kg) based on the relationship between tuna length and muscle total Hg concentration described in Houssard et al., 2019 and the assumption that 95% of total Hg is MeHg in finfish. Empirical concentrations of yellowfin tuna in various sizes across global locations were compiled by Houssard et al., 2019 unless stated otherwise; c: Modeled MeHg concentration based on the average

seawater concentration at the corresponding feeding depths (1-250 m) of the capture location; and d: data from Munoz Abril 2016. For cited literature see Li et al. (2024).

Table 2: Seafood consumption by subsistence fisher people from representative countries in the Pacific Ocean focusing on the countries with the highest tuna consumption as well as some countries with low tuna consumption. Data reported here was extracted from the Sea Around Us database and used in the analysis by Li et al. (2024)

Country	**Tuna species (%)**	**Low MeHg species (%)[a]**	**Predatory (%)[b]**	**Others (%)**
Cook Islands	62	25	12	1
Marianas	55	26	18	1
Kiribati	39	35	18	8[c]
Tuvalu	18	80	1	2
Marshall Islands	13	53	34	<1
Vietnam	11	40	49	<1
Indonesia	5.7	68	26	<1
Japan	5.5	43	28	22[d]
Australia	2.6	57	29	11[e]
French Polynesia	1.1	52	47	<1

Notes: a: The low MeHg species include shellfish, planktivores and omnivores; b: predatory includes piscivorous and other large predatory fish besides tuna and billfish; c: mostly shark and billfish; d: mostly salmon; e: mostly shark species

References

AMAP, 2021. AMAP Assessment 2021: Mercury in the Arctic. Arctic Monitoring and Assessment (AMAP). Tromso, Norway.

AMAP, UN Environment, 2019. Technical Background Report for the Global Mercury Assessment 2018. Arctic Monitoring and Assessment Programme, Oslo, Norway/UN Environment Programme, Chemicals and Health Branch. Geneva, Switzerland.

Amos, H.M., Jacob, D.J., Streets, D.G., Sunderland, E.M., 2013. Legacy impacts of all-time anthropogenic emissions on the global mercury cycle. Global Biogeochemical Cycles 27, 410–421. https://doi.org/10.1002/gbc.20040

Angot, H., Hoffman, N., Giang, A., Thackray, C.P., Hendricks, A.N., Urban, N.R., Selin, N.E., 2018. Global and Local Impacts of Delayed Mercury Mitigation Efforts. Environ. Sci. Technol. 52, 12968–12977. https://doi.org/10.1021/acs.est.8b04542

Barbosa, R.V., Point, D., Médieu, A., Allain, V., Gillikin, D.P., Couturier, L.I.E., Munaron, J.-M., Roupsard, F., Lorrain, A., 2022. Mercury concentrations in tuna blood and muscle mirror seawater methylmercury in the Western and Central Pacific Ocean. Marine Pollution Bulletin 180, 113801. https://doi.org/10.1016/j.marpolbul.2022.113801

Besada, V., 2006. Mercury, cadmium, lead, arsenic, copper and zinc concentrations in albacore, yellowfin tuna and bigeye tuna from the Atlantic Ocean. Ciencias Marinas 32, 439–445. https://doi.org/10.7773/cm.v32i22.1083

Bignert, A., Riget, F., Braune, B., Outridge, P., Wilson, S., 2004. Recent temporal trend monitoring of mercury in Arctic biota – how powerful are the existing data sets? J. Environ. Monit. 6, 351–355. https://doi.org/10.1039/B312118F

Block, B.A., Teo, S.L.H., Walli, A., Boustany, A., Stokesbury, M.J.W., Farwell, C.J., Weng, K.C., Dewar, H., Williams, T.D., 2005. Electronic tagging and population structure of Atlantic bluefin tuna. Nature 434, 1121–1127. https://doi.org/10.1038/nature03463

Bowman, K.L., Lamborg, C.H., Agather, A.M., 2020. A global perspective on mercury cycling in the ocean. Science of The Total Environment 710, 136166. https://doi.org/10.1016/j.scitotenv.2019.136166

Bowman, K.L., Hammerschmidt, C.R., Lamborg, C.H., Swarr, G.J., Agather, A.M. Distribution of mercury species across a zonal section of the eastern tropical South Pacific Ocean (U.S. GEOTRACES GP16) (2016) Marine Chemistry, 186, pp. 156-166. DOI: 10.1016/j.marchem.2016.09.005

Cai, Y., Rooker, J.R., Gill, G.A., Turner, J.P., 2007. Bioaccumulation of mercury in pelagic fishes from the northern Gulf of Mexico. Canadian Journal of Fisheries and Aquatic Sciences 64, 458–469. https://doi.org/10.1139/f07-017

Chouvelon, T., Brach-Papa, C., Auger, D., Bodin, N., Bruzac, S., Crochet, S., Degroote, M., Hollanda, S.J., Hubert, C., Knoery, J., Munschy, C., Puech, A., Rozuel, E., Thomas, B., West, W., Bourjea, J., Nikolic, N., 2017. Chemical contaminants (trace metals, persistent organic pollutants) in albacore tuna from western Indian and south-eastern Atlantic Oceans: Trophic influence and potential as tracers of populations. Science of The Total Environment 596–597, 481–495. https://doi.org/10.1016/j.scitotenv.2017.04.048

Choy, C.A., Popp, B.N., Kaneko, J.J., Drazen, J.C., 2009. The influence of depth on mercury levels in pelagic fishes and their prey. Proceedings of the National Academy of Sciences 106, 13865–13869. https://doi.org/10.1073/pnas.0900711106

Drevnick, P.E., Brooks, B.A., 2017. Mercury in tunas and blue marlin in the North Pacific Ocean. Environmental Toxicology and Chemistry 36, 1365–1374. https://doi.org/10.1002/etc.3757

FAO, 2022. The State of World Fisheries and Aquaculture 2022. FAO. https://doi.org/10.4060/cc0461en

Ferriss, B.E., Essington, T.E., 2011. Regional patterns in mercury and selenium concentrations of yellowfin tuna (Thunnus albacares) and bigeye tuna (Thunnus obesus) in the Pacific Ocean. Can. J. Fish. Aquat. Sci. 68, 2046–2056. https://doi.org/10.1139/f2011-120

Fonteneau, A., Hallier, J.-P., 2015. Fifty years of dart tag recoveries for tropical tuna: A global comparison of results for the western Pacific, eastern Pacific, Atlantic, and Indian Oceans. Fisheries Research 163, 7–22. https://doi.org/10.1016/j.fishres.2014.03.022

Fu, X., Feng, X., Zhang, G., Xu, W., Li, X., Yao, H., Liang, P., Li, J., Sommar, J., Yin, R., Liu, N., 2010. Mercury in the marine boundary layer and seawater of the South China Sea: Concentrations, sea/air flux, and implication for land outflow. J. Geophys. Res. 115, D06303. https://doi.org/10.1029/2009JD012958

Hobday, A., Evans, K., Eveson, J.P., Farley, J., Hartog, J., Basson, M., Patterson, T., 2015. Distribution and Migration—Southern Bluefin Tuna (Thunnus maccoyii), in: Biology and Ecology of Bluefin Tuna. pp. 189–210. https://doi.org/10.1201/b18714-12

Houssard, P., Lorrain, A., Tremblay-Boyer, L., Allain, V., Graham, B.S., Menkes, C.E., Pethybridge, H., Couturier, L.I.E., Point, D., Leroy, B., Receveur, A., Hunt, B.P.V., Vourey, E., Bonnet, S., Rodier, M., Raimbault, P., Feunteun, E., Kuhnert, P.M., Munaron, J.-M., Lebreton, B., Otake, T., Letourneur, Y., 2017. Trophic position

increases with thermocline depth in yellowfin and bigeye tuna across the Western and Central Pacific Ocean. Progress in Oceanography 154, 49–63. https://doi.org/10.1016/j.pocean.2017.04.008

Houssard, P., Point, D., Tremblay-Boyer, L., Allain, V., Pethybridge, H., Masbou, J., Ferriss, B.E., Baya, P.A., Lagane, C., Menkes, C.E., Letourneur, Y., Lorrain, A., 2019. A Model of Mercury Distribution in Tuna from the Western and Central Pacific Ocean: Influence of Physiology, Ecology and Environmental Factors. Environmental Science & Technology 53, 1422–1431. https://doi.org/10.1021/acs.est.8b06058

Kim, H., Lee, K., Lim, D.-I., Nam, S.-I., Han, S. hee, Kim, J., Lee, E., Han, I.-S., Jin, Y.K., Zhang, Y., 2019. Increase in anthropogenic mercury in marginal sea sediments of the Northwest Pacific Ocean. Science of The Total Environment 654, 801–810. https://doi.org/10.1016/j.scitotenv.2018.11.076

Kojadinovic, J., Potier, M., Le Corre, M., Cosson, R.P., Bustamante, P., 2006. Mercury content in commercial pelagic fish and its risk assessment in the Western Indian Ocean. Science of The Total Environment 366, 688–700. https://doi.org/10.1016/j.scitotenv.2006.02.006

Kraepiel, A.M.L., Keller, K., Chin, H.B., Malcolm, E.G., Morel, F.M.M., 2003. Sources and Variations of Mercury in Tuna. Environmental Science & Technology 37, 5551–5558. https://doi.org/10.1021/es0340679

Lamborg, C.H., Hammerschmidt, C.R., Bowman, K.L., Swarr, G.J., Munson, K.M., Ohnemus, D.C., Lam, P.J., Heimbürger, L.-E., Rijkenberg, M.J.A., Saito, M.A., 2014. A global ocean inventory of anthropogenic mercury based on water column measurements. Nature 512, 65–68. https://doi.org/10.1038/nature13563

Laufkötter, C., Vogt, M., Gruber, N., Aumont, O., Bopp, L., Doney, S.C., Dunne, J.P., Hauck, J., John, J.G., Lima, I.D., Seferian, R., Völker, C., 2016. Projected decreases in future marine export production: the role of the carbon flux through the upper ocean ecosystem. Biogeosciences 13, 4023–4047. https://doi.org/10.5194/bg-13-4023-2016

Laurier, F.J.G., Mason, R.P., Gill, G.A., Whalin, L., 2004. Mercury distributions in the North Pacific Ocean—20 years of observations. Marine Chemistry, Special Issue in honor of Dr. William F. Fitzgerald 90, 3–19. https://doi.org/10.1016/j.marchem.2004.02.025

Lavoie, R.A., Bouffard, A., Maranger, R., Amyot, M. Mercury transport and human exposure from global marine fisheries (2018) Scientific Reports, 8 (1), art. no. 6705, DOI: 10.1038/s41598-018-24938-3

Lee, C.-S., Lutcavage, M.E., Chandler, E., Madigan, D.J., Cerrato, R.M., Fisher, N.S., 2016. Declining Mercury Concentrations in Bluefin Tuna Reflect Reduced Emissions to the North Atlantic Ocean. Environmental Science & Technology 50, 12825–12830. https://doi.org/10.1021/acs.est.6b04328

Li, M-L., Thackray, C.P., Lam, V.W.Y., Cheng, W.W.L., Sunderalnd, E.M., 2024. Global fishing patterns amplify human exposure to methylmercury. PNAS 121, e2405898121

Li, C., Sonke, J.E., Le Roux, G., Piotrowska, N., Van der Putten, N., Roberts, S.J., Daley, T., Rice, E., Gehrels, R., Enrico, M., Mauquoy, D., Roland, T.P., De Vleeschouwer, F., 2020. Unequal Anthropogenic Enrichment of Mercury in Earth's Northern and Southern Hemispheres. ACS Earth Space Chem. 4, 2073–2081. https://doi.org/10.1021/acsearthspacechem.0c00220

Liu, M., Chen, L., Wang, X., Zhang, W., Tong, Y., Ou, L., Xie, H., Shen, H., Ye, X., Deng, C., Wang, H. (2016) Mercury export from Mainland China to adjacent seas and its influence on the marine mercury balance. (2016) *Environ. Sci. Technol.* **50**(12): 6224-6232. DOI: 10.1021/acs.est.5b04999

Madigan, D.J., Baumann, Z., Carlisle, A.B., Hoen, D.K., Popp, B.N., Dewar, H., Snodgrass, O.E., Block, B.A., Fisher, N.S., 2014. Reconstructing transoceanic migration patterns

of Pacific bluefin tuna using a chemical tracer toolbox. Ecology 95, 1674–1683. https://doi.org/10.1890/13-1467.1

Marumoto, K., Suzuki, N., Shibata, Y., Takeuchi, A., Takami, A., Fukuzaki, N., Kawamoto, K., Mizohata, A., Kato, S., Yamamoto, T., Chen, J., Hattori, T., Nagasaka, H., Saito, M., 2019. Long-Term Observation of Atmospheric Speciated Mercury during 2007–2018 at Cape Hedo, Okinawa, Japan. Atmosphere 10, 362. https://doi.org/10.3390/atmos10070362

Médieu, A., Lorrain, A., Point, D., 2023. Are tunas relevant bioindicators of mercury concentrations in the global ocean? Ecotoxicology. https://doi.org/10.1007/s10646-023-02679-y

Médieu, A., Point, D., Itai, T., Angot, H., Buchanan, P.J., Allain, V., Fuller, L., Griffiths, S., Gillikin, D.P., Sonke, J.E., Heimbürger-Boavida, L.-E., Desgranges, M.-M., Menkes, C.E., Madigan, D.J., Brosset, P., Gauthier, O., Tagliabue, A., Bopp, L., Verheyden, A., Lorrain, A., 2022. Evidence that Pacific tuna mercury levels are driven by marine methylmercury production and anthropogenic inputs. PNAS 119, 8. https://doi.org/10.1073/pnas.2113032119

Médieu, A., Point, D., Receveur, A., Gauthier, O., Allain, V., Pethybridge, H., Menkes, C.E., Gillikin, D.P., Revill, A.T., Somes, C.J., Collin, J., Lorrain, A., 2021. Stable mercury concentrations of tropical tuna in the south western Pacific ocean: An 18-year monitoring study. Chemosphere 263, 128024. https://doi.org/10.1016/j.chemosphere.2020.128024

Médieu, A., Point, D., Sonke, J.E., Angot, H., Allain, V., Bodin, N., Adams, D.H., Bignert, A., Streets, D.G., Buchanan, P.B., Heimbürger-Boavida, L.-E., Pethybridge, H., Gillikin, D.P., Ménard, F., Choy, C.A., Itai, T., Bustamante, P., Dhurmeea, Z., Ferriss, B.E., Bourlès, B., Habasque, J., Verheyden, A., Munaron, J.-M., Laffont, L., Gauthier, O., Lorrain, A., 2024. Stable Tuna Mercury Concentrations since 1971 Illustrate Marine Inertia and the Need for Strong Emission Reductions under the Minamata Convention. Environ. Sci. Technol. Lett. 11, 250–258. https://doi.org/10.1021/acs.estlett.3c00949

Mediodia, H.J.P., 2021. Effects of sea surface temperature on tuna catch: Evidence from countries in the Eastern Pacific Ocean. Ocean Coast. Manage. 209, art. no. 105657

Murua, H., Rodriguez-Marin, E., Neilson, J.D., Farley, J.H., Juan-Jordá, M.J., 2017. Fast versus slow growing tuna species: age, growth, and implications for population dynamics and fisheries management. Rev Fish Biol Fisheries 27, 733–773. https://doi.org/10.1007/s11160-017-9474-1

Nguyen, L.S.P., Sheu, G.-R., Lin, D.-W., Lin, N.-H., 2019. Temporal changes in atmospheric mercury concentrations at a background mountain site downwind of the East Asia continent in 2006–2016. Science of The Total Environment 686, 1049–1056. https://doi.org/10.1016/j.scitotenv.2019.05.425

Nicklisch, S.C.T., Bonito, L.T., Sandin, S., Hamdoun, A., 2017. Mercury levels of yellowfin tuna (Thunnus albacares) are associated with capture location. Environmental Pollution 229, 87–93. https://doi.org/10.1016/j.envpol.2017.05.070

Olson, R.J., Young, J.W., Ménard, F., Potier, M., Allain, V., Goñi, N., Logan, J.M., Galván-Magaña, F., 2016. Chapter Four: Bioenergetics, Trophic Ecology, and Niche Separation of Tunas, in: Advances in Marine Biology. Elsevier, pp. 199–344. https://doi.org/10.1016/bs.amb.2016.06.002

Outridge, P.M., Mason, R.P., Wang, F., Guerrero, S., Heimburger-Boavida, L-E. (2018) Updated global and oceanic mercury budgets for the United Nations Global Mercury Assessment 2018. Environ. Sci. Technol., 52: 11466-11477; DOI: 10.1021/acs.est.8b01246

Formatted: French (Switzerland)

Formatted: English (United States)

Formatted: English (United States)

Pacyna, J.M., Travnikov, O., De Simone, F., Hedgecock, I.M., Sundseth, K., Pacyna, E.G., Steenhuisen, F., Pirrone, N., Munthe, J., Kindbom, K., 2016. Current and future levels of mercury atmospheric pollution on a global scale. Atmospheric Chemistry and Physics 16, 12495–12511. https://doi.org/10.5194/acp-16-12495-2016

Schartup, A.T., Thackray, C.P., Qureshi, A., Dassuncao, C., Gillespie, K., Hanke, A., Sunderland, E.M., 2019. Climate change and overfishing increase neurotoxicant in marine predators. Nature 1–3. https://doi.org/10.1038/s41586-019-1468-9

Schmidtko, S., Stramma, L., Visbeck, M., 2017. Decline in global oceanic oxygen content during the past five decades. Nature 542, 335–339. https://doi.org/10.1038/nature21399

Shi, J., Chen, Yuping, Xu, L., Hong, Y., Li, M., Fan, X., Yin, L., Chen, Yanting, Yang, C., Chen, G., Liu, T., Ji, X., Chen, J., 2022. Measurement report: Atmospheric mercury in a coastal city of Southeast China – inter-annual variations and influencing factors. Atmospheric Chemistry and Physics 22, 11187–11202. https://doi.org/10.5194/acp-22-11187-2022

Starr, L.D., He, Y., Mason, R.P., Hammerschmidt, C.R., Newell, S.E., Lamborg, C.H. Mercury Distribution and Speciation Along the U.S. GEOTRACES GP15 Pacific Meridional Transect (2025) Journal of Geophysical Research: Oceans, 130 (4), art. no. e2024JC021672, DOI: 10.1029/2024JC021672

Stramma, L., Johnson, G.C., Sprintall, J., Mohrholz, V., 2008. Expanding Oxygen-Minimum Zones in the Tropical Oceans. Science 320, 655–658. https://doi.org/10.1126/science.1153847

Streets, D.G., Horowitz, H.M., Lu, Z., Levin, L., Thackray, C.P., Sunderland, E.M., 2019. Five hundred years of anthropogenic mercury: spatial and temporal release profiles. Environ. Res. Lett. 14, 084004. https://doi.org/10.1088/1748-9326/ab281f

Sun, X., Hu, L., Sun, X., Fan, D., Liu, M., Wang, H., Yang, Z., Cheng, P., Liu, X., Guo, Z. (2023) Mercury burial in modern sedimentary systems of the East China Marginal Seas: The role of coastal oceans in global mercury cycling. Global Biogeochemical Cycles 37(9): Art. # e2023GB007760, DOI: 10.1029/2023GB007760

Tagliabue, A., Barrier, N., Du Pontavice, H., Kwiatkowski, L., Aumont, O., Bopp, L., Cheung, W.W.L., Gascuel, D., Maury, O., 2020. An iron cycle cascade governs the response of equatorial Pacific ecosystems to climate change. Global Change Biology 26, 6168–6179. https://doi.org/10.1111/gcb.15316

Tang, Y., Wang, S., Wu, Q., Liu, K., Wang, L., Li, S., Gao, W., Zhang, L., Zheng, H., Li, Z., Hao, J., 2018. Recent decrease trend of atmospheric mercury concentrations in East China: the influence of anthropogenic emissions. Atmospheric Chemistry and Physics 18, 8279–8291. https://doi.org/10.5194/acp-18-8279-2018

Tseng, C.-M., Ang, S.-J., Chen, Y.-S., Shiao, J.-C., Lamborg, C.H., He, X., Reinfelder, J.R., 2021. Bluefin tuna reveal global patterns of mercury pollution and bioavailability in the world's oceans. Proceedings of the National Academy of Sciences 118, e2111205118. https://doi.org/10.1073/pnas.2111205118

Wang, F., Outridge, P.M., Feng, X., Meng, B., Heimbürger-Boavida, L.-E., Mason, R.P., 2019. How closely do mercury trends in fish and other aquatic wildlife track those in the atmosphere? - Implications for evaluating the effectiveness of the Minamata Convention. Science of the Total Environment 674, 58–70. https://doi.org/10.1016/j.scitotenv.2019.04.101

Zhang, Y., Zhang, L., Cao, S., Liu, X., Jin, J., Zhao, Y., 2023. Improved Anthropogenic Mercury Emission Inventories for China from 1980 to 2020: Toward More Accurate Effectiveness Evaluation for the Minamata Convention. Environ. Sci. Technol. 57, 8660–8670. https://doi.org/10.1021/acs.est.3c01065

Formatted: English (United States)

Formatted: English (United States)

Zheng, B., Tong, D., Li, M., Liu, F., Hong, C., Geng, G., Li, H., Li, X., Peng, L., Qi, J., Yan, L., Zhang, Y., Zhao, H., Zheng, Y., He, K., Zhang, Q., 2018. Trends in China's anthropogenic emissions since 2010 as the consequence of clean air actions. Atmospheric Chemistry and Physics 18, 14095–14111. https://doi.org/10.5194/acp-18-14095-2018

Great Lakes Region Case Study

Mark Burton, Biodiversity Research Institute, Portland, ME, USA
Celia Chen, Dartmouth University, Hanover, NH, USA

Description of case study

The Laurentian Great Lakes are comprised of five lakes and border eight states in the United States (US) and the Canadian Province of Ontario. They are important both for their natural resources and for recreation, transportation, industry, and commerce. The interconnected lakes contain approximately 21% of the world's surface freshwater by volume and have been impacted by anthropogenic activities, which have left a legacy of contaminants found in multiple abiotic and biotic matrices. The US and Canada have collaborated since 1972 through the Great Lakes Water Quality Agreement to protect, restore, and preserve the basin's ecosystem integrity (Visha et al. 2018). The Great Lakes and the region around it have been studied extensively for mercury (Hg) in abiotic (atmosphere, sediments) and biotic matrices (fish and birds).

In the US, atmospheric Hg emissions data are available through USEPA (2021) and mercury deposition data collected during three or more years are available at 14 Mercury Deposition Network (MDN) sites in the Great Lakes basin. Regulatory actions by both countries have led to declines in mercury emissions.

To understand the impacts of pollution, and effectiveness of subsequent regulations, on human and ecosystem health, both the US and Canada have monitoring programs for fish in the Great Lakes that include Hg and other contaminants. In the US, data are collected by the US Environmental Protection Agency (USEPA) in several programs including the National Aquatic Resources Surveys (NARS), National Coastal Condition Assessment (NCCA), and the Great Lakes Fish Monitoring and Surveillance Program (GLFMSP). The USEPA data are a combination of muscle and whole fish samples collected for evaluation of both human and ecosystem health. In Canada, data for the Great Lakes are collected by the Ontario Ministry of the Environment, Conservation and Parks (MECP). The fish samples are comprised of filet samples collected for the establishment of fish consumption advisories for the Canadian waters of the Great Lakes.

Initial results showed declines of Hg in fish tissues in the 1980's. However, more recent trends have been less clear, in some cases showing no change or others showing increases in Hg concentrations. The explanations for these trends are complex and involve not only patterns in Hg emissions but also evidence for changes in food web structure (Visha et al. 2018; Lepak et al. 2015, 2018, 2019, 2025).

Cross-media integration of observed levels/trends

Data for mercury emissions, deposition, and fish tissue were available to examine the relationships between media for spatial patterns and temporal trends. We examined national and regional emissions data for the United States, mercury deposition for sites in the basins for each of the Great Lakes, and fish muscle tissue concentrations from multiple fish species in each of the five lakes. In general, there were few relationships in the temporal trends between media in these lakes. Lakes, fish species, and years all differed widely in their mercury concentrations compounded by differences between the monitoring frequency across lakes.

The decline in atmospheric mercury emissions from anthropogenic sources in the United States since the USEPA's National Emissions Inventory (USEPA NEI) began compiling emissions data in the 1990s has been well-documented (e.g., Schmeltz et al. 2011). These reductions are attributed to a combination of regulatory actions—including incinerator regulations and the Mercury and Air Toxics Standards (MATS) rule—as well as voluntary and co-beneficial emission control technologies and broader shifts, including transitioning from coal to natural gas, with implications for mercury emissions.

However, mercury deposition patterns do not exhibit corresponding monotonic declines consistent with local to regional scale trends in mercury emissions. Depending on spatial context, factors such as changing global emissions, climatic variability, landscape geomorphology, and environmental characteristics (e.g., leaf area index) influence deposition patterns. To examine spatial and temporal patterns in wet deposition across the Great Lakes region, we analyzed data from the Mercury Deposition Network (MDN) by aggregating station observations (≥3 years of collection) within each Great Lake basin. Trend analyses were conducted using the non-parametric Mann-Kendall test and Sen's slope estimation, using the most recent range of consecutive years with available data. A significant decreasing trend in annual mercury deposition was found in the Lake Ontario basin, while a significant positive trend was detected in the Lake Huron basin (**Figure 2,** $p<0.05$). No significant trends were observed across the Lake Erie, Lake Michigan, and Lake Superior basins.

Similarly, spatial and temporal patterns in biota exhibit complex dynamics due to the complexities of mercury fate and transport. These patterns are influenced by a range of drivers including species-specific bioaccumulation dynamics, food web interactions, climate change, invasive species, and environmental factors (e.g., chemistry, habitat change) (Eagles-Smith et al. 2018). Total mercury concentrations in fish muscle (ww) tissue were selected because they made up more than 90% of the available samples. We also selected the five most sampled species (walleye, lake trout, lake whitefish, smallmouth bass, and yellow perch) for further analysis. All mercury concentrations were first length-standardized to the mean length for each species by quantifying the species-specific effect of length on muscle mercury concentrations, before being natural log transformed to improve normality.

We then used a linear mixed effects model to better understand patterns in mercury concentrations in fish in the Great Lakes. The length-standardized and log-transformed total mercury concentrations were modelled as a function of the interaction between Year, Lake, and Species, along with a random intercept for sampling site to account for site-level variation. Mercury concentrations in fish muscle varied significantly across lakes and through time, with multiple significant interactions between year, lake, and species, highlighting the spatial and temporal complexity of mercury trends in the Great Lakes (**Figure 3**) with several species-lake combinations showing significant positive or negative trends. For example, lake trout, smallmouth bass, walleye, and yellow perch all exhibited negative trends in Lake Ontario, where mercury deposition was also significantly declining (**Figure 2**), though whitefish showed a significantly increasing trend in the same lake. On the other hand, Lake Huron exhibited significantly increasing mercury deposition and mercury concentrations in lake trout and whitefish were found to be increasing, with the three other species not exhibiting a significant

trend. With the exception of whitefish, all four other species exhibited significant positive and negative trends in at least one of the Great Lakes. Lake Michigan did not exhibit a significant trend in any of the five species examined with large confidence intervals driven by sparse data with only 3 or 4 years of sampling for each species, coverage only matched by Lake Superior smallmouth bass.

Relevance to effectiveness evaluation

The decline of atmospheric emissions of mercury in the region, and nations, does not appear to be mirrored in changes in mercury deposition in each of the Great Lake basins or in the temporal trends in concentrations in fish tissue which decrease, increase, or do not change depending on the species and the lake. This suggests that there is very little linkage between atmospheric concentrations and fish tissue, which has also been documented in the literature (Lepak et al. 2025). This makes it more difficult to decipher the effectiveness of decreases in mercury emissions and releases in other compartments besides the atmosphere.

Gaps, limitations and recommendations

Based on this analysis and past studies on the Great Lakes region, cross-media integration of Hg data is complex given the different scales at which mercury is emitted, transported, and deposited as well as the differences in biogeochemical and ecological characteristics of each lake. Although long term datasets exist in both the US and Canada, the separate monitoring programs utilize separate sampling protocols and even within the USEPA Great Lakes monitoring programs, either fish filets or whole body samples are taken.

Earlier studies have indicated Hg in Great Lakes sediments, the primary sink for Hg, increased from the 1850's to 1950's before generally declining afterwards (Marvin et al. 2005; Drevnick 2012) likely due to decreases in industrial sources and increases in effluent controls. Drevnick et al. (2012) reported increasing mercury concentrations up to 1980, followed by declines potentially linked to controls on atmospheric mercury emissions. In more recent studies of the relationship between mercury concentrations in sediment and fish tissue, Lepak et al. (2018) reported an inverse pattern where Lake Superior and Lake Huron exhibited the highest total mercury concentrations in lake trout but the lowest sediment concentrations whereas the opposite was reported for Lake Ontario. This current analysis corroborates the lack of consistent relationships between temporal trends in Hg emissions, atmospheric deposition, and fish tissue mercury concentrations with the possible exception for the declines in mercury deposition and tissue concentrations in certain fish species in Lake Ontario. However, the similarities in these patterns cannot be considered causal.

Studies using stable Hg isotopes have shown that the western Great Lakes appear to receive mostly atmospheric deposition and watershed-derived loading whereas those in the east receive loading influenced mostly by watershed and anthropogenic sources (Lepak et al 2015). In fact, inputs to Lake Michigan and Lake Superior appear to be dominated by atmospheric deposition. Other studies (Lepak et al. 2019, 2025) account for changes in food web structure over time in the Great Lakes and found that while sources of Hg may be declining, concentrations in lake trout appear to be impacted by dietary shifts due to invasive species that change Hg trophic transfer. Thus, the authors hypothesize that fish Hg concentrations do not mirror atmospheric declines because zebra mussel and quagga mussel invasions in the lakes have resulted in a

reduction in plankton in the food web and this has dampened or offset the expected reductions in fish Hg due solely to reduction in emissions.

Hg concentrations in herring gulls have been studied and linked to fish concentrations but the data is not included in this integrated case study. Blukacz-Richards et al (2017) used data collected over 42 years by Environment and Climate Change Canada (ECCC) to examine Hg concentrations in herring gull eggs, lake trout, walleye and rainbow smelt. The authors found that while Hg concentrations in eggs and fish declined over the first 30 years in Lake Erie and Ontario, the trend reversed in the early 2000's, a trend also observed for Lake Superior lake trout.

When comparing the fish tissue concentrations to human health criterion for human exposure, all lakes have fish exceeding the US FDA/EPA criterion (**Figure 4**). Past studies have reported that human consumption of Great Lakes fish results in health risks of certain populations in the region. A study conducted on licensed anglers and Burmese refugees and immigrants living and fishing in and around Lake Ontario and Lake Erie had higher levels than the general US adult population (Savadatti. et al 2019; Hsu et al. 2022). Connelly et al. (2019) used a web-based diary-based method and found that women of childbearing age in the Great Lakes region ingested a disproportionate amount of Hg from locally caught fish with 18% of meals contributing 37% of Hg intake. In addition, 3.4% of the studied population exceeded the Refence Dose (RfD) based on average estimated intake over the four-month study period. Since there has not been human exposure data collected for all the lakes over time, the link to fish concentrations and consumption is difficult to make conclusively. The continuing exceedances of human health criterion for fish tissue Hg concentrations through time suggest fish concentrations in the Great Lakes could be an important exposure route for Hg and should be monitored continuously and perhaps the Lake Michigan monitoring should be increased in frequency to better understand pattens. However, across all species, size classes, lakes, and years, 61% of samples had uncorrected Hg concentrations below the lowest US FDA/EPA threshold, underscoring the importance of outreach programs promoting informed choices about species and size classes to reduce Hg exposure and maintain the nutritional benefits of fish consumption.

Figures

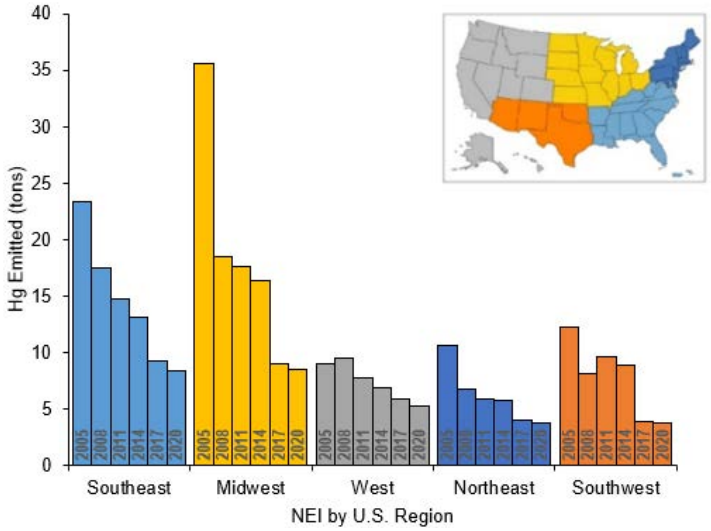

Figure 1. USEPA NEI Hg emissions (tons) by U.S. region from 2005 to 2020 (U.S. EPA 2021).

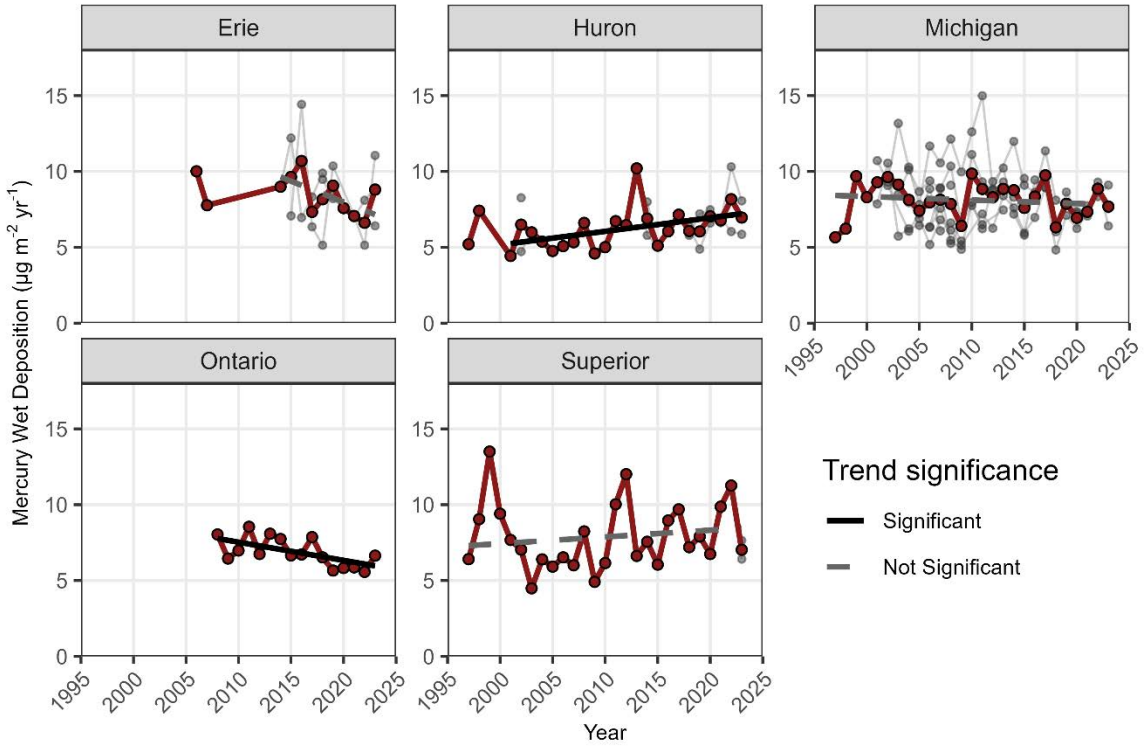

Figure 2. Annual mercury deposition for MDN sites in the Great Lakes basins from 1997-2023. Light gray lines and points are individual MDN stations within each Great Lake basin. Red lines and points are the mean annual mercury deposition for all the stations within the basin. Trend lines were derived using the Mann–Kendall test and Sen's slope estimator; solid black lines denote

statistically significant trends ($p < 0.05$), and dashed gray lines indicate non-significant trends. Trends were calculated and displayed only for the range of consecutive years with measurements

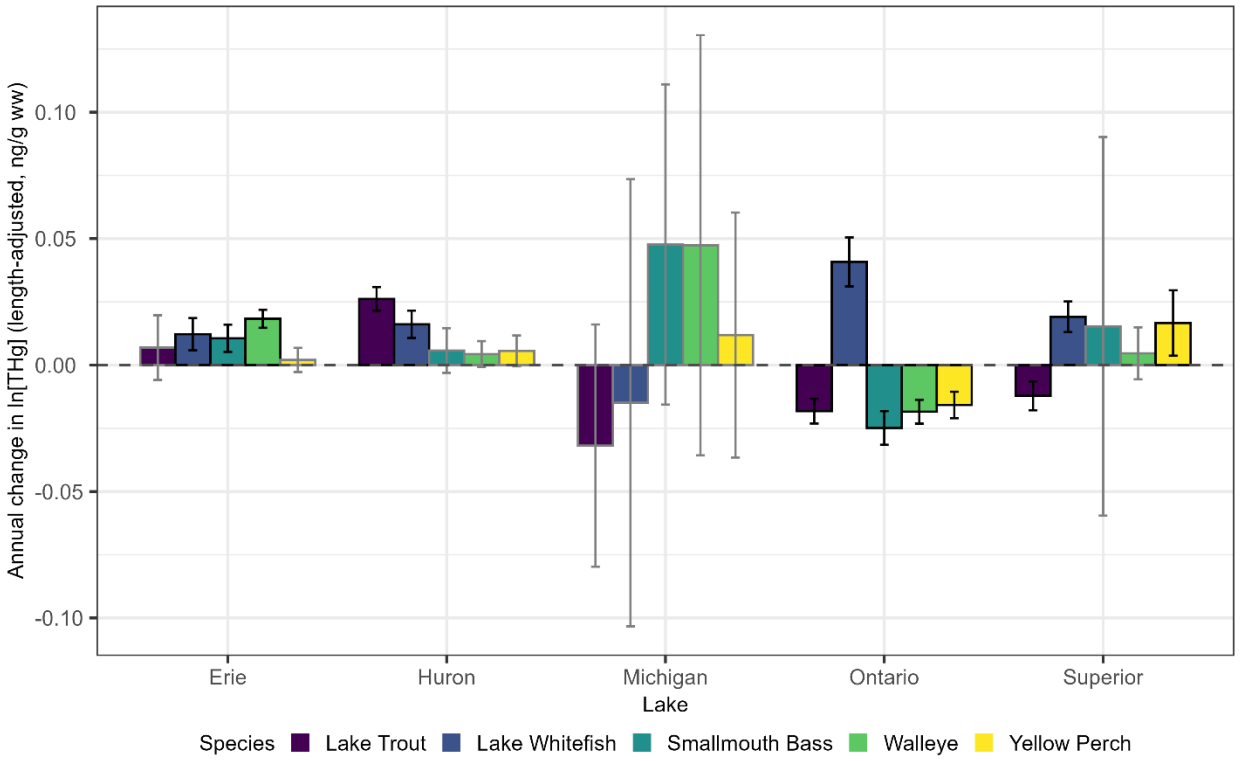

Figure 3. Estimated annual trends in length-adjusted total mercury concentrations (ln[THg], ng/g muscle wet weight) in five fish species from the five Great Lakes. Temporal trends were estimated using a linear mixed-effects model with fixed effects for Year, Lake, Species, and their interaction, and including sampling site as a random effect. Bars show model-estimated slopes for each combination of species and lakes with lines for 95% confidence intervals. Black outlines denote statistically significant trends ($p < 0.05$), while gray outlines denote non-significant trends. Only the five most-sampled species were modelled

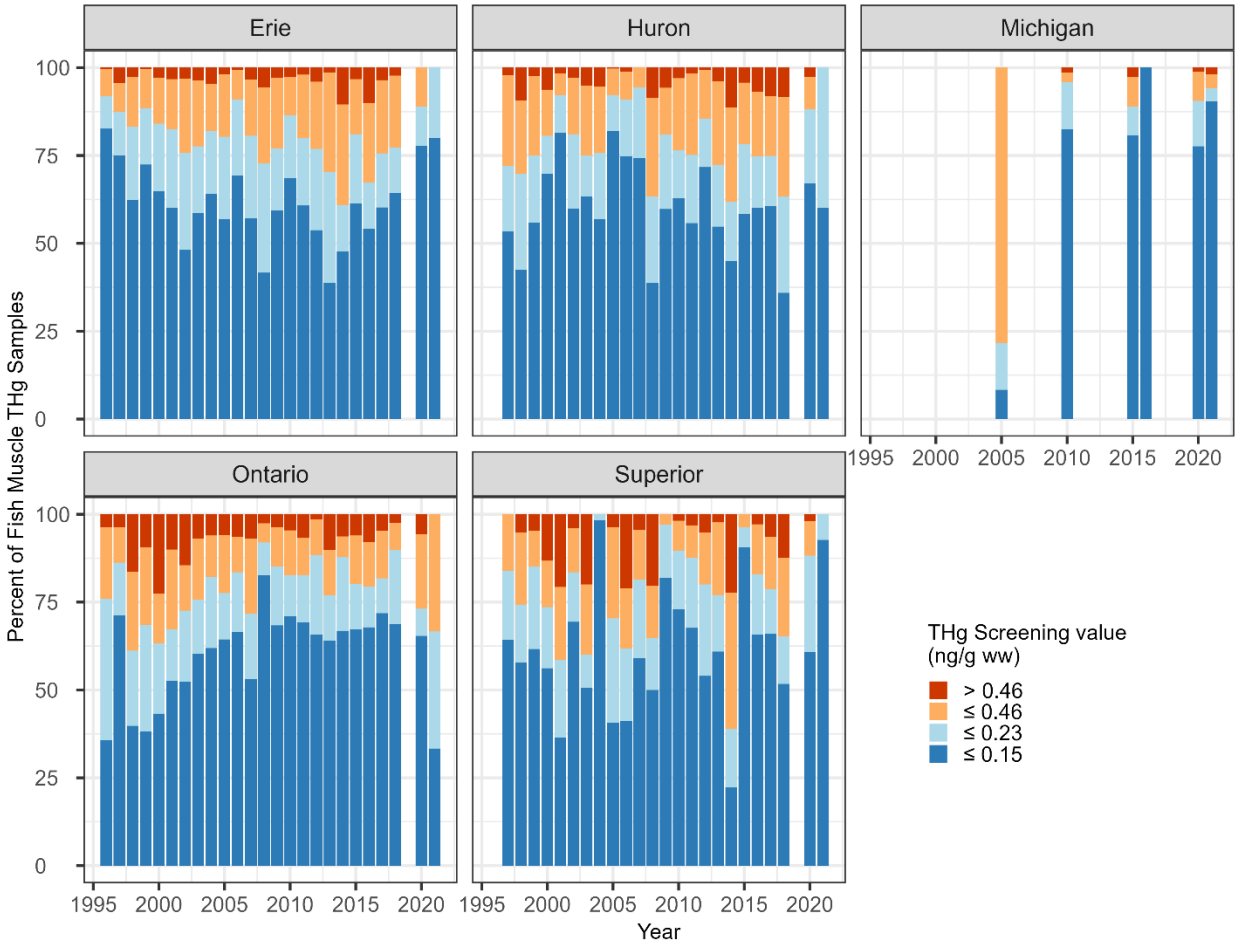

Figure 4 Percent of all fish samples in each of the five Great Lakes with mercury fish tissue concentrations categorized by the US FDA/EPA fish consumption guidelines for sensitive human populations indicating best choices (≤0.15 = 3 weekly fish servings), good choices (≤0.23 = 2 weekly fish servings or ≤0.46 = 1 weekly fish serving), or choices to avoid (>0.46 = 0 weekly fish servings) (US FDA/EPA 2024).

References

Blukacz-Richards, E.A., Visha, A., Graham, M.L., McGoldrick, D.L. de Solla, S.R., Moore, D.J.. Arhonditsis, G.B. 2017. Mercury levels in herring gulls and fish: 42 years of spatio-temporal trends in the Great Lakes. Chemos 172: 476-487. http://dx.doi.org/10.1016/j.chemosphere.2016.12.148

Connelly, N.S., Lauber, T.B., McCann, P.J., Niderdeppe, J., and Knuth, B.A. 2019. Estimated exposure to mercury from fish consumption among women anglers of childbearing age in the Great Lakes Region. Env. Res, 171: 11-17. https://doi.org/10.1016/j.envres.2019.01.005.

Drevnick, , P.E., Engstrom, D.R., Ddriscoll, C.T., Swain, E.B., Balogh, S.J., Kamman, N.C., Long, D.T., Muir, D.G.C., Parsons, M.J., Rolfhus, K.R., and Rossmann, R. 2012. Spatial and temporal patterns of mercury accumulation in lacustrine sediments across the Laurentian Great Lakes region. Env. Poll 161: 252-260. doi:10.1016/j.envpol.2011.05.025.

Eagles-Smith CA, Silbergeld EK, Basu N, Bustamante P, Diaz-Barriga F, Hopkins WA, Kidd KA, Nyland JF (2018) Modulators of mercury risk to wildlife and humans in the context of rapid global change. Ambio. 47(2):170–197. doi:10.1007/s13280-017-1011-x

Hsu, W.S.,, Zheng, Y., Svadatti, S.S., Liu, M., Lweis-Michl, E.L., Aldous, K.M., Parsons, P.J., Kannan, K., Rej, R., Wang, W., Palmer, C.D., Wattigney, W.A., Irvin-Barnwell, E., and Hwang, S.A. 2022. Biomonitoring of exposure to Great Lakes contaminant among licensed anglers and Burmese refugees in Western New York: Toxic metals and persistent organic pollutants, 2010-2015. Int. J. Hygiene Env. Health 240: 113918. https://doi.org/10.1016/j.ijheh.2022.113918

Lepak, R. F., Hoffman, J.C., Janssen, S.E., Krabbenhoft, D.P., Ogorek, J.M., DeWild, J.F., Tate, M.T., Babiarz, C.L., Yin, R., Murphy, E.W., Engstrom, D.R., Hurley, J.P. 2019. Merciruy source changes and food web shirfts alter contamination signatures of predatory fish from Lake Michigan. Proc. Nat. Acad. Sci. 116: 23600-23608.

Lepak, R.F., Hoffman, J.C., Janssen, S.E., Tate, M.T., Shanoff, M.B., Mahon, M.B., Rumschlag, S. L., Yarnes, C.T., Lenell, B.A., Krabbenhoft, D.P., Ogorek, J.M., Hurley, J.P. 2025. Ecological factors decouple Great Lakes fish mercury concentrations trends from decadal declins in Atmopherick mercury. Env. Sci. Tech. https://doi.org/10.1021/acs.est.5c01359

Lepak, R.F., Janssen, S.E., Yin, R., Krabbenhoft, D.P., Ogorek, J.M., Dewild, J.F., Tate, <M.T., Holsen, T.M., Hurley, J.P. 2018. Factors affecting mercury stable isotopic distribution in piscivorous fish of the Laurenitan Great Lakes. Env. Sci. Tech 52: 2768-2776

Lepak, R.F., Yin, R. Krabbenhoft, D.P., Ogorek, J.M., DeWild, J.F., Holsen, T.M., Hurley, J.P. 2015. Use of stable isotope signatures to determine mercury sources in the Great Lakes. Env. Sci. Technol. Letters 2: 3335-341. DOI: 10.1021/acs.estlett.5b00277

Marvin, C., Painter, S., and Rossman, R. 2004. Spatial and temporal patterns in mercury contamination in sediment of the Laurentian Great Lakes. Env. Res. 95: 351-362. doi:10.1016/j.envres.2003.09.007

Savadatti, S.S., Liu, M., Caglayan C., Reuther, J., Lewis-Michl, E.L., Aldous, K.M., Parsons P.J., Kannan, K., Rej, R., Wang, W., Palmer, C.D., Steuerwald, A.J., Wattigney, W.A., Irvin-Barnwell, E., and Hwang, S.A. 2019. Biomonitoring of populations in Western New York at

risk for exposure to Great Lakes contaminants. Env. Res. 179: 108690. https://doi.org/10.1016/j.envres.2019.108690

Schmeltz D, Evers DC, Driscoll CT, Artz R, Cohen M, Gay D, Haeuber R, Krabbenhoft DP, Mason R, Morris K, Wiener JG (2011) MercNet: a national monitoring network to assess responses to changing mercury emissions in the United States. Ecotoxicology 20(7): 1713-1725

USFDA/EPA (2024) Technical Information on Development of FDA/EPA Advice about Eating Fish for Those Who Might Become or Are Pregnant or Breastfeeding and Children Ages 1-11 Years. https://www.fda.gov/food/metals-and-your-food/technical-information-development-fdaepa-advice-about-eating-fish-those-who-might-become-or-are

Visha, A., Gandhi, N., Bhavsar, S.P., and Arhonditsis, G.B. 2016. Guiding fish consumption advisories for Lake Ontario: A Bayesian hierarchical approach. J. Great Lakes Res. 42: 70-82. http://dx.doi.org/10.1016/j.jglr.2015.11.005.